UNIVERSITA' DEGLI STUDI DI MILANO-BICOCCA

Facoltà di Scienze Matematiche Fisiche e Naturali

Dipartimento di Biotecnologie e Bioscienze

Dottorato di ricerca in Biologia, XXV ciclo

Roles of Shelterin-like proteins and Yku in *Saccharomyces cerevisiae* telomere homeostasis

Marina Martina

Anno accademico 2011-2012

Roles of Shelterin-like proteins and Yku in *Saccharomyces cerevisiae* telomere homeostasis

MARINA MARTINA
MATRICOLA 064710

TUTOR: PROF.SSA GIOVANNA LUCCHINI

DOTTORATO DI RICERCA IN BIOLOGIA XXV CICLO

UNIVERSITA' DEGLI STUDI DI MILANO-BICOCCA
PIAZZA DELL'ATENEO NUOVO 1, 20126, MILANO

DIPARTIMENTO DI BIOTECNOLOGIE E BIOSCIENZE
PIAZZA DELLA SCIENZA 2, 20126, MILANO

Index

Abstract

Abstract

Telomeres are specialized nucleoprotein complexes that distinguish the natural ends of linear chromosomes from intrachromosomal double-strand breaks. In fact, telomeres are protected from DNA damage checkpoints, homologous recombination or end-to-end fusions that normally promote repair of intrachromosomal DNA breaks. When chromosome end protection fails, dysfunctional telomeres are targeted by the DNA repair and recombination apparatus, whose outcomes range from the generation of chromosomal abnormalities, general hallmarks for human cancer cells, to permanent cell cycle arrest and cell death. While several studies address the consequences of telomere dysfunctions, the mechanisms by which telomere protection is achieved remain to be determined. During my PhD, I contributed to investigate this issue by analyzing the role of evolutionarily conserved telomeric proteins in protecting budding yeast telomeres from degradation.

In particular, the data obtained during the first year of my PhD show that the shelterin-like proteins Rif1, Rif2, and Rap1 inhibit nucleolytic processing at both *de novo* and native telomeres during G1 and G2 cell cycle phases, with Rif2 and Rap1 showing the strongest effects. Also the Yku complex prevents telomere resection in G1, independently of its role in non-homologous end joining. Yku and the shelterin-like proteins have additive effects in inhibiting DNA degradation at G1 *de novo* telomeres. In fact, while Yku plays the major role in preventing initiation, Rif2 and Rap1 act primarily by limiting extensive resection. In particular, Rap1 and Rif2 prevent telomere degradation by inhibiting MRX (Mre11-Rad50-Xrs2) access to telomeres, which are also protected from the Exo1 nuclease by Yku.

The MRX complex is also necessary to maintain telomere length by

recruiting the Tel1 kinase, and Rif2 was recently shown to interact with the C-terminus of Xrs2. As also Tel1 binds the same portion of Xrs2, it has been proposed that Rif2 and Tel1 might compete with each other for binding to MRX, with Rif2 preventing Xrs2 interaction with Tel1. This issue was explored during the second part of my PhD by taking advantage of the *TEL1-hy909* mutant allele, previously identified as a dominant suppressor of the hypersensitivity to genotoxic agents and checkpoint defects of Mec1-deficient cells (Baldo et al., 2008). The data obtained by this analysis provide evidence that regulation of telomere processing and elongation relies on a balance between Tel1 and Rif2 activities. In particular, Tel1 appears to regulate telomere nucleolytic processing by promoting MRX activity. In fact, the lack of Tel1 impairs MRX-dependent telomere resection, which is instead enhanced by the Tel1-hy909 mutant variant. Our data indicate that the Tel1-hy909 variant is more robustly associated than wild-type Tel1 to double-strand-break (DSB) ends carrying telomeric repeat sequences. Furthermore, it increases the persistence of both the MRX complex and the telomerase subunit Est1 at a DSB adjacent to telomeric repeats, which in turn likely account for the increased telomere resection and elongation in *TEL1-hy909* cells. Strikingly, Rif2 is unable to negatively regulate processing and lengthening at *TEL1-hy909* telomeres, indicating that the Tel1-hy909 variant overcomes the inhibitory activity exerted by Rif2 on MRX. Altogether, these findings highlight a primary role of Tel1 in overcoming Rif2-dependent negative regulation of MRX activity in telomere resection and elongation.

Introduction

Eukaryotic cells have evolved conserved surveillance mechanisms called checkpoints, which monitor both the integrity of the genome and its correct partitioning during cell division, and ensure that daughter cells receive complete genetic information, thus preserving genetic stability in a cell population.

In particular, the genome of living organisms can suffer both spontaneous and induced lesions. DNA double-strand breaks (DSBs), are among the most deleterious types of damage that can occur in the genome of eukaryotic cells, because failure to repair these lesions can lead to serious genetic instability. DNA breaks must be recognized as DNA damage to activated a DNA damage response (DDR) which serves at least two primary purposes: i) to activate DNA repair/recombination pathways and ii) to arrest the cell cycle in response to DNA damage, thereby coordinating cell cycle progression with DNA repair capacity.

The natural ends of linear chromosomes must be distinguished from intrachromosomal DSBs to prevent DNA damage checkpoint activation, homologous recombination or end-to-end fusions that normally promote repair of intrachromosomal DNA breaks. When this protection fails, chromosome ends are targeted by the DNA repair and recombination apparatus, whose outcomes range from the generation of chromosomal abnormalities, general hallmarks for human cancer cells, to permanent cell cycle arrest and cell death.

For this reason chromosome ends are packed into specialized protective nucleoproteic structures called telomeres.

Telomere structure and homeostasis

Telomeres are specialized nucleoprotein complexes that define the physical ends of linear chromosomes. Their basic structure is conserved among eukaryotes and consists of short tandem DNA repeats. Human telomeres bear precise C_3TA_2/T_2AG_3 repeats that can extend from 2 to up to 50 kilobase pairs, whereas *Saccharomyces cerevisiae* chromosomes ends carry 250–400 base pairs of a more heterogeneous sequence, abbreviated $C_{1-3}A/TG_{1-3}$. In both organisms, the G-rich strand extends over the complementary C-rich strand in the 3‘ direction to form a single-stranded overhang, known as the G-tail (Figure 1A). In *S. cerevisiae*, G-tails of 50–100 bases are transiently detected in late S phase, while shorter G-tails are probably present during the rest of the cell cycle.

Studies in mammalian cells support a model in which G-tails loop back and invade the duplex telomere DNA forming a t-loop (Figure 1B) (Griffith et al., 1999). Similar structures have been reported to exist also in *Kluyveromyces lactis*, ciliates and trypanosomes (Murti and Prescott 1999; Muñoz-Jordán et al. 2001; Cesare et al. 2008). Although t-loops have not been detected in yeast, yeast telomeres have a different higher-order chromatin organization in which the telomere folds back on the subtelomeric DNA (Strahl-Bolsinger et al., 1997; de Bruin et al., 2001) (Figure 1B).

Telomeres can also fold into G-quadruplex DNA, an unusual DNA conformation that is based on a guanine quartet (Parkinson et al. 2002).

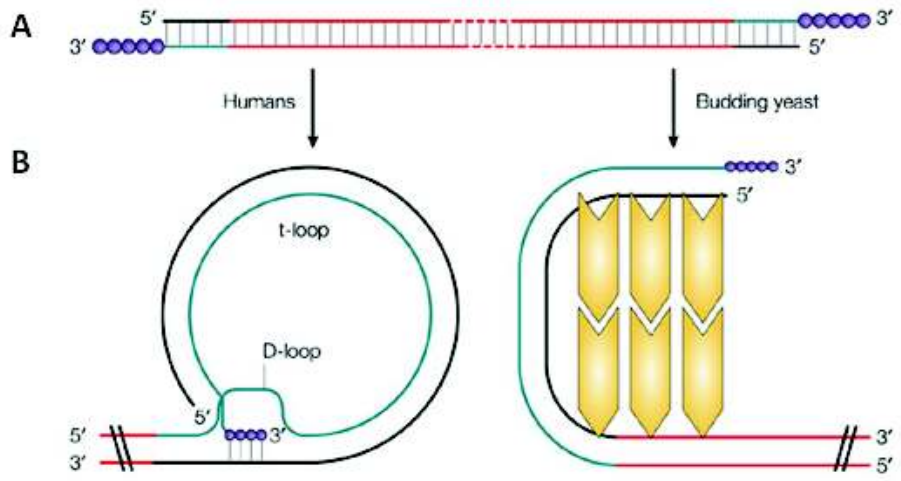

Figure 1: Telomere ends contain G-rich overhangs. A) Chromosome ends are comprised of stretches of repeated C/G-rich DNA (C-rich strand shown in black and G-rich strand shown in blue; non-telomeric DNA is in red). In both humans and yeast, the G-rich strand is longer, so that it generates a 3′ single-stranded overhang or G-tail (purple circles). **B)** Higher-order chromatin structures at the telomere in human cells and in yeast. Human telomeres end in t-loops that are formed when G-tails loop back and invade the duplex telomere DNA. Yeast telomeres fold back on the sub-telomeric DNA to form a ~3-kb region of core heterochromatin. This higher-order chromatin structure is mediated by protein–protein interactions (double-stranded DNA-binding proteins that mediate looping are shown in yellow).

The end-replication problem: the telomerase

Telomere length is maintained by a dynamic process of lengthening and shortening. Shortening can occur as a result of nucleolytic degradation and incomplete DNA replication, whereas lengthening is primarily accomplished by the action of a specialized reverse transcriptase called telomerase (Greider and Blackburn, 1985) and occasionally by homologous recombination (Liu et al., 2007).

Telomerase is needed to fully replicate telomeres and thereby to compensate the incomplete replication due to the conventional DNA replication machinery. The conventional DNA polymerases require a

short RNA primer. This primer, on the leading strand, can be extended by polymerase until it reaches the end of the chromosome to produce a blunt end. In contrast, the lagging strand is made discontinuously, and each Okazaki fragment starts with an RNA primer. Removal of the most distal RNA primer leaves a gap that cannot be filled in by a conventional DNA polymerase and thus a single stranded 3' tail. In the absence of a special end replication mechanism, the product is shorter than the starting template (Figure 2). This dilemma is the so-called end-replication problem, as classically defined (Watson 1972).

Telomerase extends the 3′ G-rich strand of a chromosome by reverse-transcribing the template region of its tightly associated RNA moiety. The conventional DNA replication machinery can then fill in the C-rich strand thus preventing any loss of DNA (for review see Hug and Lingner, 2006). Although *in vitro* telomerase activity requires both its reverse transcriptase catalytic subunit (Est2 in *S. cerevisiae* and TERT in mammals) and the RNA template (TLC1 in *S. cerevisiae* and hTR in humans) (Lingner et al., 1997), other factors are required for telomerase action *in vivo*. For instance, effective telomerase function in *S. cerevisiae* requires Est1 and Est3 that associate with Est2 and TLC1 (Lendvay et al., 1996).

Notably, by following the elongation of a single telomere in yeast it has been shown that telomerase does not act on every telomere in each cell cycle, but instead exhibits an increasing preference for telomeres as their length decline (Marcand et al., 1999), suggesting that telomeres switch between nonextendible and extendible states (Teixeira et al. 2004). It is known that telomere length affects repeat addition processivity of telomerase in vivo (Chang et al., 2007). In fact, by

examining the telomere extensions after one cell cycle, it has been shown that *S. cerevisiae* telomerase can dissociate from and reassociate to a given telomere during one round of telomere elongation. Repeat addition processivity is enhanced at extremely short telomeres, allowing cells to rapidly elongate them (Chang et al., 2007).

Telomerase-mediated lengthening is also cell-cycle regulated. In fact, although the association of telomerase with telomeres can occur throughout the cell cycle (Taggart et al., 2002), only the late S phase telomere-associated Est2 is important for telomere length regulation (Fisher et al., 2004).

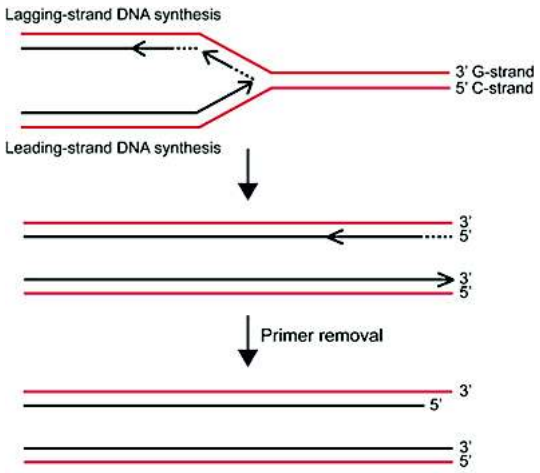

Figure 2: Telomere DNA replication. A telomere is replicated by a fork moving in a single direction, implying that the G-rich 3' strands are replicated discontinuously by the lagging-strand machinery, while the C-rich 5' strands are replicated continuously by the leading-strand machinery. The strand replicated by lagging-strand synthesis will lead to a 3' single-stranded overhang due to removal of the last RNA primer and/or to incomplete synthesis of the last Okazaki fragment, while on the leading-strand telomere replication generates a blunt end.

Telomere binding proteins

Although the presence of a functional telomerase is a necessary condition for telomere maintenance, it is not sufficient. Proteins that bind single- and double-stranded DNA with specificity for telomeric TG repeats are required to regulate telomerase activity and to protect chromosome ends from degradation and end-to-end joining events.

Three different protein complexes bind *S. cerevisiae* telomeres: the shelterin-like complex (Rap1-Rif1-Rif2) that is essential for both the protection and the lengthening of telomeres (Pardo and Marcand, 2005), an heterotrimeric complex called CST (Cdc13-Stn1-Ten1), that binds single strand G-tails and the Yku complex (Grandin et al., 1997, 2001) (Figure 3).

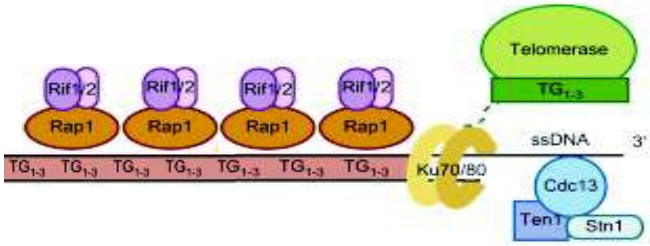

Figure 3: Budding yeast telomeric proteins. Rap1 (Repressor Activator Protein 1) binds the double-stranded telomeric sequences and recruits Rif1 and Rif2 (Rap1 Interacting Factors), which regulate telomere length. The heterodimeric Yku complex (Ku70/80) interacts with the terminal part of the telomere and, depending on the cell cycle phase, with the Ku-loop of the telomerase RNA; Cdc13 (Cell Division Control Protein 13) and the Cdc13-interacting factors Ten1 and Stn1 bind to the single strand overhang.

In *S. cerevisiae*, Cdc13 binds the single-stranded G-tail and allows telomerase recruitment to the telomeric 3' end through the interaction with the Est1 subunit (Bianchi et al. 2004; Pennock et al. 2001; Nugent et al. 1996). Moreover, Cdc13 limits telomerase-mediated telomere elongation in conjunction with Stn1 and Ten1, two essential Cdc13-

associated proteins (Grandin et al. 1997, 2001; Chandra et al. 2001). In fact, Stn1 competes with Est1 for the binding to Cdc13 (Chandra et al., 2001; Puglisi et al., 2008; Li et al., 2009)

The CST complex is also required to protect telomeres from degradation and to distinguish a telomere from a DSB. In fact, inactivation of one of its three components leads to estensive C-strand degradation, increased single-stranded DNA amounts, checkpoint activation and cell cycle arrest (Garvik et al., 1995; Grandin et al., 1997, 2001)

Double-stranded telomeric DNA repeats contains high-affinity Rap1 binding sites every ~20 bp. Therefore, given an average telomere length of 300 bp, individual telomeres are probably covered by 15–20 Rap1 molecules (Wright and Zakian, 1995). Rap1, together with Rif1 and Rif2, forms the so called shelterin-like complex, which negatively regulates telomerase by sequestering its single-stranded DNA substrate in a closed conformation. Indeed, the Rap1 protein negatively regulates telomere length (Conrad et al., 1990; Marcand et al., 1997), and the Rap1-binding proteins Rif1 and Rif2 contribute to this negative regulation (Levy and Blackburn, 2004).

A critical feature of this *in cis* negative regulation of telomerase access is the ability of the shelterin-like complex to limit telomere length based on its total telomere-bound amount, whose strength increases with increasing TG tract length (Marcand et al., 1997). Because the amount of shelterin-like proteins bound to a telomere is proportional to the length of the TG repeat array, longer telomeres are proposed to have greater probability of inhibiting telomerase access. Progressive telomere shortening causes the gradual loss of telomere-bound shelterin-like proteins, and therefore a progressive relief of its inhibitory function on

telomerase activity, thus allowing telomerase-mediated telomere elongation.

One possibility is that regulation of telomerase activity by the shelterin-like complex is achieved at the level of its association with the telomere. In fact, studies of the *S. cerevisiae* telomeric protein association to short and normal-length telomeres show that Est1 and Est2 are preferentially recruited to a shortened telomere, which is known to be a preferential substrate for telomerase (Bianchi and Shore, 2007; Sabourin et al., 2007).

Another key telomere binding factor is the yeast Ku complex (referred to as Yku), composed of the Yku70 and Yku80 subunits (Boulton and Jackson 1996; Porter et al. 1996; Gravel et al. 1998). As Yku is essential for DNA repair via non-homologous end joining (NHEJ) and telomeres are protected from NHEJ, the association of Yku with telomeres is counterintuitive. Notably, Yku complex interacts specifically with a stem–loop portion of *TLC1* RNA in yeast cells (Peterson et al., 2001; Stellwagen et al., 2003), and this interaction is essential for Est2 telomere association in G1 and early S phase (Fisher et al., 2004; Chan et al., 2008), indicating that Ku promotes telomere addition by targeting telomerase to chromosomal ends.

Both fission yeast and vertebrates telomeres are similar to those of *S. cerevisiae*. In fact, like in budding yeast, both single-stranded and double-stranded telomeric sequences are bound by specialized proteins (de Lange, 2005; Lydall, 2009; Jain and Cooper, 2010) (Figure 4). In mammalian cells, the double stranded DNA is bound by the proteins TRF1 and TRF2 (*Telomeric Repeat binding Factor* 1 e 2), whereas the single stranded G-tail is bound by POT1 (*Protection Of Telomeres* 1)

(Zhong et al., 1992; Bilaud et al., 1997; Broccoli et al., 1997; Baumann and Cech, 2001). Moreover, a Rap1 orthologous is recruited at telomeres by physical interaction with TRF2 (Li et al., 2000).

Unlike in *S.cerevisiae*, where two separate complexes bind single- and double-stranded DNA, in mammalian telomeres TIN2 (TRF1-*Interacting protein* 2) and TPP1 (TIN2-POT1 *organizing Protein* 1) proteins serve as a bridge between TRF1/TRF2/RAP1 and POT1 thus generating a single protein complex called "Shelterin" (Kim et al., 1999; Houghtaling et al., 2004; de Lange, 2005; Ye et al., 2010) (Figure 4A). This complex promotes the formation of highly ordered structures at mammalian telomeres and has a key role both in the protection and in telomerase-dependent lengthening of telomeric ends (de Lange, 2005).

Another complex similar to shelterin is present at *S. pombe* telomeres, where the double stranded DNA is bound by Taz1, similar to mammalian TRF1 and TRF2, and the single-stranded G-tail is bound by Pot1 (Cooper et al., 1997, 1998; Baumann and Cech, 2001). Moreover Rap1 is recruited at telomeres by direct interaction with Taz1, whereas the Tpz1 and Poz1 proteins link Pot1 and Taz1 (Chikashige and Hiraoka, 2001; Kanoh and Ishikawa, 2001; Miyoshi et al., 2008). Finally, Tpz1 is bound by the Ccq1 protein, which is involved in telomerase recruitment (Miyoshi et al., 2008; Tomita and Cooper, 2008) (Figure 4B).

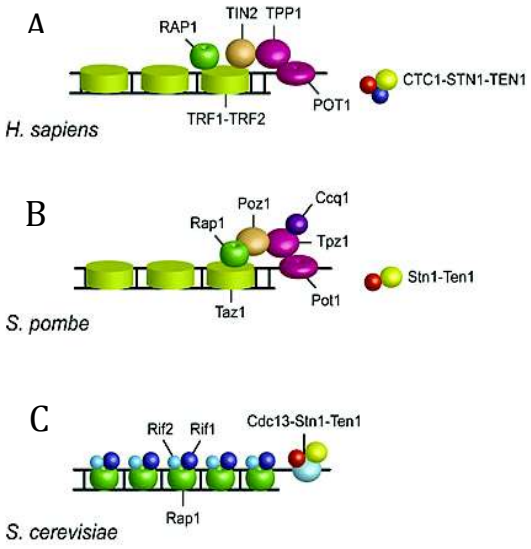

Figure 4: **Telomere-specific proteins in A) mammalian, B) *S. pombe* and C) *S. cerevisiae* cells .**

DNA damage response and telomere homeostasis

Sensing and processing of an intrachromosomal DSB

When an intrachromosomal DNA break occurs, it must be recognized as DNA damage to activate repair/recombination pathways, whose primary function is to repair the break.

In both yeast and human cells, generation of accidental DSBs triggers the activation of the DNA damage checkpoint pathway, which arrests the cell cycle and activates DNA repair pathways in response to DNA damage, thereby coordinating cell cycle progression with DNA repair capacity. Key players in the DNA damage checkpoint response belong to a protein kinase family, including mammalian Ataxia Telangiectasia Mutated (ATM) and Ataxia Telangiectasia and Rad3-related (ATR), *S. cerevisiae* Tel1 and Mec1 and *S. pombe* Tel1 and Rad3 (reviewed in Longhese et al., 2006; Shiloh, 2006). Mec1 and Rad3 are more similar to ATR, whereas Tel1 is more similar to ATM. Both yeast Tel1 and human ATM appear to bind DNA through their interaction with the MRX (Mre11, Rad50 and Xrs2)/MRN (Mre11, Rad50 and Nbs1) complex (Nakada et al., 2003; Falck et al., 2005). Rather than using MRX/MRN, Mec1, Rad3 and ATR function in a complex with Ddc2 (Paciotti et al., 2000), Rad26 (Edwards et al., 1999) and ATRIP (Cortez et al., 2001), respectively. Mec1/ATR ability to transmit and amplify the DNA damage signals is enhanced by a proliferating cell nuclear antigen (PCNA)-like complex called Ddc1-Rad17-Mec3 in budding yeast, and Rad9-Rad1-Hus1 in both mammals and *S. pombe* (Majka et al., 2006). The

checkpoint signals are then propagated through evolutionarily conserved protein kinases, which are called Rad53 and Chk1 in *S. cerevisiae*, and Chk2 and Chk1 in humans (reviewed in Longhese et al., 2006; Shiloh, 2006).

Once a DSB occurs, the highly conserved MRX/MRN complex is the first group of proteins recruited to DNA ends (Lisby et al, 2004) (Figure 5). The Ku70/Ku80 heterodimer is also loaded onto DNA ends.

If cells are in the G1 cell cycle phase, the presence of Yku prevents resection and, together with MRX, mediates recruitment of downstream NHEJ (Non Homologous End Joining) factors (Lee et al., 1998; Chen et al., 2001; Zhang et al., 2007; Clerici et al., 2008; Palmbos et al., 2008). DSB ends can then be religated by NHEJ, a process that requires the DNA ligase activity of the Dnl4-Lif1-XRCC4 heterodimer and the Nej1/XLF protein (reviewed in Daley et al., 2005). If cells are in the S or G2 cell cycle phase when a DSB is detected, processing of the 5' DSB ends generates 3'-ended ssDNA tails that inhibit NHEJ and target DSB repair to HR (Homologous Recombination) (Figure5).

In both yeast and humans, the MRN-ATM and MRX-Tel1 complexes, once recruited to DSBs, contribute to generate 3'-ended ssDNA (Falck et al., 2005; Adams et al., 2006; Jazayeri et al., 2006; Myers and Cortez, 2006; Mantiero et al., 2007), the critical intermediate structure recognized by the Mec1-Ddc2 and human ATR-ATRIP complexes (Zou and Elledge, 2003). This implies that initiation of DSB resection is a critical step for the transition from Tel1/ATM- to Mec1/ATR-dependent checkpoint activation (Figure 5).

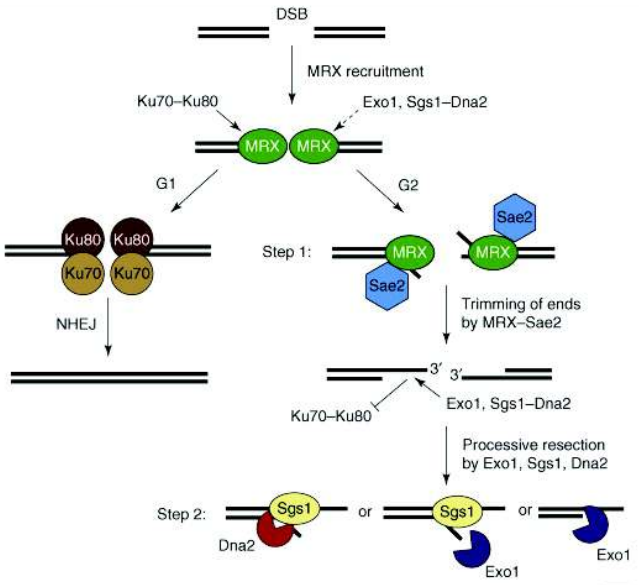

Figure 5: Model for the two-step mechanism of DSB processing. Immediately after a DSB is formed, the MRX complex (green) binds to the broken ends. If repaired by NHEJ (left), the ends should not be processed and are ligated back together with the help of the NHEJ pathway components (the Ku complex [brown], DNA ligase 4 and accessory factors). Repair of the break by HR (right) requires 5'–3' resection, which takes place in two steps. In the first step, MRX and Sae2 (blue) trim the ends around the break to create short ssDNA overhangs. These are then substrates for further processing by the concerted action of a helicase, Sgs1 (orange), and two nucleases, Exo1 (purple) and Dna2 (red).

The MRX complex and the Sae2 protein (orthologous of human CtIP) initiate together the resection of the 5' strand, possibly through an endonucleolytic cleavage. The resulting partially resected 5' DNA end can be further processed by the action of either Exo1 or Sgs1 and Dna2 (Mimitou and Symington, 2008; Zhu et al., 2008). The initial endonucleolytic cleavage of the 5' strand catalysed by MRX and Sae2 can be crucial for processing blocked ends, such as, for instance, those formed during meiosis or after exposure to methylating agents. In contrast, the MRX-Sae2 initial endonucleolytic cleavage is not essential for processing DSBs generated by endonucleases (the so-called 'clean'

DSBs), because mutants lacking Sae2 or the Mre11 nuclease activity impair only partially the processing of these DSB ends (Furuse et al., 1998; Tsubouchi and Ogawa, 1998; Moreau et al., 1999; Llorente and Symington, 2004; Clerici et al., 2005). This indicates that Exo1 and Sgs1–Dna2 can resect 'clean' DSBs even in the absence of the initial processing step.

DNA repair/recombination and DNA damage checkpoint proteins are involved in telomere homeostasis

As the previously described specialized nucleoprotein structure protects telomeres from repair and checkpoint activation, proteins involved in the DNA damage response were not expected to act at telomeres. Paradoxically, many checkpoint and DNA repair proteins associate with telomeres and critically contribute to telomeric functions, including capping.

For instance, the Yku heterodimer, which is necessary for NHEJ, is also involved in maintaining telomere length in *S. cerevisiae*, *S. pombe* and human cells, and this function appears to be distinct from Yku function in NHEJ. In particular, budding yeast Yku performs different functions at telomeres: i) it is important for recruiting telomerase to telomeres by binding to a stem-loop portion of TLC1 RNA (Peterson et al., 2001; Chai et al., 2002; Stellwagen et al., 2003; Fisher et al., 2004; Chan et al., 2008) and ii) it protects telomeres from nuclease activities (Maringele and Lydall, 2002; Vodenicharov et al., 2010). In its absence, telomeres are very short and have long G-tails throughout the cell cycle (Boulton and

Jackson, 1996; Porter et al., 1996; Gravel et al., 1998; Polotnianka et al., 1998).

Telomere structure and function depend also on proteins known to be required for DNA damage checkpoint activation. For instance, the telomerase-dependent replication of telomeres depends both on Tel1/ATM and Mec1/ATR checkpoint kinases. In fact, the lack of Tel1/ATM causes telomere shortening in *S. cerevisiae*, *S. pombe* and human cells (Greenwell et al., 1995; Metcalfe et al., 1996; Dahlen et al., 1998; Matsuura et al., 1999). However, in contrast to what observed at DSBs, Tel1 association with short telomeres does not elicit a checkpoint response, a difference that is not fully understood.

In any case, cells that lack Tel1 show short but stable telomeres, whereas the concomitant inactivation of both Tel1/ATM and Mec1/ATR kinases in *S. cerevisiae* and *S. pombe* leads to chromosome self-circularization and complete loss of telomeric sequences, similar to that seen in cells lacking active telomerase (Naito et al., 1998; Ritchie et al., 1999; Nakamura et al., 2002). Moreover, as observed with *TEL1* inactivation, the lack of *RAD50* in a *mec1* mutant leads to telomere erosion (Ritchie et al., 1999; Ritchie and Petes, 2000).

Tel1 binds telomeres (Bianchi and Shore, 2007; Hector et al., 2007; Sabourin et al., 2007) during S phase via the interaction with the Xrs2 subunit of MRX. Indeed, Tel1 interacts preferentially with short telomeres and is thought to be involved in telomerase recruitment.

Although the kinase activity of Tel1 is required for its role in telomere length maintenance (Mallory and Petes, 2000), its critical targets at telomeres are not yet identified. Cdc13 is a good candidate as a Tel1 target because it contains 11 SQ/TQ motifs, which are preferred

phosphorylation sites for ATM/ATR-like kinases (Mallory and Petes, 2000; Tseng et al., 2006). In vitro, Tel1 phosphorylates Cdc13 on three serine residues (S225, 249 and 255). Moreover, simultaneous mutation of two of these residues (S249 and S255) results in an EST (Ever Shorter Telomeres) phenotype. In addition, if Est1 is targeted to the telomere using a ^{DBD}Cdc13–Est1 fusion protein, phosphorylation of these residues is no longer required for telomerase action.

The phenotype of *cdc13-S249A, S255A* cells makes a strong argument that their phosphorylation is critical for Cdc13–Est1 interaction (Tseng et al. 2006). However, cells expressing a *cdc13* allele in which each of the SQ/TQ motifs is mutated to AQ supports near wild-type–length telomeres (Gao et al., 2010). One possible way to reconcile these data is that perhaps *cdc13-S249A, S255A* cells are telomerase defective because these mutations destabilize the recruitment domain (RD) rather than preventing it from being phosphorylated. In any case, the key sites of Tel1-dependent phosphorylation of Cdc13 that are relevant for telomerase recruitment have probably not been identified.

It has been shown that Tel1 is important for telomerase processivity at short telomeres (Chang et al., 2007). By definition, telomeres progressively loose Rap1 binding sites concomitantly with loss of telomeric DNA. Thus, an appealing model is that short telomeres are marked for MRX binding by their low content of Rif1 and Rif2. Surprisingly, short telomeres show about the same amount of Rif1 binding as wild-type–length telomeres (Sabourin et al., 2007; McGee et al., 2010). Thus, short telomeres are not distinguished from long telomeres by their Rif1 content, although Rif1 may be selectively modified at short telomeres. In contrast, Rif2 content at short telomeres

is lower than at long telomeres, suggesting that its absence might mark short telomeres for elongation.

A mechanistic explanation for the effects of Rif2 on Tel1 binding comes from studies on DSBs made adjacent to telomeric DNA (Hirano et al., 2009). Tel1 binding to these DSBs is increased in *rif2Δ* cells, suggesting that Rif2 inhibits Tel1 association with the break. Moreover, tethering Rif2 to a nontelomeric DSB decreases the binding of Tel1 but not of MRX to the break. Finally, coimmunoprecipitation shows that the N-terminus of Rif2, but not Rif1, interacts with the C-terminus of Xrs2. As Tel1 also binds this portion of Xrs2, Rif2 and Tel1 probably compete with each other for binding to MRX. According to this data, Rif2 might sequester Xrs2 in a manner that prevents its interaction with Tel1 (Figure 6).

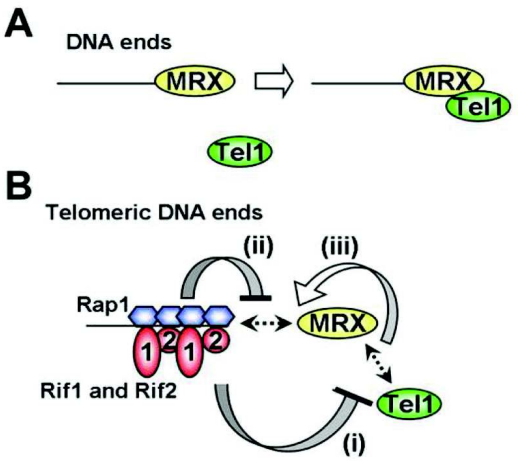

Figure 6: A Model for Localization of MRX and Tel1 to Telomeric DNA Ends A) MRX-dependent localization of Tel1 to DNA ends. MRX recognizes DNA ends and associates with DNA ends independently of Tel1, but then recruits Tel1 to the DNA ends. B) Inhibitory network for MRX and Tel1 localization at telomeric DNA ends. (i) Rif1 and Rif2 by themselves inhibit MRX-dependent Tel1 localization to DNA ends and Rif2 competes with Tel1 for binding to the C terminus of Xrs2. It is not known how Rif1 inhibits Tel1 localization to DNA ends. (ii) MRX does not efficiently localize to Rap1-bound DNA ends in the absence of Tel1. (iii) MRX-Tel1 interaction could stabilize MRX association with Rap1-bound DNA ends. If Rif1 and Rif2 disrupt Tel1-MRX interaction at DNA ends, MRX could no longer associate efficiently with Rap1-bound DNA ends.

The connections between telomeres and the DNA damage checkpoint are not limited to Mec1/ATR and Tel1/ATM. Telomere length maintenance in *S. cerevisiae* is also influenced by the checkpoint kinase Rad53, and by the Rad17-Mec3-Ddc1 complex (Longhese et al., 2000). Notably, this role for Rad17-Mec3-Ddc1 is evolutionarily conserved in fission yeast and *C. elegans* (Dahlen et al., 1998; Amhed and Hodgkin, 2000; Hoffmann et al., 2000; Nakamura et al., 2002). Moreover, the human Rad9-Hus1-Rad1 complex is constitutively associated with telomeres in both human and mouse cells, and the lack of Hus1 leads to a dramatic telomere shortening (Francia et al., 2006).

Generation of ssDNA overhangs at telomeres

Although telomeric ends are apparently shielded from being recognized as DSBs, chromosome ends and accidental interruptions in duplex DNA molecules share important similarities. In fact, accidental DSBs are resected by 5'-3' exonucleases to generate 3'-ended ssDNA tails, which are channelled into different homology-dependent recombination pathways. The ends of chromosomes in humans, mice, ciliates, yeast, trypanosomes and plants also carry ssDNA G-tails that serve as substrate for telomerase. Single-stranded G-tails of 50-100 nucleotides are transiently detected in *S. cerevisiae* telomeres in late S phase (Wellinger et al., 1993), while G-tails of 12-14 nucleotides are present outside of S phase during the rest of the cell cycle (Larrivée et al., 2004). These single-stranded G-tails have a central function in modulating telomere homeostasis. In fact, they provide a substrate for telomerase, a

specialized reverse transcriptase that needs a single-stranded 3' overhang to anneal it to its associated RNA moiety for iterative reverse transcription of the RNA template. In *S. cerevisiae*, the single-stranded G-tails are bound by the ssDNA-binding protein Cdc13, which is necessary for the recruitment of telomerase through an interaction with the telomerase subunit Est1 (reviewed in Shore and Bianchi, 2009).

As already mentioned, single-stranded telomeric G-tails can be generated during lagging-strand replication after removal of the last RNA primer, whereas leading-strand polymerases are expected to fully replicate their template, thus generating blunt ends (Figure 2). However, in the large majority of eukaryotes, 3' single-stranded overhangs can be detected at both daughter telomeres (Wellinger et al, 1996; Makarov et al, 1997), implying that the 5' strand of the leading-strand telomere must be resected to convert blunt ends into 3' overhangs.

Notably, similar resection machineries create 3' overhangs at both telomeres and DSBs (Diede and Gottschling, 2001; Larrivée et al., 2004; Bonetti et al., 2009). The MRX complex and Sae2 have been shown to be important for C-strand resection, with MRX having the major function (Diede and Gottschling, 2001; Bonetti et al., 2009). It has been recently shown that the MRX complex is present only at the leading-strand telomere (Faure et al., 2010). In contrast, Cdc13 and telomerase are recruited at both leading- and lagging-strand telomeres, but only their binding at leading-strand telomeres requires MRX (Faure et al., 2010). As MRX is necessary to resect telomeric DNA, the above data suggests that leading-strand blunt ends are resected to generate ssDNA, whereas the 3' ssDNA on lagging-strand telomeres could be generated by RNA

primer removal and/or MRX-independent processing. How MRX is targeted only at leading-strand telomeres remains to be determined.

Sgs1 and Exo1 provide compensatory activities to initiate end processing in the absence of Sae2. As seen for DSB resection, Sae2 and MRX act in the same telomere resection pathway, whereas Sgs1 functions in conjunction with Dna2 (Bonetti et al., 2009). The involvement of Dna2 in telomere resection has been observed also in *S. pombe* (Tomita et al., 2004). In any case, 3'-ended ssDNA at telomeres is less far reaching than that at DSBs. In fact, the lack of Sgs1, Exo1 or Dna2 by itself does not affect telomere resection (Bonetti et al., 2009), suggesting that the initial resection catalysed by MRX-Sae2 could be sufficient to generate 3'-ended ssDNA that can be long enough to allow telomerase action. In turn, Exo1 and Sgs1–Dna2 may provide a back-up mechanism for telomere resection when Sae2-MRX activity is compromised. Alternatively, MRX and Sae2 could be specialized in resecting the 5' strand on the leading-strand telomere, whereas Exo1, Sgs1 and Dna2 may extend the single-stranded overhangs generated by RNA primer removal at the lagging- strand telomere.

Consistent with the requirement of 3'-ended ssDNA to allow telomerase action, the absence of nucleolytic activities should impair telomere elongation. However, in the absence of both Sae2 and Sgs1 there is not the complete telomere loss that is observed upon lack of telomerase activity, suggesting that other nuclease activities may resect telomeres even in the absence of Sae2 and Sgs1. Consistent with this hypothesis, telomere shortening in *sae2Δ sgs1Δ* double mutant cells can be partially suppressed by overexpressing Exo1, but not its nuclease-defective

variant, thus confirming a key role of this nuclease in telomere resection (Bonetti et al., 2009) (Figure 7).

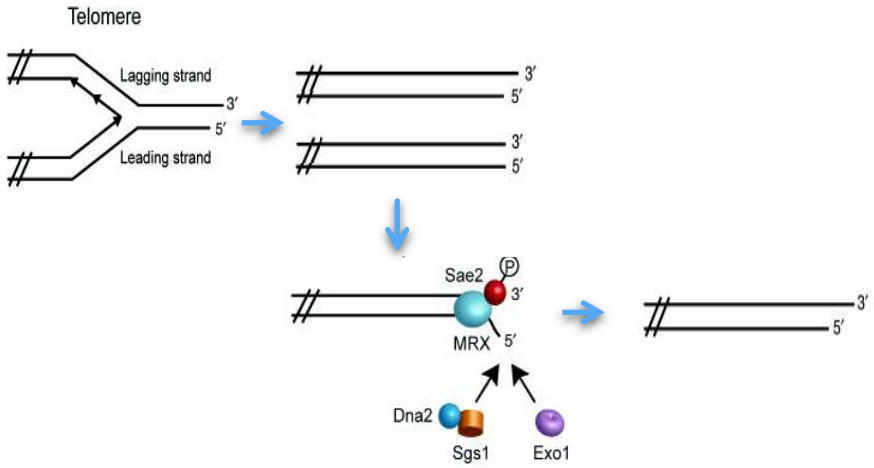

Figure 7: DNA end resection at telomeres. Telomere DNA replication is expected to leave a short 30 overhang on the lagging strand (upon RNA primer removal) and a blunt end on the leading strand. End processing at the leading-strand telomere can then be initiated by Sae2/MRX, with Sae2 activity requiring Cdk1-mediated phosphorylation. Sgs1 and Exo1 can provide compensatory activities to resect the 5′ C-strand, with Sgs1 acting in conjunction with Dna2.

Cell cycle regulation of DNA end resection

Generation of ssDNA at both DSBs and telomeres requires the activity of the Cdk1 cell cycle kinase (Cdc28-Clb in *S. cerevisiae*), whose sequential action determines cell cycle progression. Low Cdk1 activity in *S. cerevisiae* cells, such as during the G1 cell cycle phase, does not allow resection and repair by HR of a single endonuclease-induced DSB (Aylon et al., 2004; Ira et al., 2004). This observation supports a model in which only NHEJ is allowed in haploid G1 cells, whereas Cdk1 activation in S and G2 phases leads to generation of 3’ ssDNA tails and subsequent HR. Cdk1 activity is also required to promote formation of 3’ overhangs at telomeres (Frank et al., 2006; Vodenicharov and Wellinger, 2006).

As Cdk1 activity is low in G1, resection at telomeres can occur only during S/G2, coinciding with the time frame in which the length of the G-tails increases (Wellinger et al., 1993) and telomerase elongates telomeres (Marcand et al., 2000).

The Cdk1-mediated control of resection at both mitotic DSBs and telomeres involves phosphorylation of Sae2 Ser267 (Huertas et al., 2008; Bonetti et al., 2009), a mechanism that is conserved in the Sae2 vertebrate homologue CtIP (Huertas and Jackson, 2009).

Aim of the work

A highly ordered nucleoprotein complex called “telomere” prevents the ends of linear chromosomes from being recognized as DNA double-strand breaks (DSBs). This evolutionary conserved structure is extremely important for genome stability. In fact, the outcomes of telomeres dysfunctions range from the generation of chromosomal abnormalities, general hallmarks for human cancer cells, to permanent cell cycle arrest and cell death.

Although telomere ends are apparently shielded from being recognized as DSBs, they share important similarities with intrachromosomal DSBs. In fact, DSBs are resected to generate 3’-ended single-stranded DNA (ssDNA) tails, which channel their repair into HR. Similarly, the tips of human, mouse, ciliate, yeast and plant telomeres terminate with 3’ overhangs, that serve as substrate for telomerase, due to the protrusion of the G-strand over its complementary C-strand. Furthermore, several proteins such as the MRX (Mre11-Rad50-Xrs2) complex, Sae2, Sgs1, Exo1 and Dna2 are required for generation of ssDNA at both telomeres and intrachromosomal DSBs (Mimitou and Symington, 2008; Zhu et al., 2008; Bonetti et al., 2009), and both DSB and telomere resection is promoted by the activity of the cyclin-dependent protein kinase Cdk1 (Ira et al., 2004; Frank et al., 2006; Vodenicharov and Wellinger, 2006). Noteworthy, although the nuclease requirements at DSBs and telomeres are similar, the single-stranded G-tails of budding yeast telomeres are shorter then those generated at DSB ends. This finding suggests an inherent resistance of telomeric ends to exonuclease attack, which could contribute to avoid telomeres from being sensed as DNA damage.

While several studies address the consequences of telomere dysfunctions, the mechanisms by which telomere protection is achieved

remain to be determined. For this reason, during the first year of my PhD I aimed at studying the role of evolutionarily conserved telomeric proteins, such as the shelterin-like proteins (Rap1/Rif1/Rif2) and the Yku complex, in protecting budding yeast telomeres from degradation. The data obtained are described in the first chapter of the "Results" section and demonstrate the inhibitory role of Rif2 on MRX-dependent 5'-end resection at telomeres. These data have been published in PLoS Genetics (Bonetti D, Anbalagan S, Clerici M, Martina M, Lucchini G, Longhese MP *"Shelterin proteins and Yku inhibit nucleolytic processing of Saccharomyces cerevisiae telomeres"*, PLoS Genetics, 2009).

The MRX complex is also necessary to maintain telomere length by recruiting the Tel1 kinase and Rif2 was recently shown to interact with the C-terminus of the Xrs2 subunit of the MRX complex. As Tel1 also binds the same portion of Xrs2, Hirano and collegues proposed that Rif2 and Tel1 might compete with each other for binding to MRX (Hirano et al., 2009). Furthermore, MRX localization at telomeres is reduced in *tel1Δ* cells compared to wild-type cells (Hirano et al., 2009), raising the possibility that Tel1, after its MRX-dependent loading onto telomeric ends, can enhance MRX activity. As MRX is required to generate telomeric single-stranded DNA (ssDNA), this Tel1-dependent regulation of MRX might influence resection and elongation of telomeric ends. In this contest, during the second part of my PhD I investigated the physiological consequences of the Tel1-mediated feedback loop on MRX, as well as the role of Rif2 in counteracting Tel1/MRX function. To explore this issue, we took advantage of the *TEL1-hy909* mutant allele, previously identified to be a dominant suppressor of the hypersensitivity to genotoxic agents and checkpoint defects of Mec1-

deficient cells (Baldo et al., 2008). The data obtained by this analysis are described in the second chapter of the "Results" section and have been published in Molecular and Cellular Biology (Martina M, Clerici M, Baldo V, Bonetti D, Lucchini G, Longhese MP *"A balance between Tel1 and Rif2 activities regulates nucleolytic processing and elongation at telomeres"* **Molecular and Cellular Biology**, 2012).

Moreover, some of the data presented in this thesis are reported in the following review of which I am co-author:

Longhese MP, Anbalagan S, Martina M, Bonetti D *"The role of shelterin in maintaining telomere integrity"* **Frontiers in Biosciences**, 2012.

Results

PLOS GENETICS,
May 2010, Vol. 6, N°5: e1000966
doi:10.1371/journal.pgen.1000966

Shelterin-Like Proteins and Yku Inhibit Nucleolytic Processing of *Saccharomyces cerevisiae* Telomeres

Diego Bonetti, Michela Clerici, Savani Anbalagan, Marina Martina, Giovanna Lucchini, Maria Pia Longhese

Dipartimento di Biotecnologie e Bioscienze, Piazza della Scienza 2, Università di Milano-Bicocca, 20126 Milan, Italy.

Received 16 February 2010, **Accepted** 21 April 2010, **Published** 27 May 2010

Intrachromosomal double-strand breaks (DSBs) elicit a DNA damage response, which comprises DNA repair pathways and surveillance mechanisms called DNA damage checkpoints. By contrast, telomeres are by definition stable and inert natural ends of linear chromosomes, as they are protected from checkpoints, as well as from homologous recombination (HR) or end-to-end fusions that normally promote repair of intrachromosomal DSB (Longhese, 2008). Telomere basic structure is conserved among eukaryotes and consists of short tandem DNA repeats, which are G-rich in the strand containing the 3′ end (G-strand).

Although telomere ends are apparently shielded from being recognized as DSBs, they share important similarities with intrachromosomal DSBs. In fact, DSBs are resected to generate 3′-ended single-stranded DNA (ssDNA) tails, which channel their repair into HR. Similarly, the tips of

human, mouse, ciliate, yeast and plant telomeres terminate with 3′ overhangs due to the protrusion of the G-strand over its complementary C-strand. Furthermore, several proteins such as the MRX complex, Sae2, Sgs1, Exo1 and Dna2 are required for generation of ssDNA at both telomeres and intrachromosomal DSBs, with Sae2 and MRX belonging to the same pathway, while the helicase Sgs1 acts in conjunction with the nuclease Dna2 (Mimitou and Symington, 2008; Bonetti et al., 2009). Finally, both DSB and telomere resection is promoted by the activity of cyclin-dependent protein kinase Cdk1 (Ira et al., 2004; Vodenicharov and Wellinger, 2006), which phosphorylates Sae2 Ser267 (Bonetti et al., 2009).

It is well known that ssDNA accumulation at DSBs invokes an ATR/Mec1-dependent DNA damage response when it exceeds a certain threshold (Zierhut and Diffley, 2008). Noteworthy, the single-stranded G-tails of budding yeast telomeres are short (about 10–15 nucleotides) for most of the cell cycle, and their length increases transiently at the time of telomere replication in late S phase (Larrivée et al., 2004). As the nuclease requirements at DSBs and telomeres are similar (Bonetti et al., 2009), this finding suggests an inherent resistance of telomeric ends to exonuclease attack, which could contribute to avoid telomeres from being sensed as DNA damage. One report suggests that an elongating telomere formed at a TG-flanked DSB actually exerts an "anticheckpoint" effect on the non-TG-containing side of the break (Michelson et al., 2005), though the origin of this checkpoint attenuation has been questioned (Hirano and Sugimoto, 2007).

In budding yeast, telomere protection is achieved through single- and double-stranded DNA binding proteins. In particular, the heterodimeric

Yku complex (Yku70-Yku80) contributes to protect telomeres, as Yku lack causes shortened telomeres and Exo1-dependent accumulation of telomeric ssDNA (Gravel et al., 1998; Polotnianka et al., 1998; Maringele and Lydall, 2002; Bertuch and Lundblad, 2004), as well as checkpoint-mediated cell cycle arrest at elevated temperatures (Barnes and Rio, 1997; Maringele and Lydall, 2002; Bertuch and Lundblad, 2004). Furthermore, Cdc13 inactivation leads to C-rich strand degradation, with subsequent accumulation of long ssDNA regions that extend into non-telomeric sequences (Garvik et al., 1995; Nugent et al., 1996; Booth et al., 2001). Finally, the Rap1 protein, together with its interactors Rif1 and Rif2, binds telomeric double-stranded DNA repeats and inhibits both telomere fusions by non-homologous end joining (NHEJ) (Marcand et al., 2008) and telomerase-dependent telomere elongation (Hardy et al., 1992; Marcand et al., 1997). The Rap1 C-terminal domain is sufficient for interaction with Rif1 and Rif2 (Hardy et al., 1992; Moretti et al., 1994; Wotton and Shore, 1997) and is responsible for Rap1-mediated inhibition of both NHEJ and telomere elongation. In fact, deletion of Rap1 C-terminus causes both NHEJ-dependent telomeric fusions, due to the lack of Rif2 and Sir4 at telomeres (Marcand et al., 2008), and an increase in telomere length, which is similar to the one observed when both Rif1 and Rif2 are lacking (Wotton and Shore, 1997).

Proteins negatively regulating telomerase and NHEJ are found at telomeres also in other eukaryotes, such as fission yeast (Cooper et al., 1997) and mammals, where they form a complex called shelterin that functionally recapitulates the Rap1-Rif1-Rif2 complex (reviewed in de Lange, 2005).

Several studies address the consequences of telomere dysfunctions, while the mechanisms by which telomere protection is achieved remain to be determined. Here, we investigate this issue by analyzing the role of key telomeric proteins in protecting budding yeast telomeres from degradation. By using an inducible short telomere assay, we show that loss of Rif1 or Rif2, as well as deletion of Rap1 C-terminus, promotes C-rich strand degradation at an HO-derived telomere in G1 and enhances it in G2. The lack of Rap1 C-terminus or Rif2 shows the strongest effect at the induced short telomere and also causes ssDNA accumulation at native telomeres in cycling cells.

Moreover, Yku prevents telomere resection in G1 at both native and HO-induced telomeres independently of its role in NHEJ. Resection of the HO-induced telomere in G1-arrested *yku70Δ* cells is restricted to the DNA regions closest to the telomeric tips, likely due to the action of Rap1, Rif1 and Rif2, whose inactivation extends telomere processing in *yku70Δ* G1 cells. Finally, ssDNA generation at both native and HO-induced telomeres requires Exo1 in *yku70Δ* G1 cells, whereas it depends primarily on MRX in both *rap1ΔC and rif2Δ* cells, where recruitment of the MRX subunit Mre11 to the HO-induced telomere is enhanced.

Thus, while Yku protects telomeres from Exo1 action, the shelterin-like proteins prevent telomere degradation by inhibiting MRX loading onto telomeric ends.

Rap1, Rif1, and Rif2 inhibit 3′ single-stranded overhang generation at a *de novo* telomere in both G1 and G2

Nucleolytic degradation of telomeric ends is inhibited in G1, when Cdk1 (Cdc28/Clb in yeast) activity is low, whereas it occurs in G2/M cells, where Cdk1 activity is high (Frank et al., 2006; Vodenicharov and Wellinger, 2006). We investigated whether the shelterin-like proteins Rif1, Rif2 and Rap1 regulated 3′ overhang generation at *Saccharomyces cerevisiae* telomeres by examining the effects of their inactivation on telomeric ssDNA formation in both G1 and G2. We used an inducible short telomere assay (Figure 8A) (Diede and Gottschling, 2001; Michelson et al., 2005) that allows generation of a single short telomere without affecting the length of the other telomeres in the same cell. In this system, galactose-induced HO endonuclease generates a single DSB at an HO cleavage site adjacent to an 81-base pair TG repeat sequence that is inserted at the *ADH4* locus, 15 kb from the left telomere of chromosome VII (Figure 8A). After HO galactose-induction, the fragment distal to the break is lost, and, over time, the short telomeric "seed" sequence is elongated by telomerase (Diede and Gottschling, 2001; Michelson et al., 2005). Length changes of either the 5′ C-strand or the 3′ G-strand of the newly created HO-induced telomere can be followed by using two single-stranded riboprobes (probes A and B in Figure 8) that detect the 5′ C-strand or the 3′ G-strand, respectively, by hybridizing to a DNA region spanning 212 bp from the HO site (Figure 8A).

HO was induced by galactose addition in G1-arrested *rap1ΔC*, *rif1Δ* and *rif2Δ* cells (Figure 8B), the latter lacking the Rap1 C-terminus (residues

670–807) that is sufficient for both telomere length regulation and Rap1 interaction with Rif1 and Rif2 (Moretti et al., 1994; Wotton and Shore, 1997). When the 5′ C-strand was analyzed with its complementary probe A in EcoRV and RsaI double-digested genomic DNA (Figure 8C), the predicted EcoRV-HO band (166 bp; cut C-strand) corresponding to the 5′ C-rich strand of the HO-induced telomere was detected in all cell cultures about 2 hours after HO induction.

Consistent with the requirement of Cdk1 activity for telomere resection (Frank et al., 2006; Vodenicharov and Wellinger, 2006), the C-strand signal was stable in G1-arrested wild type cells (Figure 8C and 8D). By contrast, it progressively decreased in both *rap1ΔC and rif2Δ* G1-arrested cells (Figure 8C and 8D), indicating that C-strand resection in these two mutants had proceeded beyond the hybridization region. C-strand degradation at the HO-derived telomere occurred also in *rif1Δ* cells, although less efficiently than in *rap1ΔC* and *rif2Δ* cells (Figure 8C and 8D). The decrease of single-stranded 5′ C-strand signal in all these mutants was due to DNA degradation and not to elongation by the coordinated action of telomerase and lagging strand DNA synthesis, as we observed a similar decrease also in *rif1Δ*, *rap1ΔC and rif2Δ* G1 cells lacking the catalytic subunit of telomerase (data not shown).

The 3′ G-strand of the HO-induced telomere was analyzed in the same DNA samples by using the G-strand complementary probe B (Figure 8E and 8F). Because EcoRV and RsaI do not cleave ssDNA, the 166 nt EcoRV-HO 3′ G-strand fragment is converted into slower migrating r1 and r2 DNA fragments as 5′ to 3′ resection proceeds beyond the EcoRV up to the two RsaI restriction sites located 304 and 346 bp, respectively, from the HO cutting site (Figure 8A).

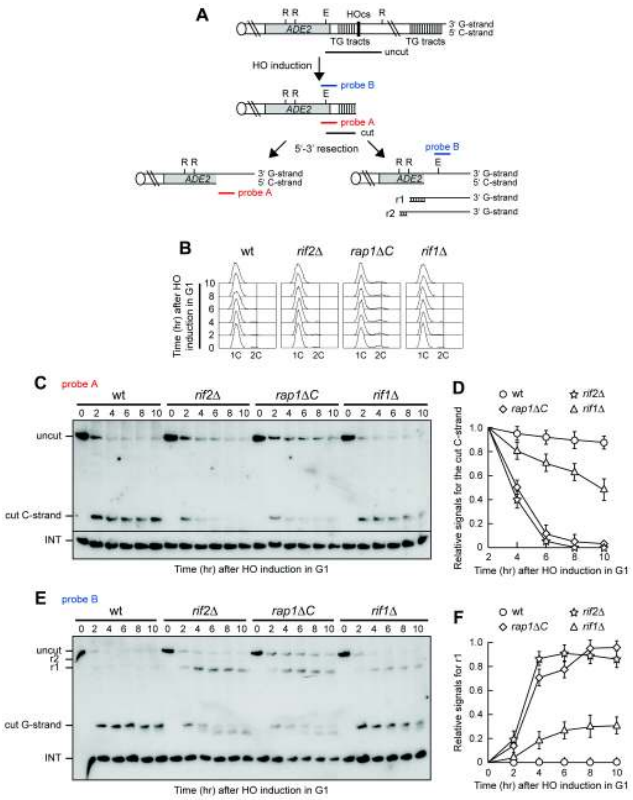

Figure 8: **A)** The HO-induced telomere system. Galactose-induced HO endonuclease generates a single DSB at an HO cleavage site (HOcs) adjacent to an 81-bp TG repeat sequence (TG tracts) that is inserted at the ADH4 locus on chromosome VII. RsaI- and EcoRV-digested genomic DNA was hybridized with two single-stranded riboprobes, which anneal to either the 5′ C-strand (probe A) or the 3′ G-strand (probe B) to a site located 212 bp from the HO cutting site. Both probes reveal an uncut 390 nt DNA fragment (uncut), which is converted by HO cleavage into a 166 nt fragment (cut) that can be detected by both probe A (5′ C-strand) and probe B (3′ G-strand). Degradation of the 5′ C-strand leads to disappearance of the probe A signal as resection proceeds beyond the hybridization region. Furthermore, it eliminates the cutting sites for the EcoRV (E) and RsaI (R) restriction enzymes, thus converting the 3′ cut G-strand into longer r1 (304 nt) and r2 (346 nt) DNA fragments detected by probe B. Both probes also detects a 138 nt fragment from the *ade2*-101 locus on Chr. XV (INT), which serves as internal loading control. **(B–F)** HO expression was induced at time zero by galactose addition to α-factor-arrested wild type (YLL2599) and otherwise isogenic *rif2Δ*, *rap1ΔC* and *rif1Δ* cell cultures that were then kept arrested in G1. **B)** FACS analysis of DNA content. **C)** RsaI- and EcoRV-digested genomic DNA was hybridized with probe A. Degradation of the 5′ C-strand leads to the disappearance of the 166 nt signal (cut C-strand) generated by this probe. **D)** Densitometric analysis. Plotted values are the mean value ±SD from three independent experiments as in (C). **E)** The same RsaI- and EcoRV-digested genomic DNA analyzed in (C) was hybridized with probe B. Degradation of the 5′ C-strand leads to the conversion of the 3′ cut G-strand 166 nt fragment into the slower migrating r1 DNA fragment described in (A). **F)** Densitometric analysis. Plotted values are the mean value ±SD from three independent experiments as in (E).

The amount of the predicted EcoRV-HO fragment (cut G-strand), which was constant in G1-arrested wild type cells, decreased over time in *rif1Δ*, *rap1ΔC* and *rif2Δ* cells that also showed r1 3′-ended resection products (Figure 8E and 8F), indicating that resection had proceeded beyond the EcoRV site towards the RsaI site located 304 bp from the HO cut. Again, the amount of the resection products was higher in *rap1ΔC* and *rif2Δ* cells than in *rif1Δ* cells (Figure 8E and 8F), indicating a stronger role for Rap1 and Rif2 in protecting telomeres from degradation in G1.

Consistent with previous observations (Diede and Gottschling, 2001), 3′ G-strand length of the HO-induced telomere decreased by ~10 nucleotides in both *rap1ΔC and rif2Δ* cells (Figure 8E).

This very limited G-strand degradation was not specifically caused by the lack of Rif2 or Rap1, as it was detectable after HO induction also in G2-arrested wild type cells undergoing telomere resection (Figure 9B). A similar phenomenon has been described at intrachromosomal DSBs, where both the 5′ and the 3′ strands disappear with time in wild type cells after HO cleavage, and the 5′ strand is processed faster than the 3′ strand (Zierhut and Diffley, 2008).

Telomere protection by the shelterin-like proteins occurred also outside G1, as shown by the analysis of 3′ single-stranded G-tail generation at the HO-induced telomere in G2-arrested *rif1Δ*, *rap1ΔC* and *rif2Δ* cells (Figure 9). As expected, r1 resection products were detectable in G2-arrested wild type cells, but their amount in these cells was significantly lower than in *rif2Δ*, *rap1ΔC* and *rif1Δ* cells (Figure 9B and 9C). Both *rap1ΔC and rif2Δ* G2 cells showed also some r2 resection products

(Figure 9B), indicating that they allowed resection to proceed beyond the first RsaI site. The ~10 nucleotides decrease in length of the 3′ G-strand occurring in G2-arrested wild type cells was not detectable in *rap1ΔC and rif2Δ* G2 cells (Figure 9B), likely because the 3′ G-strand in these two mutants was converted into longer r1 resection products much more efficiently than in wild type cells. Thus, Rif1, Rif2 and Rap1 inhibit degradation of the HO-induced telomere in both G1 and G2, with Rif2 and Rap1 playing the major role.

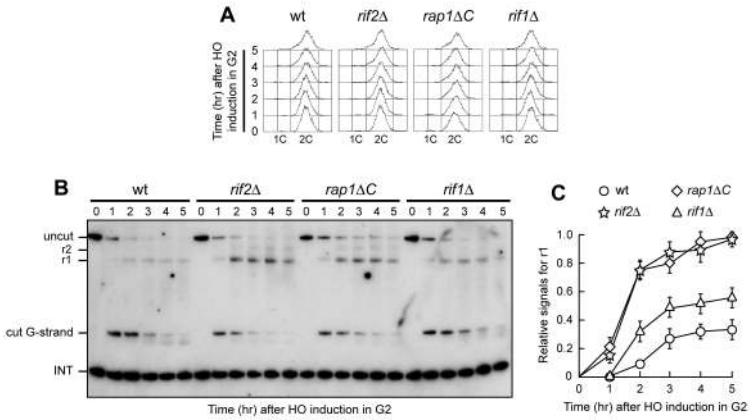

Figure 9: HO expression was induced at time zero by galactose addition to nocodazole-arrested wild type (YLL2599) and otherwise isogenic *rif2Δ*, *rap1ΔC* and *rif1Δ* cell cultures that were then kept arrested in G2. **A)** FACS analysis of DNA content. **B)** RsaI- and EcoRV-digested genomic DNA was hybridized with probe B as in Figure 8E. **C)** Densitometric analysis. Plotted values are the mean value ±SD from three independent experiments as in (B).

Yku inhibits 3′ single-stranded overhang generation at a *de novo* telomere in G1

Yku lack accelerates 5′-to-3′ nucleolytic degradation of intrachromosomal DSBs in yeast cells with low Cdk1 activity (Clerici et al., 2008). This effect is partially due to NHEJ defects that might increase

the time available to the resection machinery, as DSB processing is also increased in G1-arrested cells lacking the NHEJ DNA ligase IV (Dnl4/Lig4), although to a lesser extent than in *yku70Δ* cells (Clerici et al., 2008).

We investigated the possible role of Yku and/or Dnl4 in preventing telomere resection by analyzing the effect of their loss on the kinetics of 5′ C-strand degradation at the HO-induced telomere in both G1 and G2. We also evaluated how the lack of Yku and Dnl4 influenced 5′-strand degradation at an HO-induced DSB lacking the terminal TG repeats (Figure 10G) (Michelson et al., 2005), in order to highlight possible differences in the regulation of DNA degradation at DSBs versus telomeres. Similar to what was found at intrachromosomal DSBs (Michelson et al., 2005), Yku absence did not enhance processing of the HO-induced telomere in G2, as G2-arrested wild type and *yku70Δ* cells (Figure 10A) displayed very similar kinetics of 5′ C-strand degradation (Figure 10B and 10C). By contrast, the amount of 5′ C-strand of the HO-induced telomere decreased in G1-arrested *yku70Δ* cells, while it remained constant in both wild type and *dnl4Δ* cells under the same conditions (Figure 10D–10F). As expected (Michelson et al., 2005), the 5′-strand at the HO-induced DSB lacking the TG repeats (Figure 10G) was degraded much more efficiently in both G1-arrested *yku70Δ* and *dnl4Δ* cells than in wild type, with *yku70Δ* cells showing the strongest effect (Figure 10H–10L). Thus, Dnl4 does not block telomere resection in G1, whereas Yku does, indicating that the role of Yku in telomere protection is not related to its NHEJ function. This finding also highlights differences in the regulation of nucleolytic processing at DSBs versus telomeres.

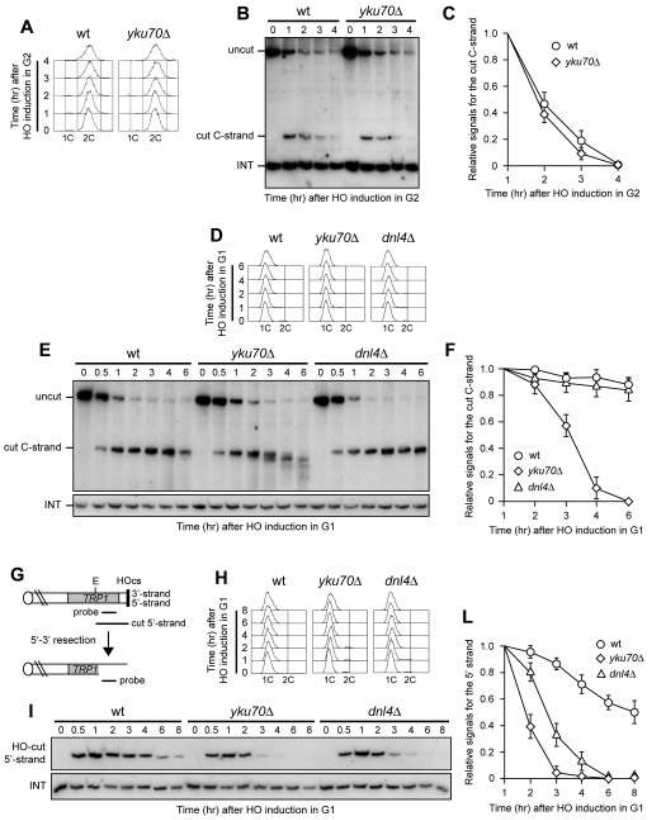

Figure 10: **(A–C)** HO expression was induced at time zero by galactose addition to nocodazole-arrested wild type (YLL2599) and otherwise isogenic *yku70Δ* cell cultures that were then kept arrested in G2. **A)** FACS analysis of DNA content. **B)** RsaI- and EcoRV-digested genomic DNA was hybridized with probe A as described in Figure 8C. **C)** Densitometric analysis. Plotted values are the mean value ±SD from three independent experiments as in (B). **(D–F)** HO expression was induced at time zero by galactose addition to α-factor-arrested wild type (YLL2599) and otherwise isogenic *yku70Δ* and *dnl4Δ*Cell cultures that were then kept arrested in G1. **D)** FACS analysis of DNA content. **E)** RsaI-digested genomic DNA was hybridized with the single-stranded riboprobe A described in Figure 8, which anneals to the 5′ C-strand and reveals an uncut 460 nt DNA fragment (uncut). After HO cleavage, this fragment is converted into a 304 nt fragment (cut) detected by the same probe (cut C-strand). **F)** Densitometric analysis. Plotted values are the mean value ±SD from three independent experiments as in (E). **G)** The system used to generate an HO-induced DSB. Hybridization of EcoRV-digested genomic DNA with a probe that anneals to the 5′ strand to a site located 215 nt from the HO cutting site reveals a 430 nt HO-cut 5′-strand fragment. Loss of the 5′ strand beyond the hybridization region leads to disappearance of the signal generated by the probe. **(H–L)** HO expression was induced at time zero by galactose addition to α-factor-arrested wild type (YLL2600) and otherwise isogenic *yku70Δ* and *dnl4Δ* cells, all carrying the system in (G). Cells were then kept arrested in G1. **H)** FACS analysis of DNA content. **I)** EcoRV-digested genomic DNA was hybridized with the probe indicated in (G). The INT band, corresponding to a chromosome IV sequence, serves as internal loading control. **L)** Densitometric analysis. Plotted values are the mean value ±SD from three independent experiments as in (I).

Rif1, Rif2, and Rap1 limit resection at a *de novo* telomere in *yku70Δ* G1 cells

Interestingly, G1-arrested *yku70Δ* cells converted the 5′ C-strand fragment of the HO-induced telomere into discrete smaller DNA fragments (Figure 10E), suggesting that C-strand degradation under these conditions is limited to the terminal part. In order to confirm this observation, we monitored the 3′ G-strand of the HO-induced telomere in *yku70Δ* cells. As shown in Figure 11A and 11B, the 3′ cut G-strand was not converted into the longer resection products r1 and r2 in G1-arrested *yku70Δ* cells. Therefore, exonucleolytic degradation did not proceed beyond the EcoRV site located 166 bp from the HO site.

Thus, other proteins might limit resection of the HO-induced telomere in G1 even in the absence of Yku70, and the shelterin-like proteins appear to exert this effect. In fact, 3′-ended r1 resection products were clearly detectable in G1-arrested *yku70Δ rif2Δ*, *yku70Δ rap1ΔC* and, although to a lesser extent, *yku70Δ rif1Δ* cells (Figure 11A and 11B). Furthermore, the smaller C-strand fragments that accumulated in G1-arrested *yku70Δ* cells were only slightly detectable in similarly treated *yku70Δ rif2Δ* (Figure 11C) and *yku70Δ rap1ΔC* cells (data not shown), indicating that 5′ C-strand degradation in these cells had proceeded beyond 166 bp from the HO site. Thus, Rap1, Rif2 and, to a lesser extent, Rif1 limit telomeric ssDNA generation in G1 cells lacking Yku.

Notably, although telomere resection in *yku70Δ* G1 cells was confined to the telomere tip, the 166 nt 5′ C-strand signal decreased faster in *yku70Δ* than in *rif2Δ* G1 cells (Figure 11C and 11D). Furthermore, the ~10 nucleotides decrease in length of the 3′ G-strand was more efficient

in *yku70Δ* than in *rif2Δ* G1-arrested cells (Figure 11E). Thus, more resection events are initiated at G1 telomeres in the absence of Yku than in the absence of Rif2. These findings, together with the observation that the shelterin-like proteins still inhibit extensive resection in Yku-lacking cells, suggest that Yku has a major role in preventing initiation of telomere processing, while the shelterin-like proteins are primarily responsible for limiting extensive resection. Accordingly, the concomitant lack of Yku70 and Rif2 showed additive effects on *de novo* telomere degradation in G1. In fact, both C-strand degradation (Figure 11C and 11D) and generation of r1 resection products (Figure 11E and 11F) occurred more efficiently in G1-arrested *yku70Δ rif2Δ* double mutant cells than in either *yku70Δ* or *rif2Δ* single mutants.

Similar to what we observed after inactivation of Rap1, Rif1 or Rif2 in G2 cells with functional Yku (Figure 9), r1 amounts were higher in *yku70Δ rif2Δ*, *yku70Δ rap1ΔC* and *yku70Δ rif1Δ* cells than in *yku70Δ* single mutant cells after galactose addition in G2 (Figure 11G and 11H), indicating that Rap1, Rif2 and Rif1 inactivation promotes telomere processing in G2 also in the absence of Yku70. The finding that the r1 resection products accumulated with similar kinetics in G2-arrested wild type (Figure 9C) and *yku70Δ* single mutant cells (Figure 11H) further confirms that Yku70 loss does not affect telomere resection in G2.

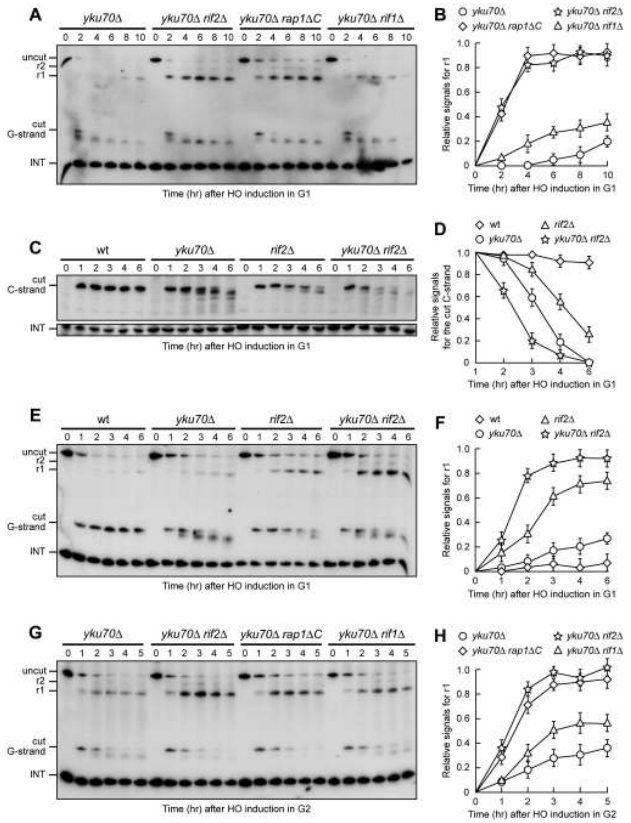

Figure 11: **(A–C)** HO expression was induced at time zero by galactose addition to nocodazole-arrested wild type (YLL2599) and otherwise isogenic *yku70Δ* cell cultures that were then kept arrested in G2. **A)** FACS analysis of DNA content. **B)** RsaI- and EcoRV-digested genomic DNA was hybridized with probe A as described in Figure 8C. **C)** Densitometric analysis. Plotted values are the mean value ±SD from three independent experiments as in (B). **(D–F)** HO expression was induced at time zero by galactose addition to α-factor-arrested wild type (YLL2599) and otherwise isogenic *yku70Δ* and *dnl4ΔC*ell cultures that were then kept arrested in G1. **D)** FACS analysis of DNA content. **E)** RsaI-digested genomic DNA was hybridized with the single-stranded riboprobe A described in Figure 8A, which anneals to the 5′ C-strand and reveals an uncut 460 nt DNA fragment (uncut). After HO cleavage, this fragment is converted into a 304 nt fragment (cut) detected by the same probe (cut C-strand). **F)** Densitometric analysis. Plotted values are the mean value ±SD from three independent experiments as in (E). **G)** The system used to generate an HO-induced DSB. Hybridization of EcoRV-digested genomic DNA with a probe that anneals to the 5′ strand to a site located 215 nt from the HO cutting site reveals a 430 nt HO-cut 5′-strand fragment. Loss of the 5′ strand beyond the hybridization region leads to disappearance of the signal generated by the probe. **(H–L)** HO expression was induced at time zero by galactose addition to α-factor-arrested wild type (YLL2600) and otherwise isogenic *yku70Δ* and *dnl4Δ* cells, all carrying the system in (G). Cells were then kept arrested in G1. **H)** FACS analysis of DNA content. **I)** EcoRV-digested genomic DNA was hybridized with the probe indicated in (G). The INT band, corresponding to a chromosome IV sequence, serves as internal loading control. **L)** Densitometric analysis. Plotted values are the mean value ±SD from three independent experiments as in (I).

Yku70, Rif2, and Rap1 inhibit G-strand overhang generation at native telomeres

The above findings prompted us to investigate whether the key role of Yku, Rif2 and Rap1 in preventing ssDNA generation at *de novo* telomeres could be extended to native telomeres. As Yku inhibits HO-induced telomere processing specifically in G1, we asked whether Yku70 loss could cause deprotection of native telomeres in G1 cells. To this end, we took advantage of previous data (Maringele and Lydall, 2002) showing that incubation at 37°C of *yku70Δ* cells causes checkpoint-dependent cell cycle arrest and accumulation of telomeric ssDNA as measured by ssDNA quantitative amplification (QAOS). Thus, we incubated G1-arrested wild type and *yku70Δ* cells at either 23°C or 37°C for 4 hours in the presence of α-factor (Figure 12B). Genomic DNA was then analyzed by non-denaturing in gel hybridization with a C-rich radiolabeled oligonucleotide detecting the G-rich single-stranded telomere overhangs (Dionne and Wellinger, 1996). As expected, no telomeric ssDNA signals were detectable in G1-arrested wild type cells at either 23°C or 37°C (Figure 12A). In contrast, single-stranded G-tail signals appeared in G1-arrested *yku70Δ* cells even at 23°C, and their intensity increased after incubation at 37°C (Figure 12A), thus highlighting an important role of Yku in protecting native telomeres in G1.

Also Rif2 and Rap1 turned out to inhibit exonucleolytic degradation at native telomeres (Figure 12C). Their role in this process was analyzed in cycling cells, because both proteins protect the HO-induced telomere from degradation in both G1 and G2 cells (Figure 8 and Figure 9). Single-

stranded G-tails were not detectable in wild type cycling cells, whereas they accumulated in both *rap1ΔC and rif2Δ* cells, which showed longer native telomeres than wild type, as expected (Figure 12C).

It is well known that a Mec1-dependent DNA damage response is invoked when accumulation of ssDNA at DSBs reaches a certain threshold (Zierhut and Diffley, 2008). We found that G1-arrested *yku70Δ* cells incubated at either 23°C or 37°C in the presence of α-factor did not show Rad53 electrophoretic mobility shifts that signal Mec1-dependent Rad53 phosphorylation and subsequent checkpoint activation (Figure 12D). Thus, Yku inactivation in G1 does not cause checkpoint activation. By contrast, and consistent with previous data (Maringele and Lydall, 2002), Rad53 phosphorylation was induced when exponentially growing *yku70Δ* cells were incubated at 37°C (Figure 12D).

We did not observe Rad53 phosphorylation even when G1-arrested *rap1ΔC and rif2Δ* cells were released into the cell cycle (Figure 12E), although they accumulated higher amounts of telomeric ssDNA at the HO-induced telomere than *yku70Δ* G1 cells. This lack of checkpoint activation might be due to either limited C-strand resection or general inability to phosphorylate Rad53. We then combined the *rif2Δ* allele with the temperature sensitive *cdc13-1* allele, which is well known to cause C-rich strand degradation and activation of the DNA damage checkpoint after incubation at 37°C (Garvik et al., 1995; Nugent et al., 1996; Booth et al., 2001)(Figure 12F).

When G1-arrested *cdc13-1 rif2Δ* cells were released into the cell cycle at 28°C (semi-permissive temperature for *cdc13-1*), they showed a higher amount of phosphorylated Rad53 than similarly treated *cdc13-1* single

mutant cells (Figure 12F). Thus, loss of Rif2 (and possibly of Rap1) enhances the checkpoint response in the presence of partially unprotected telomeres, suggesting that the amount of telomeric ssDNA formation caused by the lack of shelterin-like proteins does not reach the threshold level for the checkpoint response.

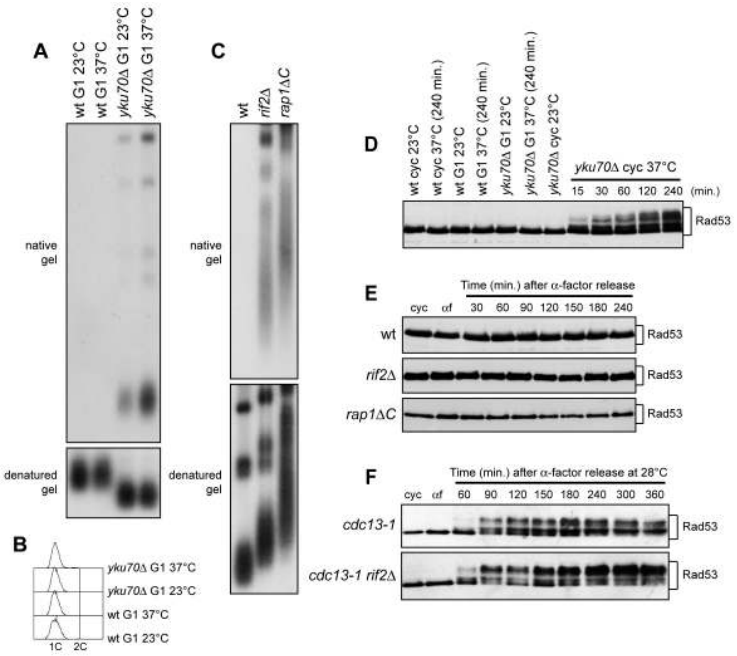

Figure 12: **A,B)** G1-arrested (G1) wild type (YLL2599) and otherwise isogenic *yku70Δ* cell cultures were incubated at either 23°C or 37°C for 4 hours in the presence of α-factor. **A)** Genomic DNA was digested with XhoI and single-stranded telomere overhangs were visualized by in-gel hybridization (native gel) using an end-labeled C-rich oligonucleotide (Dionne and Wellinger, 1996). The same DNA samples were separated on a 0.8% agarose gel, denatured and hybridized with the end-labeled C-rich oligonucleotide for loading and telomere length control (denatured gel). **B)** FACS analysis of DNA content. **C)** Genomic DNA prepared from wild type (YLL2599) and otherwise isogenic *rap1ΔC and rif2Δ* cell cultures, exponentially growing at 25°C, was digested with XhoI and the single-stranded telomere overhangs were visualized by in-gel hybridization as in (A). **D)** Wild type (YLL2599) and otherwise isogenic *yku70Δ* cell cultures exponentially growing (cyc) at 23°C were incubated at 37°C for the indicated time points. G1-arrested wild type and *yku70Δ* cells (G1) were incubated at either 23°C or 37°C for 4 hours. Rad53 was visualized at the indicated times by western analysis with anti-Rad53 antibodies. **E)** α-factor arrested wild type (YLL2599) and otherwise isogenic *rap1ΔC and rif2Δ* cell cultures were released into the cell cycle at 25°C. Rad53 was visualized as in (D). **F)** α-factor-arrested *cdc13-1* and *cdc13-1 rif2Δ* cells were released into the cell cycle at 28°C. Rad53 was visualized as in (D).

Different nucleases are required for telomeric ssDNA generation in the absence of Yku or shelterin-like proteins

As the *yku70Δ*, *rap1ΔC and rif2Δ* alleles increased ssDNA generation at native telomeres, we asked which nucleolytic activities were involved in this process. The nuclease Exo1 turned out to be required in both cycling and G1-arrested *yku70Δ* cells. In fact, ssDNA at native telomeres was undetectable in DNA samples prepared from either G1-arrested or exponentially growing *yku70Δ mre11Δ* double mutant cells incubated at 37°C for 4 hours (Figure 13A and 13B). Under the same conditions, MRE11 deletion only slightly suppressed accumulation of telomeric ssDNA in G1-arrested *yku70Δ* cells (Figure 13A), and did not significantly influence it in cycling *yku70Δ* cells (Figure 13B), indicating that ssDNA generation at native telomeres in the absence of Yku depends primarily on Exo1.

Mre11 was instead required at *rap1ΔC and rif2Δ* native telomeres to generate G-rich ssDNA, which was almost completely absent in both *rif2Δ mre11Δ* (Figure 13C) and *rap1ΔC mre11Δ* cycling cells (Figure 13D). By contrast, EXO1 deletion did not affect the same process in *rap1ΔC and rif2Δ* cycling cells (Figure 13C and 13D). Thus, native telomere nucleolytic degradation that is normally inhibited by Rif2 and Rap1 is mainly Mre11-dependent.

The absence of Mre11 leads to telomere shortening in *yku70Δ*, *rap1ΔC* and *rif2Δ* cells (Figure 13), likely because it prevents loading of the Tel1 kinase, which in turn allows recruitment of the Est1 telomerase subunit by phosphorylating Cdc13 (Bianchi et al., 2004; Goudsouzian et al., 2006; Tseng et al., 2006). In order to rule out possible artifacts caused

by telomere structure alterations, we analyzed the effects of the *mre11Δ* and *mre11Δ* alleles also at the newly created HO-induced telomere in G1 cells that cannot elongate this telomere due to the low Cdk1 activity.

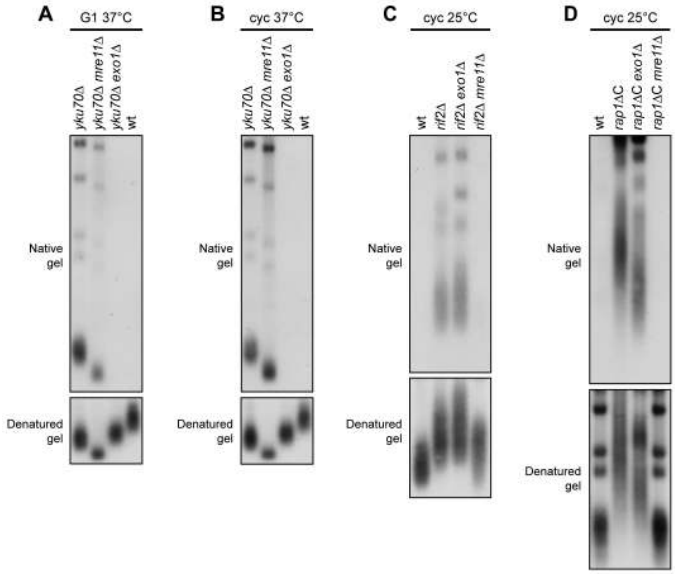

Figure 13: **A)** G1-arrested cells were incubated at 37°C for 4 hours in the presence of α-factor. Genomic DNA was analyzed as in Figure 12A. **B)** Exponentially growing cells were incubated at 37°C for 4 hours. Genomic DNA was analyzed as in Figure 12A. **C,D)** Genomic DNA prepared from exponentially growing cells at 25°C was analyzed as in Figure 12A.

Similar to what we observed at native telomeres, 5′ C-strand degradation in G1-arrested *yku70Δ* cells was abolished in the absence of Exo1, whereas it occurred in *yku70Δ mre11Δ* cells (Figure 14A–14C). Conversely, the lack of Exo1 did not affect 5′ C-strand degradation in G1-arrested *rif2Δ* cells, where degradation of the same strand was instead abolished in the absence of Mre11 (Figure 14D–14F). Unfortunately, we were unable to synchronize *rap1ΔC mre11Δ* and *rap1ΔC mre11Δ* cell cultures due to their growth defects (data not shown). Altogether, these data indicate that Exo1 is primarily responsible for telomeric DNA

degradation in the absence of Yku70, whereas the same process is mainly Mre11-dependent in *rap1ΔC* and *rif2Δ* cells, suggesting that Yku and shelterin-like proteins specifically prevent the action of different nucleases.

Rif2 and Rap1 inhibit Mre11 association at a *de novo* telomere in G1

Our data indicate that Mre11 plays a key role in telomeric ssDNA generation in the absence of Rif2 or Rap1, and Rif2 has been shown to regulate MRX recruitment at telomeres in cycling cells by inhibiting Tel1 association at telomeric ends (Hirano et al., 2009). We then monitored Mre11 recruitment at the HO-induced telomere in G1-arrested wild type, *rap1ΔC and rif2Δ* cells carrying a fully functional MYC-tagged MRE11 allele. Sheared chromatin from formaldehyde cross-linked cell samples taken at different time points after galactose addition was immunoprecipitated with anti-Myc antibodies. Quantitative real-time polymerase chain reaction (qPCR) was then used to monitor coimmunoprecipitation of a DNA fragment located 640 bp centromere-proximal to the HO site (TEL) and of a nontelomeric ARO1 fragment (CON). The TEL/CON ratio, which was used to measure Mre11 association with the HO-induced telomere, was much higher in both *rap1ΔC and rif2Δ* cells than in wild type (Figure 14G), indicating that Rif2 and Rap1 prevent Mre11 association at telomeric ends in G1. This finding, together with the observation that Mre11 is required to generate telomeric ssDNA in the absence of Rif2 or Rap1, suggests that Rif2 and Rap1 might inhibit telomere processing by preventing Mre11 binding.

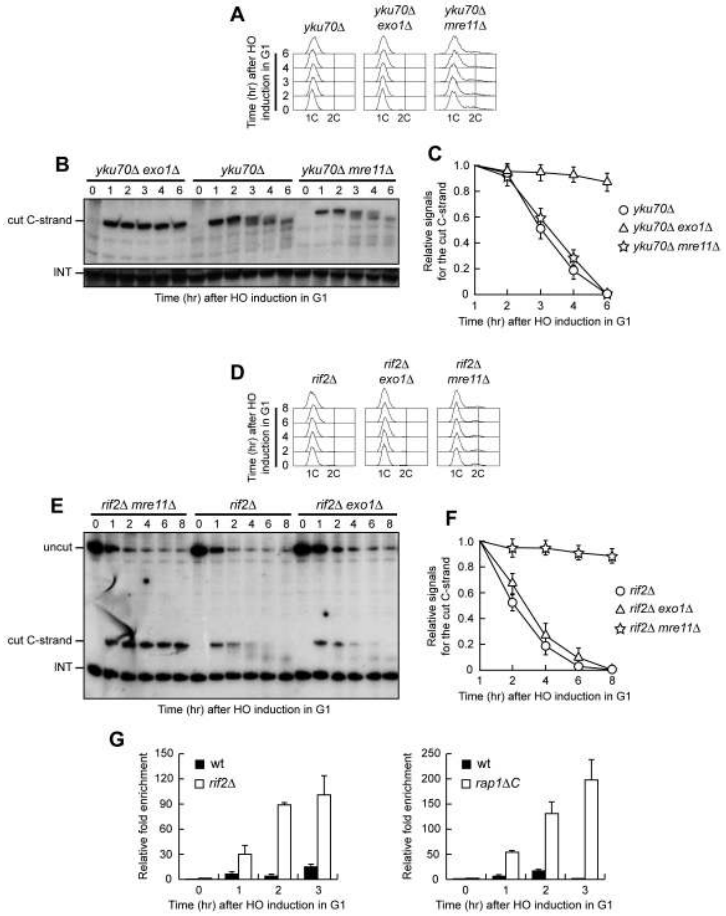

Figure 14: **(A–C)** HO expression was induced at time zero by galactose addition to α-factor-arrested *yku70Δ*, *yku70Δ mre11Δ* and *yku70Δ mre11Δ* cell cultures that were then kept arrested in G1. **A)** FACS analysis of DNA content. **B)** RsaI-digested genomic DNA was hybridized with probe A as in Figure 10E. **C)** Densitometric analysis. Plotted values are the mean value ±SD from three independent experiments as in (B). **(D–F)** HO expression was induced at time zero by galactose addition to α-factor-arrested *rif2Δ*, *rif2Δ mre11Δ* and *rif2Δ exo1Δ* cell cultures that were then kept arrested in G1. **D)** FACS analysis of DNA content. **E)** RsaI- and EcoRV-digested genomic DNA was hybridized with probe A as described in Figure 8C. **F)** Densitometric analysis. Plotted values are the mean value ±SD from three independent experiments as in (E). **G)** HO expression was induced at time zero by galactose addition to α-factor-arrested wild type, *rap1ΔC and rif2Δ* cells, all expressing a fully functional MRE11-MYC tagged allele. Cells were then kept arrested in G1 and chromatin samples taken at different times after HO induction were immunoprecipitated with anti-Myc antibody. Coimmunoprecipitated DNA was analyzed by quantitative real-time PCR (qPCR) using primer pairs located at the nontelomeric ARO1 fragment of chromosome IV (CON) and 640 bp proximal to the HO site (TEL), respectively. Data are expressed as relative fold enrichment of TEL over CON signal after normalization to input signals for each primer set. The data presented are the mean of those obtained in three independent experiments. Error bars indicate SD.

MOLECULAR AND CELLULAR BIOLOGY,
May 2012, pag. 1604-1617, Vol. 32, N°9
0270-7306/12/$12.00 doi: 10.1128/MCB.06547-11

A balance between Tel1 and Rif2 activities regulates nucleolytic processing and elongation at telomeres

Marina Marina, Michela Clerici, Veronica Baldo*, Diego Bonetti, Giovanna Lucchini, Maria Pia Longhese

Dipartimento di Biotecnologie e Bioscienze, Piazza della Scienza 2, Università di Milano-Bicocca, 20126 Milan, Italy.
*Present address: Ludwig Institute for Cancer Research, University of California, San Diego, La Jolla, California, USA

Received 8 November 2011, **Returned for modification** 13 December 2011, **Accepted** 10 February 2012

A highly ordered nucleoprotein complex called the telomere prevents the ends of linear chromosomes from being recognized as DNA double-strand breaks (DSBs) (reviewed in Longhese, 2008). Another key function of telomeres is to compensate for the incomplete replication of chromosome ends caused by discontinuous DNA synthesis. In most eukaryotes, telomeric DNA comprises tandemly repeated G-rich sequences (TG_{1-3} repeats in *Saccharomyces cerevisiae* yeast and T_2AG_3 in vertebrates), ending in a single-stranded 3' overhang (G tail) (reviewed in Goudsouzian et al., 2006). The addition of telomeric repeats depends

on the action of telomerase, a specialized reverse transcriptase that extends the TG-rich strand of chromosome ends (Greider and Blackburn, 1985). The yeast telomerase complex consists of a reverse transcriptase subunit (Est2), a template RNA (TLC1), and two accessory proteins (Est1 and Est3), which are required for telomerase activity *in vivo* but not *in vitro*.

The single-stranded G tails of budding yeast telomeres are short (about 10 to 15 nucleotides [nt]) for most of the cell cycle, but their length increases transiently to 50 to 100 nucleotides in late S phase (Wellinger et al., 1993; Dionne and Wellinger, 1996). While telomeric G tails can be generated during lagging-strand replication by removal of the last RNA primer, the 5' C-strand of the telomere generated by leading-strand synthesis must be nucleolytically processed (resected) to generate 3' overhangs (Wellinger et al., 1996; Makarov et al., 1997). Cyclin-dependent kinase (Cdk1 in *S. cerevisiae*) activity is required for this telomeric C-strand resection (Frank et al., 2006; Vodenicharov and Wellinger, 2006), which occurs only during S and G2 cell cycle phases, when Cdk1 activity is high and telomeres are elongated by telomerase (Marcand et al., 2000). The MRX (Mre11-Rad50-Xrs2) complex and Sae2 have been shown to be important for resection of telomeric ends, with MRX playing the major role (Diede and Gottschling, 2001; Larrivée et al., 2004; Bianchi and Shore, 2007; Longhese et al., 2010). Moreover, Exo1 and Sgs1-Dna2 can provide a backup mechanism for telomere resection when Sae2-MRX activity is compromised (Bonetti et al., 2009).

In the yeast *Saccharomyces cerevisiae*, telomerase lengthens telomeres only in late S/G2 phase (Marcand et al., 2000) Although chromatin immunoprecipitation (ChIP) studies have found that Est2 is associated

to telomeres from G1 to late S phase (Taggart et al., 2002), the use of live-cell imaging has shown that a subset of TLC1 molecules clusters and stably associates with telomeres only in late S phase (Gallardo et al., 2011). This clustering has been proposed to represent actively elongating telomeres (Gallardo et al., 2011), suggesting that regulation of telomerase activity is achieved at the level of its association with the telomere. In agreement with this hypothesis, budding yeast telomerase is preferentially enriched at short telomeres (Bianchi and Shore, 2007; Sabourin et al., 2007), which are its preferred substrate (Marcand et al., 1999; Teixeira et al., 2004).

Telomere length maintenance depends on the checkpoint kinase Tel1, whose localization to chromosome ends requires the MRX complex (Nakada et al., 2003). The function of Tel1 at telomeres relies on its kinase activity, since *tel1* kinase-dead cells have short telomeres like *tel1Δ* cells (Greenwell et al., 1995; Mallory and Petes, 2000). However, how Tel1 regulates telomere length is still unknown. Cells lacking Tel1 have a decreased frequency of telomerase-mediated telomere elongation (Arnerić and Lingner, 2007). Furthermore, Tel1 has been shown to specifically associate with short telomeres (Bianchi and Shore, 2007; Hector et al., 2007; Sabourin et al., 2007) and is needed for preferential binding of Est1 and Est2 to them (Goudsouzian et al., 2006). These findings suggest that length-dependent binding of Tel1 to telomeres is a critical step in the regulation of telomerase association with telomeres in S phase. In budding yeast, telomerase recruitment at telomeres relies on a direct interaction between Est1 and the telomere end-binding protein Cdc13 (Evans and Lundblad, 1999; Pennock et al., 2001; Bianchi et al., 2004; Chan et al., 2008). It has been proposed that

Tel1 promotes Est1-Cdc13 interaction by phosphorylating the telomerase recruitment do- main of Cdc13 (Tseng et al., 2006), although this model has recently been questioned (Gao et al., 2010). Tel1 is also important for increasing telomerase processivity at critically short telomeres (Chang et al., 2007). However, since the occurrence of critically short telomeres (~125 bp in length) should be relatively infrequent, the primary cause of the short *tel1Δ* telomeres has been proposed to be a reduced frequency of elongation by telomerase, rather than a reduced telomerase processivity (Chang et al., 2007).

The identity of *S. cerevisiae* telomeres also relies on a protein complex formed by the Rap1, Rif1, and Rif2 proteins, which inhibit telomerase-dependent telomere elongation (Conrad et al., 1990; Hardy et al., 1992; Wotton and Shore, 1997; Levy and Blackburn, 2004). Rif2 physically interacts with MRX *in vitro* (Hirano et al., 2009) and inhibits MRX-dependent 5'-end resection at telomeres (Bonetti et al., 2010a, 2010b). Furthermore, the lack of Rif2 enhances MRX and Tel1 association at telomeres (Hirano et al., 2009; Bonetti et al., 2010a), suggesting that Rif2 regulates nucleolytic processing of telomeres by inhibiting MRX recruitment. However, the artificial tethering of Rif2 at DNA ends leads to decreased Tel1 binding, but not MRX binding, to these ends (Hirano et al., 2009), indicating that Rif2 counteracts Tel1 association to DNA ends. This observation, together with the finding that MRX localization at telomeres is reduced in *tel1Δ* cells compared to wild-type cells (Hirano et al., 2009), raises the possibility that Tel1, after its MRX-dependent loading onto telomeric ends, can enhance MRX activity. As MRX is required to generate telomeric single-stranded DNA (ssDNA), this Tel1-dependent regulation of MRX might influence resection of

telomeric ends. Consistent with this hypothesis, loss of Tel1 in telomerase-negative cells attenuates the onset of senescence (Ritchie et al., 1999; Gao et al., 2010), whose primary signal has been proposed to be telomeric ssDNA (Abdallah et al., 2009).

To study the physiological consequences of the Tel1-mediated feedback loop on MRX, as well as the role of Rif2 in counteracting Tel1/MRX function, we took advantage of the *TEL1-hy909* mutant allele, previously identified to be a dominant suppressor of the hypersensitivity to genotoxic agents and checkpoint defects of Mec1-deficient cells (Baldo et al., 2008). Here we provide evidence that Tel1 regulates G-tail generation at telomeres by promoting MRX function. In fact, the lack of Tel1 impairs MRX-dependent generation of ssDNA at telomeres, whereas the Tel1-hy909 variant enhances both resection and elongation of telomeric ends. Moreover, Tel1-hy909 is more robustly associated to DSBs adjacent to telomeric tracts than wild-type Tel1 and also enhances MRX and Est1 binding at these DNA ends. These findings, together with the observation that *TEL1-hy909* telomeres escape the negative regulation exerted by Rif2 on both processing and elongation, indicate that Rif2-mediated inhibition of Tel1/MRX activity is important to regulate nucleolytic processing and elongation of telomeres.

Tel1-hy909 causes MRX- and telomerase-dependent telomere overelongation

In a screening for *TEL1* mutations that suppressed the hypersensitivity to genotoxic agents of *mec1Δ* cells, we previously identified 7 *TEL1-hy* alleles which can partially bypass the Mec1 requirement for checkpoint

activation (Baldo et al., 2008). Most of the Tel1-hy variants displayed enhanced kinase activity *in vitro* compared to wild-type Tel1, but only the Tel1-hy909 variant causes an impressive telomere elongation (Baldo et al., 2008) (Figure 15).

The overelongated telomere phenotype of *TEL1-hy909* cells is dominant and requires Tel1 kinase activity. In fact, *TEL1-hy909* heterozygous and homozygous diploid cells exhibited very similar telomere lengths (Figure 15A). Furthermore, cells expressing a Tel1-hy909 variant carrying the G2611D, D2612A, N2616K, and D2631E amino acid changes (Tel1-hy909kd in Figure 15B), which were shown to destroy Tel1 kinase activity (Mallory and Petes, 2000), had telomeres as short as those of *tel1Δ* cells (Figure 15B). These data further support previous findings that Tel1 acts as a kinase to maintain telomere length (Mallory and Petes, 2000).

The MRX complex is required to load Tel1 onto DNA ends (Nakada et al., 2003). MRX is properly assembled and binds DSBs in *xrs2-11* cells, which express truncated Xrs2 lacking the C-terminal 162 amino acids, but Tel1 binding to DSBs is compromised in the same cells (Nakada et al., 2003). As shown in Figure 15A, telomeres in *xrs2-11 TEL1-hy909* double mutant cells were as short as in *xrs2-11* single mutant cells, indicating that Tel1-hy909 action at telomeres does not bypass MRX requirement.

Telomere elongation is primarily accomplished by telomerase and occasionally by homologous recombination, but the latter does not seem to have a role in Tel1-hy909-induced telomere overelongation. In fact, the lack of the recombination protein Rad51 or Rad52 in *TEL1-hy909* cells did not modify telomere length (Figure 15C). We then assessed the

contribution of the telomerase enzyme to this *TEL1-hy909* phenotype by dissecting meiotic tetrads from a diploid strain heterozygous for the *est2Δ* and *TEL1- hy909* alleles. After 2 days of incubation at 25°C (approximately 25 generations), spore clones were streaked for successive times, and aliquots of cells from the indicated streaks were propagated in YEPD liquid medium for 5 h to prepare genomic DNA for telomere length analysis (Figure 15D). Telomeres underwent progressive shortening in *TEL1-hy909* est2*Δ* clones (Figure 15D), indicating that *TEL1-hy909*-dependent telomere overelongation requires telomerase activity.

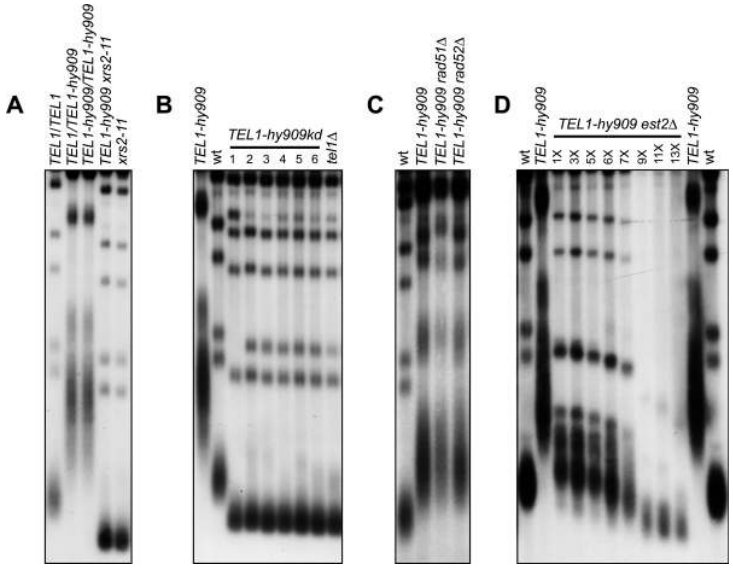

Figure 15: Telomere overelongation in *TEL1-hy909* cells. (A to C) XhoI-cut genomic DNA from exponentially growing cells (YEPD at 25°C) was subjected to Southern blot analysis using a radiolabeled poly(GT) telomere-specific probe. For panel **B)**, 6 independent *TEL1-hy909kd* transformant clones were analyzed (lanes 1 to 6). **D)** Meiotic tetrads from *EST2/est2Δ TEL1/TEL1-hy909* diploid cells were dissected on YEPD plates. After ~25 generations, *TEL1-hy909 est2Δ* spore clones were streaked for successive times (1 to 13 times) and aliquots of cells from the indicated streaks were propagated in YEPD liquid medium for 5 h to prepare genomic DNA for telomere length detection, as in panels A to C. Each subsequent streak represents ~25 generations of growth. wt, wild type.

The *tel1Δ* and *TEL1-hy909* mutations exert opposite effects on ssDNA generation at a DSB adjacent to telomeric repeat sequences

Because the absence of Tel1 attenuates the senescence phenotype of telomerase-negative cells, it was suggested that Tel1 has additional functions at telomeres besides directly affecting telomerase action (Ritchie et al., 1999; Gao et al., 2010). Tel1 recruitment at telomeres requires the MRX complex (Nakada et al., 2003), which is necessary to generate 3'-ended ssDNA at telomeric ends (Diede and Gottschling, 2001; Larrivée et al., 2004; Bonetti et al., 2009). MRX association to telomeres is decreased in *tel1Δ* cells (Hirano et al., 2009), suggesting that Tel1 may be involved in stimulating resection of the telomeric ends by promoting MRX activity. To assess whether Tel1 exerts a positive-feedback loop on MRX *in vivo*, we analyzed resection of telomeric ends in *tel1Δ* and *TEL1-hy909* cells. We used an assay initially developed to examine *de novo* telomere formation (Diede and Gottschling, 1999, 2001), where an 81-bp TG repeat sequence is placed immediately adjacent to an HO endonuclease cut site (Figure 16A). The strain carries this HO cleavage site inserted into the *ADH4* locus on chromosome VII and expresses the HO endonuclease gene from a galactose-inducible promoter. Upon cleavage by HO, the centromere-proximal TG side of the break is "healed" by telomerase and gives rise to a bona fide telomere (Diede and Gottschling, 1999, 2001). DNA degradation was assessed by Southern blotting under denaturing conditions, using a single-stranded riboprobe that recognizes the 5' C-strand (Figure 16A). Upon digestion of genomic DNA with EcoRV and RsaI restriction enzymes, the probe reveals an uncut 390-nt DNA fragment (uncut), which is converted by

HO cleavage into a 166-nt fragment (cut C-strand) (Figure 16A). Degradation of the 5' C-strand leads to disappearance of the probe signal when resection proceeds beyond the hybridization region.

As generation of ssDNA at telomeres occurs during S and G2/M cell cycle phases, when Cdk1 activity is high (Frank et al., 2006; Vodenicharov and Wellinger, 2006), we monitored 5'-3' resection of the TG DSB end by inducing HO expression in *tel1Δ*, *TEL1-hy909*, and *mre11Δ* cells that were kept arrested in G2 with nocodazole (Figure 16B). Degradation of the band corresponding to the cut 5' C-strand (cut C-strand) occurred more slowly in G2-arrested *tel1Δ* cells than in wild type, and it was completely abolished, as expected (Diede and Gottschling, 2001; Larrivée et al., 2004), in G2-arrested *mre11Δ* cells (Figure 16C and D). In contrast, 5' C-strand degradation was more efficient in *TEL1-hy909* cells than in wild type (Figure 16C and D). Thus, the lack of Tel1 impairs resection at DSB ends adjacent to telomeric DNA, while Tel1-hy909 increases its efficiency. These observations, together with the notion that 5' C-strand degradation in G2-arrested cells requires the MRX complex (Figure 16C and D) (Diede and Gottschling, 2001; Larrivée et al., 2004), indicate that Tel1 influences 5'-3' nucleolytic processing of these DNA ends by promoting MRX activity. Interestingly, MRX function is not completely abrogated by the lack of Tel1, as 5' C-strand degradation in *tel1Δ* cells was reduced but not completely abolished as it was in *mre11Δ* cells (Figure 16C and D).

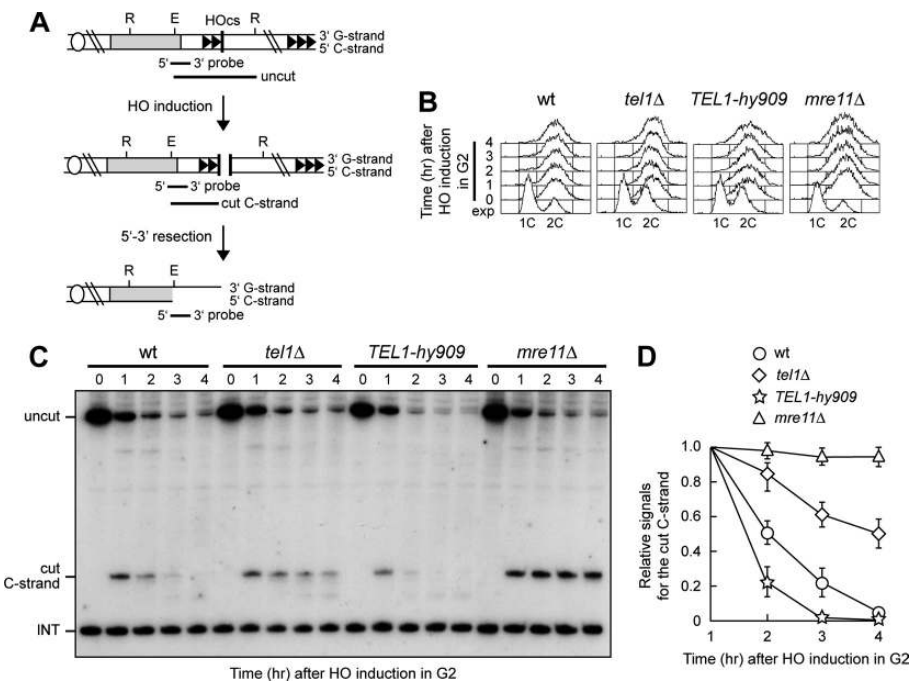

Figure 16: Effects of the *tel1Δ* and *TEL1-hy909* mutations on ssDNA generation at a DSB end carrying telomeric repeats. A) Schematic representation of the HO cleavage site (HOcs) with the TG repeat sequences (81 bp; two arrowheads) that were placed centromere proximal to the HO site at the *ADH4* locus on chromosome VII-L. The centromere is shown as a circle on the left. The probe used to monitor nucleolytic degradation of the 5' C-strand is also indicated. R, RsaI; E, EcoRV. **(B to D)** HO expression was induced at time zero by galactose addition to nocodazole-arrested cell cultures that were kept arrested in G2. **B)** Fluorescence-activated cell sorter analysis of DNA content. exp, exponentially growing cells. **C)** RsaI- and EcoRV-digested genomic DNA was hybridized with a single-stranded riboprobe that anneals to the 5' C-strand to a site located 212 bp from the HO cutting site. The probe reveals an uncut 390-nt DNA fragment (uncut), which is converted by HO cleavage into a 166-nt fragment (cut C-strand). Degradation of the 5' C-strand leads to disappearance of the probe signal as resection proceeds beyond the hybridization region. The probe also detects a 138-nt fragment from the *ade2-101* locus on chromosome XV (INT), which serves as internal loading control. **D)** Densitometric analysis. Plotted values are means ±SDs from three independent experiments, as in panel C.

The Tel1-hy909 variant might enhance nucleolytic processing at telomeres by hyperactivating the MRX complex. As nucleolytic degradation at telomeres requires Cdk1 activity (Frank et al., 2006; Vodenicharov and Wellinger, 2006), which is thought to activate the MRX-dependent resection machinery (Bonetti et al., 2010a, 2010b), we

asked whether the Tel1-hy909 variant bypasses Cdk1 requirement for resection of a DSB adjacent to telomeric repeat sequences.

To this end, the HO cut was induced in G1-arrested wild-type and *TEL1-hy909* cells (Figure 17A) carrying the system described in Figure 16A. Consistent with the requirement of Cdk1 activity for DNA end resection, the 5' C-rich strand signal was stable in G1-arrested wild-type cells (Figure 17B and C). In contrast, it progressively decreased in G1-arrested *TEL1-hy909* cells (Figure 17B and C), indicating that the *TEL1-hy909* mutation allows Cdk1-independent nucleolytic processing of a DSB end with telomeric repeats. This ability of Tel1-hy909 to bypass Cdk1 requirement for resection depends on Tel1 kinase activity, as 5' C-strand degradation was prevented in G1-arrested *TEL1-hy909kd* cells (Figure 17A to C). Furthermore, this Tel1-hy909-dependent resection specifically requires MRX, because it was abolished in G1-arrested *TEL1-hy909 mre11Δ* cells, whereas it took place in *TEL1-hy909* cells lacking the Exo1 nuclease (Figure 17D and E). As Cdk1 has been proposed to induce DSB resection by increasing the efficiency of the MRX- dependent resection machinery (Bonetti et al., 2010a, 2010b), these data are consistent with the hypothesis that Tel1-hy909 hyperactivates MRX.

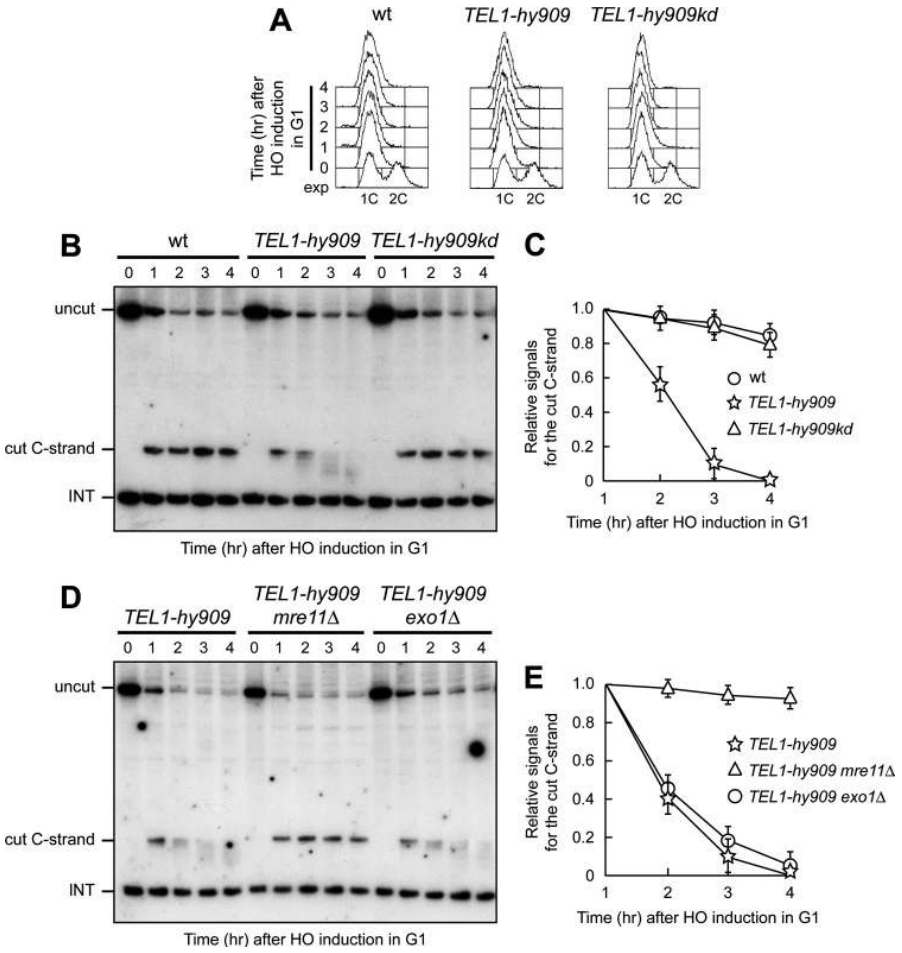

Figure 17: Tel1-hy909 allows resection in G1 of a DSB adjacent to telomeric repeats. (A to C) HO expression was induced at time zero by galactose addition to α-factor-arrested cells, all carrying the system described in Figure 16A. Cells were kept arrested in G1. **A)** Fluorescence-activated cell sorter analysis of DNA content. **B)** RsaI- and EcoRV-digested genomic DNA was analyzed as described in the legend to Figure 16C. **C)** Densitometric analysis. Plotted values are means ± SDs from three independent experiments, as in panel B. **(D and E)** HO expression was induced at time zero by galactose addition to α-factor-arrested cells that were kept arrested in G1. Cell cycle arrest was verified by fluorescence-activated cell sorter analysis (data not shown). **D)** RsaI- and EcoRV-digested genomic DNA was analyzed as described in the legend to Figure 16C. **E)** Densitometric analysis. Plotted values are means ± SDs from three independent experiments, as in panel D.

Tel1-hy909 does not bypass Cdk1 requirement to generate ssDNA at DSB ends lacking telomeric repeats.

We have previously shown that Tel1-hy909 increases ssDNA generation at intrachromosomal DSBs in G2-arrested cells (Baldo et al., 2008). Thus, we asked whether the Tel1-hy909 variant could bypass Cdk1 requirement for ssDNA generation at an HO-induced DSB devoid of telomeric repeats, as it does when the DSB is adjacent to telomeric tracts (Figure 17). HO expression was induced in G1-arrested wild-type and *TEL1-hy909* cell cultures that carried an HO cut site with no TG repeats (Figure 18A) and that were kept arrested in G1 with α-factor (Figure 18B). In contrast to what happens at a DSB end carrying telomeric repeats, whose resection was completely abolished in G1 (Figure 17B and C), a degradation of the 5' DSB end with no TG repeats still occurred in G1-arrested wild-type cells (Figure 18C and D), although it was less efficient than that detected at the same DSB in G2 (data not shown) (Ira et al., 2004). On the other hand, *TEL1-hy909* G1 cells showed a behavior very similar to that of wild type (Figure 18C and D), indicating that Tel1-hy909 does not promote Cdk1-independent 5'-3' nucleolytic processing at DSB ends that do not carry telomeric DNA sequences. This hypothesis was further confirmed by the observation that both wild-type and *TEL1-hy909* G1 cells generated very similar small amounts of 3'-ended single-stranded resection products at an irreparable HO-induced DSB generated at the *MAT* locus (see Table 1). Thus, we can conclude that Tel1-hy909 in G1 exerts its action preferentially at DNA ends adjacent to telomeric repeats.

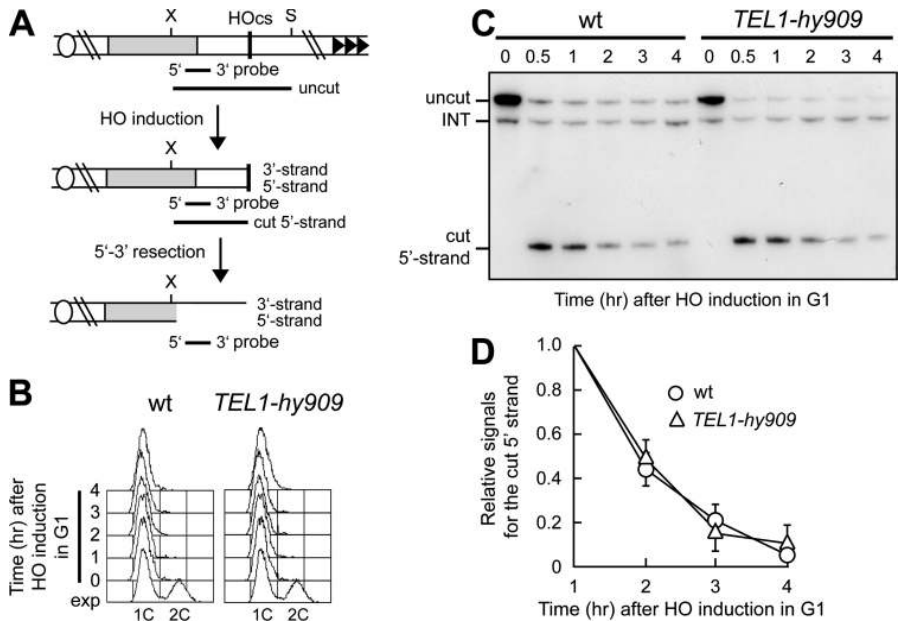

Figure 18: Tel1-hy909 does not enhance nucleolytic processing in G1 of a DSB with no telomeric repeats. A) Schematic representation of the system used to generate the HO-induced DSB on chromosome VII. SspI- and XbaI-digested genomic DNA is hybridized with the indicated single-stranded probe that anneals to the 5' strand to a site located 248 nt from the HO cutting site, revealing an uncut 897-nt DNA fragment (uncut), which is converted by HO cleavage into a 286-nt fragment (cut 5' strand). Loss of the 5' strand beyond the hybridization region of the probe leads to disappearance of the signal generated by the probe. S, SspI; X, XbaI. **(B to D)** HO expression was induced at time zero by galactose addition to α-factor-arrested wild-type and *TEL1-hy909* cells, all carrying the system depicted in panel A. Cells were kept arrested in G1. **B)** Fluorescence-activated cell sorter analysis of DNA content. **C)** SspI- and XbaI-digested genomic DNA was hybridized with the probe described in panel A. **D)** Densitometric analysis. Plotted values are means ± SDs from four independent experiments, as in panel C.

The *tel1Δ* and *TEL1-hy909* mutations exert opposite effects at native telomeres

The above-described findings prompted us to investigate whether the role of Tel1 in promoting ssDNA generation at DSB ends carrying TG repeats could be extended to native telomeres. To assess the presence of ssDNA at natural chromosome ends, genomic DNA prepared from exponentially growing cells was analyzed by nondenaturing in-gel

hybridization with a C-rich radiolabeled oligonucleotide that detect the G-rich single- stranded telomere overhangs (Dionne and Wellinger, 1996). Because *tel1Δ* telomeres have fewer TG sequences than wild-type telomeres, the TG-ssDNA signals were normalized to the total amount of TG repeats revealed by the same probe after denaturation of the gel. Consistent with a role of Tel1 in promoting single-stranded overhang generation also at native chromosome ends, the amount of ssDNA was lower at *tel1Δ* telomeres than at wild-type telomeres (Figure 19A and B). As previously observed (Diede and Gottschling, 2001; Larrivée et al., 2004), *mre11Δ* telomeres also displayed a reduced amount of telomeric ssDNA compared to wild type (Figure 19A and B). However, similar to what happens at the DSB ends carrying telomeric repeats (Figure 16C and D), the single-stranded G-tail signal was lower in *mre11Δ* than in *tel1Δ* cells (Figure 19A and B), indicating that MRX activity at telomeres is not completely abolished by the lack of Tel1.

The same analysis showed a stronger intensity of the G-tail signal in exponentially growing *TEL1-hy909* cells than in wild- type cells (Figure 19A and B). The ssDNA formation at *TEL1-hy909* telomeres depends on the MRX complex, as the lack of Mre11 reduced the amount of the G-tail signal in *TEL1-hy909* cells to the level observed in *mre11Δ* cells (Figure 19A and B). Furthermore, the strong ssDNA signal at *TEL1-hy909* telomeres was due to resection rather than to telomerase action, because similar amounts of telomeric ssDNA were detected during successive streaks of *TEL1- hy909* cells that shortened telomeres due to the absence of the telomerase subunit Est2 (Figure 19C and D).

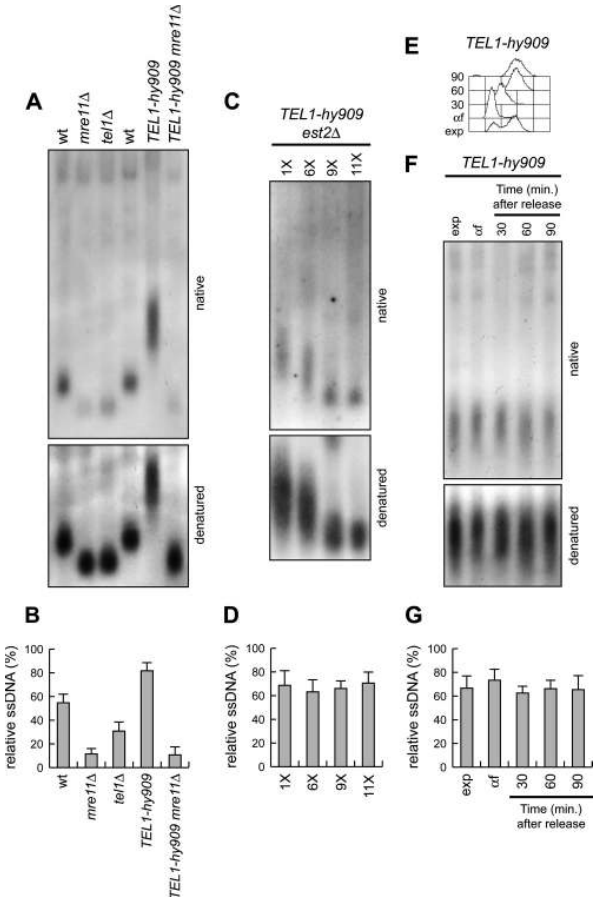

Figure 19: Effects of *tel1Δ* and *TEL1-hy909* alleles on ssDNA formation at native telomeres. A) Genomic DNA prepared from exponentially growing cells was digested with XhoI, and single-stranded G tails were visualized by in-gel hybridization (native) using an end-labeled C-rich oligonucleotide as a probe. The gel was then denatured and hybridized again with the same probe for loading control (denatured). **B)** The amount of native TG-ssDNA, as in panel A, was normalized to the total amount of TG sequences detected in each denatured sample. **(C and D)** Meiotic tetrads from *EST2/est2Δ TEL1/tel1-hy909* diploid cells were dissected on YEPD plates. **C)** After ~25 generations, *TEL1-hy909 est2Δ* spore clones were streaked for successive times (1 to 11 times), and aliquots of cells from the indicated streaks were propagated in YEPD liquid medium for 5 h to prepare genomic DNA for telomeric ssDNA detection, as in panel A. **D)** The amount of native TG-ssDNA, as in panel C, was normalized to the total amount of TG sequences detected in each denatured sample. **(E to G)** Exponentially growing (exp) *TEL1-hy909* cells were arrested in G1 with α-factor (αf) and released into the cell cycle. **E)** Fluorescence-activated cell sorter analysis of DNA content. **F)** Genomic DNA prepared at the indicated time points after release from the α-factor block was analyzed for telomeric ssDNA detection, as in panel A. **G)** The amount of native TG-ssDNA, as in panel F, was normalized to the total amount of TG sequences detected in each denatured sample. Plotted values in panels B, D, and G are means ± SDs from three independent experiments.

The Tel1-hy909 variant allows resection of a DSB end with telomeric repeats even in G1 (Figure 17), and this property is extended to native telomeres. In fact, when *TEL1-hy909* cells were arrested in G1 with α-factor and released into the cell cycle (Figure 19E), the intensity of the telomeric ssDNA signal in G1-arrested cells was similar to that observed both during exponential growth and at different times after release (Figure 19F and G). Thus, the Tel1-hy909 variant appears to bypass Cdk1 requirement for ssDNA generation even at native telomeres. Because ssDNA at telomeres has been proposed to signal the onset of senescence (Abdallah et al., 2009), we could expect differences in the decline of growth of *est2Δ* versus *est2Δ TEL1-hy909* cells. Meiotic tetrads were dissected from a diploid strain heterozygous for both *est2Δ* and *TEL1-hy909*. After incubation for 2 days at 25°C (approx. 25 generations), spore clones were streaked for successive times (Figure 20A) and an aliquot of cells from each streak was propagated in YEPD liquid medium for 5 h to prepare genomic DNA for telomere length analysis (Figure 20B). As the *TEL1-hy909* allele also causes telomere overelongation under heterozygous conditions (Figure 15A), *est2Δ* and *est2Δ TEL1-hy909* spores started with similar very long telomeres, which shortened during the subsequent subculturings (Figure 20B). Consistent with the enhanced resection promoted by Tel1-hy909, the telomeres shortened slightly faster in *est2Δ TEL1-hy909* than in *est2Δ* cells (Figure 20B). Furthermore, *TEL1-hy909 est2Δ* cells showed a senescent phenotype at the 5th passage, whereas *est2Δ* cells lost viability only at the 11th subculturing (Figure 20A), indicating that Tel1-hy909 accelerates the onset of senescence in telomerase-negative cells. If ssDNA is the primary signal triggering senescence, as proposed

(Abdallah et al., 2009), these data suggest that the increased amount of ssDNA in *TEL1-hy909 est2Δ* compared to *est2Δ* cells might explain the accelerated senescence phenotype of the *TEL1-hy909 est2Δ* cells.

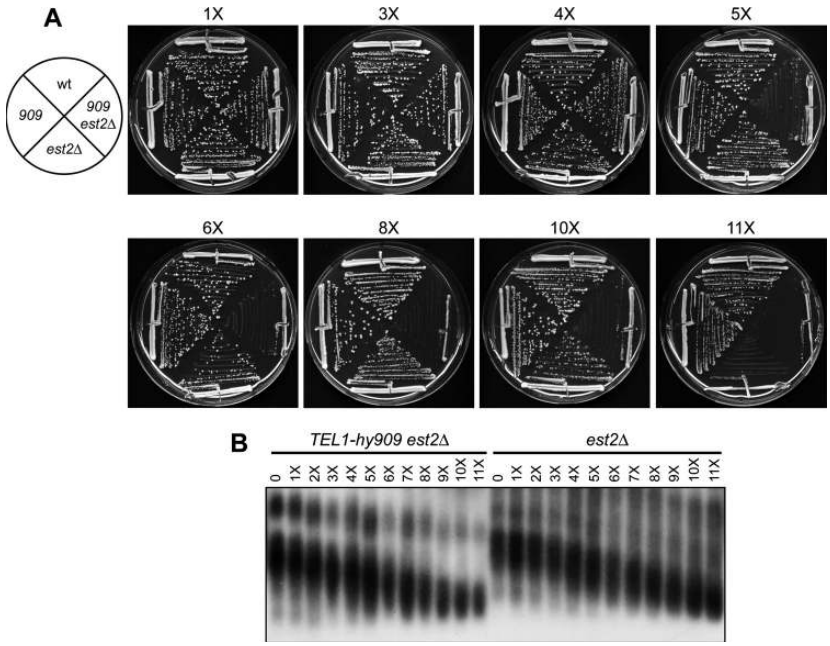

Figure 18: The *TEL1-hy909* mutation accelerates the onset of senescence in *est2Δ* cells. Meiotic tetrads from an *EST2/est2Δ TEL1/tel1-hy909* diploid strain were dissected on YEPD plates. **A)** After ~25 generations, spore clones from 15 tetrads were streaked for successive times (1 to 11 times). **B)** An aliquot of cells from the indicated streaks was propagated in YEPD liquid medium for 5 h to prepare genomic DNA for telomere length determination by Southern blot analysis. All tetratype tetrads behaved as the one shown in panel A.

TEL1-hy909 telomeres escape Rif2-mediated inhibition of nucleolytic processing and elongation

Rif2 inhibits MRX-dependent ssDNA generation at telomeres during both G1 and G2 cell cycle phases (Bonetti et al., 2010a, 2010b). Since Rif2 has been proposed to compete with Tel1 for binding to MRX

(Hirano et al., 2009), the Tel1-hy909 variant might bypass the Rif2-mediated negative regulation of MRX activity. To address this possibility, we compared resection of the DSB adjacent to telomeric repeats in *TEL1-hy909*, *rif2Δ*, and *rif2Δ TEL1- hy909* cells. We found that the 5' C-strand at the TG side of the HO cut was degraded with very similar kinetics in G1-arrested *TEL1- hy909*, *rif2Δ*, and *rif2Δ TEL1-hy909* cells (Figure 21A and B). Similar results were also obtained when degradation of the 5' C-strand was analyzed in the same strains arrested in G2 (data not shown). Thus, nucleolytic degradation at *TEL1-hy909* telomeres is not sensitive to the inhibitory activity of Rif2, indicating that the increased resection of *TEL1-hy909* telomeres likely reflects failure of Rif2 to negatively regulate their processing.

As Rif2 inhibits telomerase-dependent telomere elongation (Wotton and Shore, 1997; Levy and Blackburn, 2004), we investigated whether Tel1-hy909 also overcomes this Rif2-mediated negative regulation of telomere length. We first used the system described in Figure 16A to analyze the effect of a lack of Rif2 on the kinetics of telomere addition at the DSB end carrying TG sequences in *TEL1-hy909* cells. As a control, we also analyzed the same process in otherwise isogenic *TEL1-hy909* cells lacking Rif1, which negatively regulates telomere length by acting in a pathway different from that involving Rif2 (Wotton and Shore, 1997; Levy and Blackburn, 2004). When the HO cut was induced in exponentially growing cells, *rif2Δ* cells elongated the TG DSB end more efficiently than wild-type cells under the same conditions (Figure 21C), as expected.

Sequence addition to this DSB side was also enhanced in *TEL1-hy909* cells (Figure 21C), indicating that the Tel1-hy909 variant also increases

the efficiency of telomere elongation in this assay. Interestingly, telomere addition took place with very similar efficiency in *TEL1-hy909 rif2Δ* double mutant cells and in *rif2Δ* or *TEL1-hy909* single mutants (Figure 21C), indicating that *TEL1-hy909* telomere length escapes the Rif2-dependent negative control. Differently from Rif2, Rif1 still acts as a negative regulator of telomere length in *TEL1- hy909* cells. In fact, sequence addition to the telomeric DSB side was enhanced in *TEL1-hy909 rif1Δ* double mutant cells compared to both *TEL1-hy909* and *rif1Δ* single mutants (Figure 21D), although *RIF1* deletion had a more modest effect than *RIF2* deletion in allowing telomere addition (Figure 21D) (Hirano et al., 2009; McGee et al., 2010).

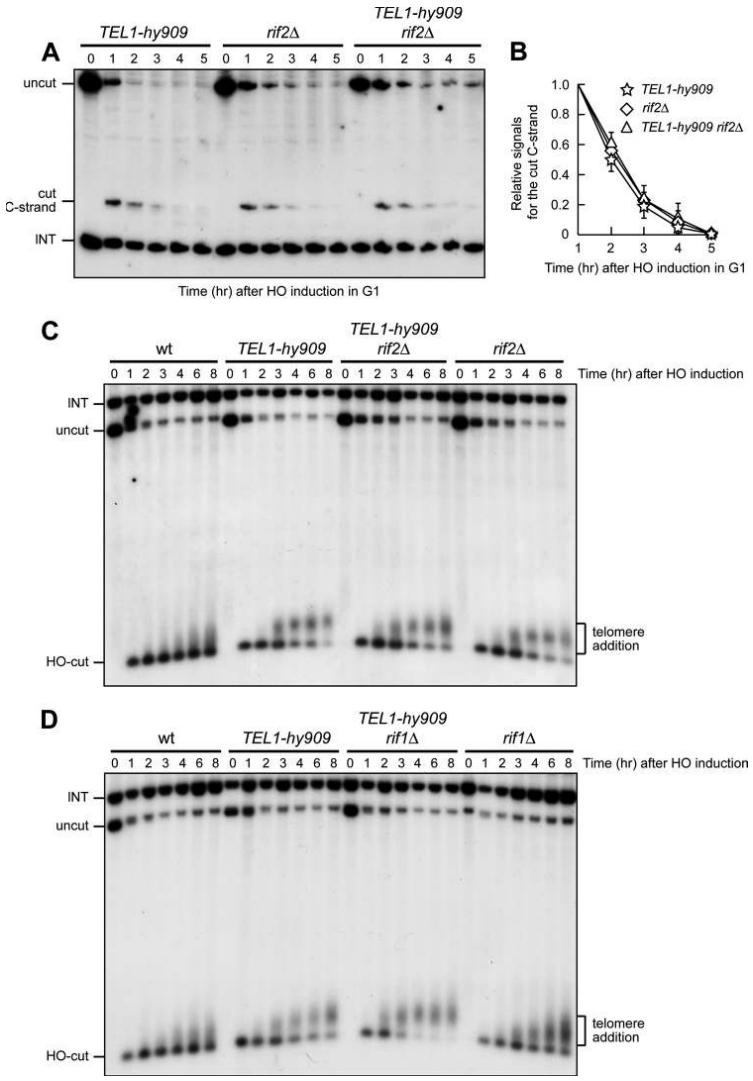

Figure 21: Processing and elongation of a DSB end carrying TG tracts in *TEL1-hy909* cells are not affected by *RIF2* deletion. (A and B) HO expression was induced at time zero by galactose addition to α-factor-arrested cells, all carrying the system described in Figure 16A. Cells were kept arrested in G1, and cell cycle arrest was verified by fluorescence-activated cell sorter analysis (data not shown). **A)** RsaI- and EcoRV-digested genomic DNA was analyzed as described in the legend to Figure 16C. **B)** Densitometric analysis. Plotted values are means ± SDs from three independent experiments, as in panel A. **(C and D)** HO expression was induced at time zero by galactose addition to exponentially growing cells. AvaI- and NdeI-digested genomic DNA was subjected to Southern blot analysis using a *TRP1* probe, which reveals the ~800-bp AvaI-HO fragment exposing the TG repeats, whose length progressively increases as new telomere repeats are added. A bracket points out new telomere repeats added to the exposed TG-HO sequence.

We then analyzed the epistatic relationships between *TEL1- hy909*, *rif2Δ*, and *rif1Δ* alleles in the control of native telomere length. Diploid strains heterozygous for *TEL1-hy909* and either *rif1Δ* or *rif2Δ* were sporulated, and the resulting tetrads were dissected. Because mutations affecting telomere length often exhibit a phenotypic lag, we examined telomere lengths by Southern blot analysis of genomic DNA prepared from subcultures of the haploid clones derived from the spores. Telomeres of *TEL1-hy909 rif1Δ* double mutant cells were longer than those of both *TEL1- hy909* and *rif1Δ* single mutants (Figure 22), whereas *RIF2* deletion did not cause further telomere lengthening in *TEL1-hy909* cells (Figure 22). Thus, while Rif1 still negatively controls the length of native telomeres in *TEL1-hy909* cells, the same cells also escape the Rif2- mediated negative regulation at native telomeres. Interestingly, *TEL1-hy909* cells had longer telomeres than *rif2Δ* cells (Figure 22), indicating that *TEL1-hy909* telomere overelongation cannot be solely attributed to the lack of Rif2-mediated inhibition of telomerase.

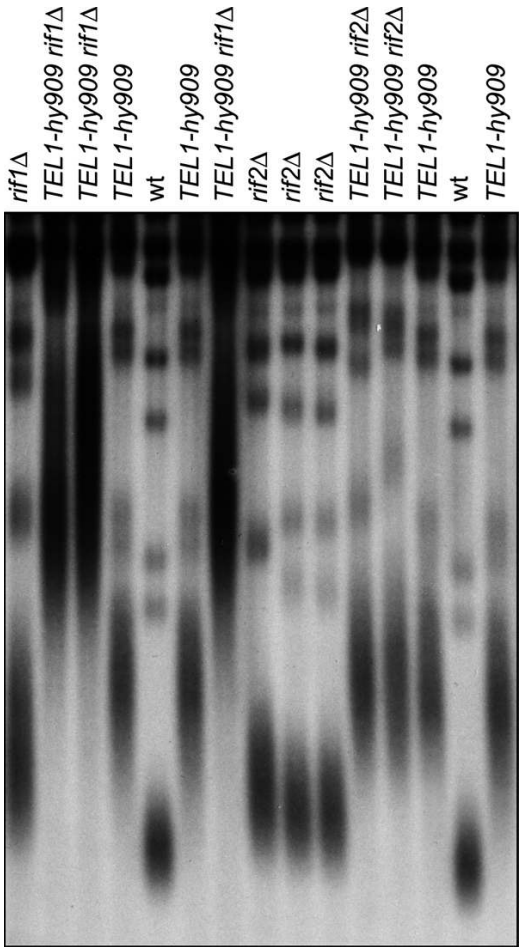

Figure 22: Different effects of *RIF1* and *RIF2* deletion on the length of native *TEL1-hy909* telomeres. XhoI-cut genomic DNA from exponentially growing cell cultures with the indicated genotypes was analyzed as described in the legend to Figure 15.

Tel1-hy909 is more robustly associated than wild-type Tel1 to DSB ends carrying telomeric repeat sequences

Rif2 is thought to inhibit telomere elongation by counteracting Tel1 association to telomeric DNA (Hirano et al., 2009). Thus, one possibility is that Rif2 is unable to inhibit telomere processing and elongation in

TEL1-hy909 cells because Tel1-hy909 is more robustly associated to the telomeric ends than wild-type Tel1. To investigate this hypothesis, we analyzed by ChIP experiments the binding of HA-tagged Tel1 and Tel1-hy909 variants at the telomeric (TG-HO) and nontelomeric (HO) sides of the HO-induced DSB depicted in Fig. 9A. The HO cut was induced by galactose addition in G1- or G2-arrested *TEL1-HA* and *TEL1-hy909-HA* cell cultures that were kept arrested in G1 (Fig. 9B) or in G2 (Fig. 9E), respectively. Consistent with the notion that Tel1 association at telomeres is inhibited by Rif2 (Hirano et al., 2009), the amount of wild-type Tel1-HA bound at the TG-HO side of the break was greatly reduced compared to that associated to the nontelomeric (HO) side during both G1 (Fig. 9C and D) and G2 (Fig. 9F and G) arrest. Interestingly, the amount of Tel1- hy909-HA bound at the TG-HO DSB end was dramatically higher than that of wild-type Tel1-HA in both G1 and G2 (Fig. 9C and F), indicating that Tel1-hy909 is more robustly associated than wild-type Tel1 to DNA ends carrying telomeric DNA. In contrast, the amount of Tel1-hy909-HA that associated to the HO end with no telomeric repeats was similar to that of wild-type Tel1-HA in G1 cells (Fig. 9D), whereas it was slightly increased in G2 cells (Fig. 9G), in agreement with the observation that Tel1-hy909 can enhance resection of a nontelomeric DSB end in G2, but not in G1.

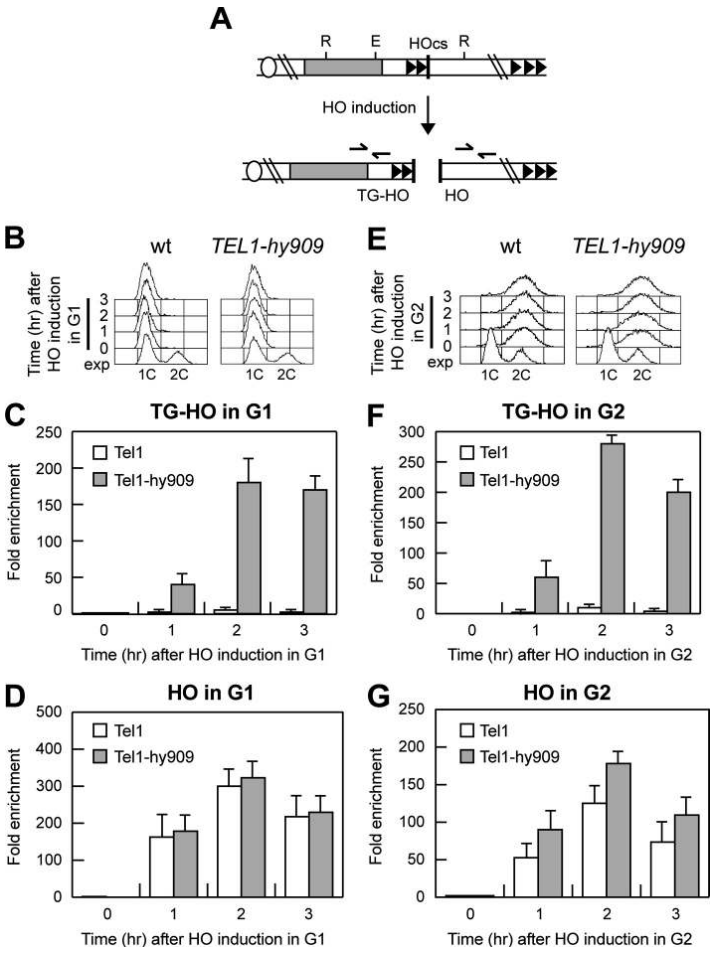

Figure 23: Association of Tel1-HA and Tel1-hy909-HA to DNA ends. A) The system described in Figure 16A was used to generate TG-HO and HO DNA ends, and the primers used to detect protein association centromere proximal (TG-HO) or centromere distal (HO) to the HO-induced DSB are represented by arrows in the bottom part of the panel. **(B to G)** HO expression was induced at time zero by galactose addition to G1-arrested **(B to D)** or G2-arrested **(E to G)** *TEL1-HA* (wild-type) and *TEL1-hy909-HA* (*TEL1-hy909*) cells, which were kept arrested in G1 or G2 by α-factor and nocodazole, respectively. **(B and E)** Fluorescence- activated cell sorter analysis of DNA content. **(C to G)** Chromatin samples taken at the indicated times after HO induction were immunoprecipitated with anti-HA antibody. **(C and F)** Coimmunoprecipitated DNA was analyzed by qPCR using primer pairs located 640 bp centromere proximal to the HO cleavage site (HOcs; TG-HO) and at the nontelomeric *ARO1* fragment of chromosome IV (CON). **(D and G)** Coimmunoprecipitated DNA was analyzed by qPCR using primer pairs located 550 bp centromere distal to the HO cleavage site (HOcs; HO) and at the nontelomeric *ARO1* fragment of chromosome IV (CON). In all graphs, data are expressed as relative fold enrichment of the TG-HO or HO signal over the CON signal after normalization to input signals for each primer set. The data presented are means ± SDs from three different experiments.

Tel1-hy909 increases MRX and Est1 persistence at DSB ends carrying telomeric repeats

If Tel1 promotes MRX activity by facilitating MRX persistence onto DNA ends, then the more robust association to telomeric ends of Tel1-hy909 than wild-type Tel1 might lead to increased MRX binding at these ends, thus eventually leading to enhanced telomere resection. We therefore also analyzed G1- or G2-arrested wild-type and *TEL1-hy909* cells for the binding of MYC-tagged Mre11 to either the TG-HO telomeric end or the HO nontelomeric end of the HO-induced DSB depicted in Fig. 9A. The association of Mre11 to the TG-HO DSB end was greatly increased in both G1- and G2-arrested *TEL1-hy909* cells compared to wild type (Figure 15A and B). In contrast, Mre11 binding to the nontelomeric DSB end was similar in G1-arrested wild-type and *TEL1-hy909* cells (Figure 15C), whereas it was slightly increased in *TEL1-hy909* G2 cells (Figure 15D), consistent with the finding that the enhanced resection of DSB ends with no TG sequences in *TEL1-hy909* cells is restricted to the G2 cell cycle phase (Baldo et al., 2008).

As Tel1 is thought to regulate telomere length by promoting telomerase recruitment at telomeres, increased association of Tel1-hy909 at telomeric ends might also enhance telomerase association to the same ends. Indeed, the amount of MYC-tagged Est1 bound to the TG-HO side of the HO-induced DSB was much higher in G2-arrested *TEL1-hy909* cells than in wild type (Figure 15E), suggesting that enhanced Est1 association at *TEL1-hy909* telomeres may account for their overelongation.

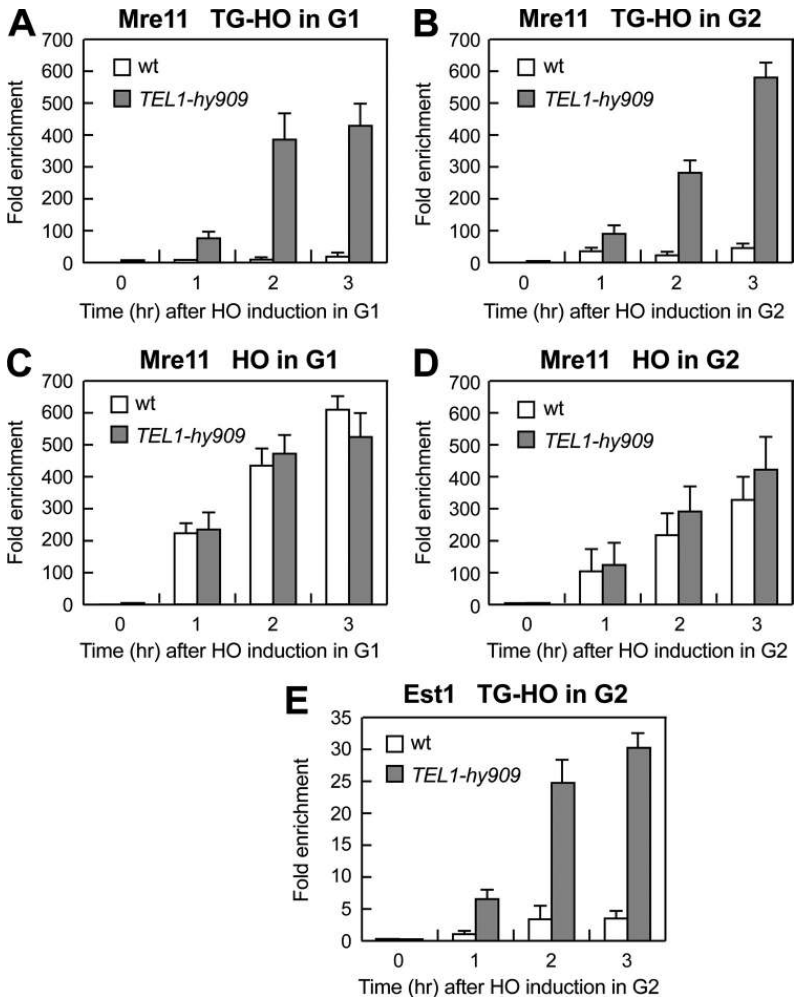

Figure 24: Mre11 and Est1 association to DNA ends in wild-type and *TEL1-hy909* cells. G1- or G2-arrested wild-type and *TEL1-hy909* cells carrying the TG-HO system described in Figure 16A and expressing fully functional MYC-tagged Mre11 **(A to D)** or MYC-tagged Est1 **E)** were treated as described in the legend to Fig. 9, and cell cycle arrest was verified by fluorescence-activated cell sorter analysis (data not shown). Chromatin samples taken at the indicated times after HO induction were immunoprecipitated with anti-MYC antibody. **(A, B, and E)** Coimmunoprecipitated DNA was analyzed by qPCR with the primer pairs used for Fig. 9C and F. **(C and D)** Coimmunoprecipitated DNA was analyzed by qPCR with the primer pairs used for Fig. 9D and G. In all graphs, data are expressed as relative fold enrichment of the TG-HO or HO signal over the CON signal after normalization to input signals for each primer set. The data presented are means ± SDs from three different experiments.

Discussion

Telomeres are specialized nucleoprotein complexes that distinguish the natural ends of linear chromosomes from intrachromosomal double-strand breaks. In fact, telomeres are protected from DNA damage checkpoints, homologous recombination or end-to-end fusions that normally promote repair of intrachromosomal DNA breaks.

The results reported in this study highlight the role of key telomeric proteins in protecting budding yeast telomeres from nucleolytic degradation. In particular, lack of Rif1, Rif2 or C-terminus of Rap1 promote C-rich strand degradation at an HO-derived telomere in G1 and enhance it in G2. Moreover, cycling cells devoid of Rif2 or Rap1 C-terminus display accumulation of ssDNA also at native telomeres. Interestingly, ssDNA generation at both native and HO-induced telomeres is increased to the same extent in *rif2Δ* and *rap1ΔC* cells, suggesting that the effect exerted by Rap1 is likely mediated by Rif2. In fact, Rap1 recruits Rif2 to the TG tracts through its C-terminal domain (Wotton and Shore, 1997). On the other hand, also Rif1 is recruited by Rap1 to TG tracts (Hardy et al., 1992; Moretti et al., 1994), but Rif1 loss has a minor effect on C-strand resection, indicating different functions for Rif1 and Rif2 in inhibiting nucleolytic telomere processing. Similarly, Rif2, but not Rif1, prevents telomeric fusions by NHEJ (Marcand et al., 2008).

Also Yku has a role in inhibiting telomere resection, but it acts specifically in G1. In fact, ssDNA generation at both HO-induced and native telomeres is increased in G1-arrested *yku70Δ* cells compared to wild type, whereas no significant differences are observed in G2/M. The Yku-mediated inhibitory effect on telomeric processing is independent on Yku role in NHEJ, as Dnl4 loss does not promote ssDNA generation at

the HO-induced telomere in G1, unlike at intrachromosomal DSBs (Clerici et al., 2008; Zierhut and Diffley, 2008). This finding is consistent with the observation that NHEJ is inhibited at telomeres (Pardo and Marcand, 2005), possibly because its components are excluded from telomeric ends. Interestingly, resection at the HO-induced telomere in G1-arrested *yku70Δ* cells does not proceed beyond 166 bp from the HO site. It is noteworthy that this limited processing is due to the inhibitory action of Rap1, Rif1 and Rif2, as their inactivation allows extensive resection not only in wild type but also in *yku70Δ* G1 cells.

Although C-strand degradation in the absence of Yku is restricted to the regions closest to the telomeric tip, this degradation is more efficient in G1-arrested *yku70Δ* cells than in *rif2Δ* cells. This observation, together with the finding that the shelterin-like proteins limit extensive resection in Yku-lacking cells, suggests that Yku is mainly involved in inhibiting initiation, whereas Rif1, Rif2 and Rap1 act primarily by limiting extensive resection. Consistent with the different inhibitory functions of Yku and shelterin-like proteins, the concomitant lack of Yku and Rif2 has additive effects on de novo telomere degradation in G1. In fact, both C-strand degradation and generation of r1 resection products occur more efficiently in G1 *yku70Δ rif2Δ* double mutant cells than in *rif2Δ* and *yku70Δ* single mutants.

It is worth pointing out that telomere processing in the absence of Yku, Rif2, Rap1 or Rif1 takes place in G1 independently of the low Cdk1 activity. As DSB resection is not completely abolished in G1 (Ira et al., 2004; Clerici et al., 2008), the Cdk1 role might be simply to potentiate the resection machineries, thus explaining why Cdk1 requirement for

telomere resection can be bypassed by inactivation of negative regulators of this process.

The resection extent at the HO-induced telomere is higher in *rif2Δ* and *rap1ΔC* cycling cells than in *yku70Δ* G1 cells, but ssDNA at native telomeres does not elicit the DNA damage checkpoint in any of these mutant cells, suggesting that other mechanisms might prevent a DNA damage response at telomeres. One possibility is that the ssDNA accumulated in the absence of Yku or the shelterin-like proteins is still covered by Cdc13, which has been shown to inhibit Mec1 association to DNA ends (Hirano and Sugimoto, 2007). Consistent with this hypothesis, the lack of Rif2 enhances checkpoint activation in cells crippled for Cdc13 activity (Figure 12F). Alternatively, or in addition, as Mec1 is the main responder to DSBs in yeast and its activation needs ssDNA (Zou and Elledge, 2003), the amount of telomeric ssDNA in these cells may be insufficient to elicit a checkpoint response. In mammalian cells, loss of the shelterin protein TRF2 leads to ATM-dependent DNA damage response that does not require extensive degradation of the telomeric 5' strand (Celli and de Lange, 2005). The knowledge that the ATM yeast ortholog, Tel1, has a very minor role in the checkpoint response to DSBs compared to Mec1 (Mantiero et al., 2007) might explain this difference between yeast and mammals in the response to telomere alterations.

The inhibitory actions of Yku and shelterin-like proteins seem to target different nucleases. In fact, Exo1 appears to be important for telomeric ssDNA generation at both native and HO-induced telomeres in *yku70Δ* G1 cells, suggesting that Yku might hide the telomeric ends from Exo1 association. By contrast, telomeric ssDNA generation in both *rif2Δ* and *rap1ΔC* cells depends primarily on Mre11, whose recruitment in G1 to

the HO-induced telomere is enhanced in *rif2Δ* and *rap1ΔC* cells. Thus, while Yku protects telomeres towards Exo1 in G1, Rap1 and Rif2 likely prevent telomere processing by inhibiting loading of the MRX complex onto telomeric ends in both G1 and G2 (Figure 23). However, we cannot exclude that Yku might protect G1 telomeres also from MRX (Figure 23), as it has been observed at intrachromosomal DSB (Clerici et al., 2008), because MRX action in *yku70Δ* G1 cells is anyhow inhibited by Rap1, Rif1 and Rif2. As some MRX association at the HO-induced telomere can be detected in wild type G1 cells, Rap1 and Rif2 might impair 5'-end resection also by inhibiting MRX activity besides its association to DNA. In any case, telomere processing can take place in G2, likely because Cdk1 activity potentiates the resection machinery and Yku does not exert its inhibitory effect in this cell cycle phase (Figure 23).

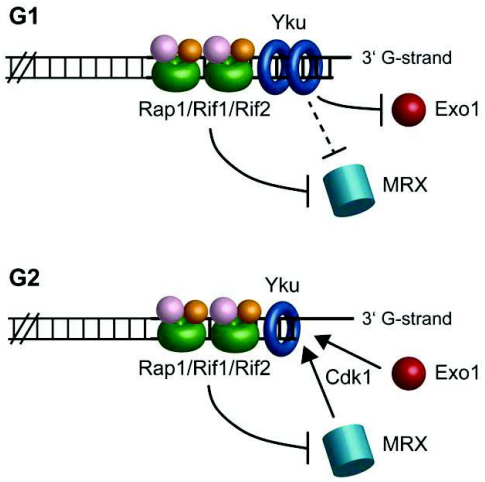

Figure 23: A working model for limiting DNA degradation at telomeres. In G1, Yku protects telomeres from Exo1, while Rap1, Rif1 and Rif2 mainly act by preventing MRX access. As MRX action is still inhibited by Rap1, Rif1 and Rif2 in *yku70Δ* G1 cells, Yku might protect G1 telomeres also from MRX. In G2, only Rap1 and Rif2 still exert their inhibitory effects on telomere processing. Telomere resection can take place in G2 because Yku does not exert its inhibitory effect and Cdk1 activity potentiates nuclease actions.

The data described so far increase our knowledge of telomere protecting mechanisms, as they highlight a role of evolutionarily conserved proteins in protecting chromosome ends during different cell cycle phases by preventing the action of different nucleases.

The Rap1/Rif2 complex is crucial to limit MRX recruitment and activity at telomeres. Consistent with our findings, end processing and Mre11 binding have been shown to be reduced at an HO-induced telomere with 250 bp TG tracts compared to one with 81 bp TG tracts (Negrini et al., 2007), which likely bind a smaller number of shelterin-like complexes than the former (Marcand et al., 1997; Levy and Blackburn, 2004).

The MRX complex is also necessary to maintain telomere length by recruiting the Tel1 kinase (Nakada et al., 2003) and Rif2 was recently shown to interact with the C-terminus of the Xrs2 subunit of the MRX complex (Hirano et al., 2009). As Tel1 also binds the same portion of Xrs2, Hirano and collegues proposed that Rif2 and Tel1 might compete with each other for binding to MRX (Hirano et al., 2009). Furthermore, MRX localization at telomeres is reduced in *tel1Δ* cells compared to wild-type cells (Hirano et al., 2009), raising the possibility that Tel1, after its MRX-dependent loading onto telomeric ends, can enhance MRX activity. As MRX is required to generate telomeric single-stranded DNA (ssDNA), this Tel1-dependent regulation of MRX might influence resection and elongation of telomeric ends. However, the physiological relevance of this control was unknown. By studying the effects on telomere processing and elongation of the lack of Tel1 compared with the effects of the dominant Tel1-hy909 variant, we provide evidence that Tel1 is crucial for counteracting Rif2-dependent negative regulation of telomere resection and elongation.

We show that the lack of Tel1, which is known to cause telomere shortening (Greenwell et al., 1995), decreases both MRX-dependent resection at a DSB end carrying telomeric repeats and the amount of ssDNA formation at native telomeres. Together with the notion that MRX association at telomeres is impaired by the lack of Tel1 (Hirano et al., 2009), these data indicate that Tel1, once loaded onto DNA ends by MRX, regulates 5'-3' nucleolytic degradation of telomere ends by promoting MRX activity. This role of Tel1 is not restricted to telomere ends, as the lack of Tel1 was shown to slightly impair generation of ssDNA also at intrachromosomal DSBs (Mantiero et al., 2007).

Consistent with a role of Tel1 in regulating telomere end resection, the *TEL1-hy909* mutation, which causes telomerase-dependent telomere overelongation, increases the amount of ssDNA at telomeres. This increase becomes apparent even in the absence of telomerase, indicating that it is due to an enhanced resection rather than to telomerase action. Moreover, the *TEL1-hy909* mutation accelerates the onset of senescence of telomerase-negative cells. As telomeric ssDNA has been proposed to trigger senescence (Abdallah et al., 2009), this finding further supports the hypothesis that the Tel1-hy909 variant enhances nucleolytic degradation at telomeres. Accordingly, the lack of Tel1, which reduces the amount of telomeric ssDNA, attenuates the senescence phenotype of telomerase-negative cells (Ritchie et al., 1999; Gao et al., 2010).

How does Tel1-hy909 enhance telomere processing and elongation? Both the enhanced resection and elongation of *TEL1- hy909* telomeres require Tel1-hy909 kinase activity, further confirming that Tel1 acts as a kinase at telomeres (Mallory and Petes, 2000). Like most of the other

Tel1-hy variants that we found by virtue of their ability to suppress the hypersensitivity to genotoxic agents of *mec1Δ* cells, the Tel1-hy909 variant has enhanced kinase activity *in vitro* compared to wild-type Tel1 (Baldo et al., 2008). However, only the Tel1-hy909 variant confers a striking telomere overelongation phenotype (Baldo et al., 2008), implying that this phenotype cannot be entirely ascribed to the high Tel1-hy909 kinase activity.

Tel1-hy909 is more robustly associated than wild-type Tel1 to DSB ends carrying telomeric repeats during both the G1 and G2 cell cycle phases, likely leading to increased MRX and Est1 persistence at telomeric ends. In fact, the amounts of Mre11 and Est1 bound to telomeric DNA ends are higher in *TEL1-hy909* cells than wild-type cells. While enhanced MRX association could explain the increased efficiency of *TEL1-hy909* telomere resection, stabilization of Est1 binding to telomeric ends may account for the overelongation of *TEL1-hy909* telomeres. Because MRX is required to load Tel1 onto DNA ends (Nakada et al., 2003) and to support Tel1-hy909 activities, this robust Tel1-hy909 association to telomeres may be due to an increased ability of Tel1-hy909 to interact with MRX compared to wild-type Tel1, as also suggested by the dominant effects of the *TEL1-hy909* allele. Unfortunately, we have so far been unable to co-immunoprecipitate Tel1 with MRX to assess this possibility.

In the first part of this thesis we reported that MRX-dependent generation of ssDNA at telomeres is prevented by Rif2 during both G1 and G2. On the contrary, neither processing nor elongation of *TEL1-hy909* telomeres is inhibited by Rif2, indicating a failure of Rif2 to counteract MRX activity in the presence of the Tel1-hy909 variant. As

Rif2 has been proposed to compete with Tel1 for binding to MRX (Hirano et al., 2009), the dominant Tel1-hy909 variant might escape the Rif2-mediated negative control by binding to MRX more efficiently than wild-type Tel1. Because Tel1 exerts a positive-feedback loop on MRX, this robust Tel1-hy909 recruitment may in turn stabilize MRX association to telomeric ends, possibly through phosphorylation events.

The action of Tel1-hy909 is not restricted to telomeric ends, as Tel1-hy909 also enhances resection at intrachromosomal DSBs (Baldo et al., 2008). However, this Tel1-hy909 function is restricted to the G2 cell cycle phase, since MRX-dependent resection in G1 (when Cdk1 activity is low) is counteracted by Yku, which exerts this inhibitory role only in G1 (Clerici et al., 2008). This inability does not prevent Tel1-hy909 from enhancing MRX-dependent resection at telomeres, because, as previously described, Yku protects them mainly from Exo1 and not from MRX. Interestingly, the resection kinetics of DSB ends in G1-arrested wild-type cells is similar to that occurring at an HO-telomere in G1-arrested *TEL1-hy909* cells (compare Figure 10 and 11). Furthermore, the amount of MRX bound a DSB in wild-type cells is similar to the MRX amount that is recruited at an artificial telomere in *TEL1-hy909* cells. Thus, the difference in terms of ssDNA generation at DSBs versus telomeric DNA ends appears to rely on Rif2-mediated inhibition of Tel1 and, hence, of MRX activity.

Thus, the evidences presented so far suggest a model in which the regulation of telomere processing and elongation appears to rely on a balance between Tel1 and Rif2 activities. As Tel1 hyperactivation can improve both telomere resection and telomerase action, Rif2-dependent inhibition of Tel1/MRX function at telomeres is important to ensure the

maintenance of telomere identity by limiting ssDNA generation and elongation. In contrast, such a control appears to be dispensable at intrachromosomal DSBs, where generation of ssDNA is necessary to repair the break.

However the molecular mechanism underlying Tel1-mediated regulation of telomere length has not yet been solved. Our findings that the amount of telomeric G-tails is reduced by the lack of Tel1, whereas it is increased in *TEL1-hy909* cells, leads to a model, also suggested by Lundblad and colleagues (Gao et al., 2010), where Tel1 function in telomere length maintenance can be linked to its role in generating telomeric G-tails, which are the substrates of telomerase. In this model, the telomere length defect observed in *tel1Δ* cells might be a consequence of the reduced ssDNA amount at the telomeric ends, whereas the increased ssDNA generation at *TEL1-hy909* telomeres might improve telomerase-dependent elongation by increasing the substrates available for the telomerase enzyme. However, the finding that the single-stranded G-tail signal was lower in *mre11Δ* cells than in *tel1Δ* cells, which display a similar telomere length defect and are likely defective in the same telomere length maintenance pathway (Ritchie and Petes, 2000), is inconsistent with the idea that Tel1 function in telomere length maintenance is limited to ssDNA generation.

Moreover the correlation between telomere overelongation and increased Est1 binding at *TEL1-hy909* telomeres provides additional support for a model in which Tel1 is a positive activator of telomerase. Because the kinase activity of Tel1 is needed for its role in telomere maintenance (Mallory and Petes, 2000), and telomere overelongation is completely abolished in *Tel1-hy909kd* mutant (Figure 15),

phosphorylation of one or more telomere binding proteins by Tel1 could increase the frequency of elongation by making the telomeric chromatin more accessible to telomerase. In this scenario, the robust association of hyperactive Tel1-hy909 kinase at telomeres may improve the efficiency of this process.

Unfortunately, no Tel1 targets have been identified so far. MRX itself was previously shown to be target of Tel1-dependent phosphorylation during DSB-induced checkpoint activation (Mantiero et al., 2007), but the biological relevance of this control is so far unknown. Further studies will be needed to better understand how Tel1-mediated regulation of telomere length is achieved.

Materials and Methods

Yeast and bacterial strains

Yeast strains

Strain genotypes used for this work are listed in Table 1.

Strain	Relevant genotype	Source or Ref.
UCC5913	*MATa-inc ade2-101 lys2-801 his3-Δ200 trp1-Δ63 ura3-52 leu2-Δ1::GAL1-HO-LEU2 VII-L::ADE2-TG(1-3)-HO site-LYS2*	(Diede and Gottschling, 2001)
YLL2554	UCC5913 *MRE11-18MYC::TRP1*	This study
YLL2599	UCC5913 *bar1Δ::HPHMX*	This study
YLL2612	UCC5913 *yku70Δ::URA3 bar1Δ::HPHMX*	This study
YLL2613	UCC5913 *dnl4Δ::NATMX bar1Δ::HPHMX*	This study
YLL2646	UCC5913 *yku70Δ::URA3 rif1Δ::NATMX bar1Δ::HPHMX*	This study
YLL2647	UCC5913 *yku70Δ::URA3 rif2Δ::NATMX bar1Δ::HPHMX*	This study
YLL2649	UCC5913 *rif1Δ::NATMX bar1Δ::HPHMX*	This study
YLL2650	UCC5913 *rif2Δ::NATMX bar1Δ::HPHMX*	This study
YLL2651	UCC5913 *rap1Δ::KANMX4* [*CEN-HIS3-rap1Δ670-807*] *bar1Δ::HPHMX*	This study
YLL2655	UCC5913 *yku70Δ::URA3 rap1Δ::KANMX4* [*CEN-HIS3-rap1Δ670-807*] *bar1Δ::HPHMX*	This study
YLL2670	UCC5913 *MRE11-18MYC::TRP1 bar1Δ::HPHMX*	This study
YLL2672	UCC5913 *MRE11-18MYC::TRP1 rap1Δ::KANMX4* [*CEN-HIS3-rap1Δ670-807*] *bar1Δ::HPHMX*	This study
YLL2694	UCC5913 *MRE11-18MYC::TRP1 rif2Δ::NATMX*	This study
YLL2725	UCC5913 *rif2Δ::NATMX mre11Δ::KANMX4 bar1Δ::HPHMX*	This study
YLL2728	UCC5913 *yku70Δ::URA3 exo1Δ::NATMX bar1Δ::HPHMX*	This study
YLL2730	UCC5913 *yku70Δ::URA3 mre11Δ::NATMX bar1Δ::HPHMX*	This study
YLL2731	UCC5913 *rif2Δ::NATMX exo1Δ::URA3 bar1Δ::HPHMX*	This study
YLL2733	UCC5913 *rap1Δ::KANMX4* [*CEN-HIS3-rap1Δ670-807*] *exo1Δ::URA3 bar1Δ::HPHMX*	This study

YLL2736	UCC5913 *rap1Δ::KANMX4* [*CEN-HIS3-rap1Δ670-807*] *mre11Δ::NATMX bar1Δ::HPHMX*	This study
YLL2820	UCC5913 *tel1Δ::HIS3 bar1Δ::HPHMX*	This study
YLL2831	UCC5913 *mre11Δ::KANMX4 bar1Δ::HPHMX*	This study
YLL2836	UCC5913 *TEL1-hy909::KANMX4 bar1Δ::HPHMX*	This study
YLL2860	UCC5913 *exo1Δ::URA3 TEL1-hy909::KANMX4 bar1Δ::HPHMX*	This study
YLL2861	UCC5913 *MRE11-MYC::HIS3 TEL1-hy909::KANMX4 bar1Δ::HPHMX*	This study
YLL2874	UCC5913 *rif2Δ::TRP1 TEL1-hy909::KANMX4 bar1Δ::HPHMX*	This study
YLL2876	UCC5913 *mre11Δ::NATMX TEL1-hy909::KANMX4 bar1Δ::HPHMX*	This study
YLL3003	UCC5913 *NATMX::TEL1-hy909-HA::KANMX4 bar1Δ::HPHMX*	This study
YLL3060	UCC5913 *EST1-MYC::HIS3 bar1Δ::HPHMX*	This study
YLL3061	UCC5913 *EST1-MYC::HIS3 TEL1-hy909::KANMX4 bar1Δ::HPHMX*	This study
YLL3068	UCC5913 *TEL1-HA::NATMX bar1Δ::HPHMX*	This study
YLL3130	UCC5913 *TEL1-hy909kd::KANMX4 bar1Δ::HPHMX*	This study
RMY169	*MATa-inc ade2-101 lys2-801 his3-Δ200 trp1-Δ63 ura3-52 leu2-Δ1::GAL1-HO-LEU2 VII-L::TRP1-HO site-LYS2*	(Michelson et al., 2005)
YLL2600	RMY169 *bar1Δ::KANMX4*	This study
YLL2606	RMY169 *yku70Δ::URA3 bar1Δ::HPHMX*	This study
YLL2607	RMY169 *dnl4Δ::NATMX bar1Δ::HPHMX*	This study
YLL3053	RMY169 bar1Δ::HPHMX	This study
YLL3066	RMY169 *TEL1-hy909::KANMX4 bar1Δ::HPHMX*	This study
DMP2156/15B	W303 (*MATa ade2-1 can1-100 his3-11,15 leu2-3,112 trp1-1 ura3-1 rad5-535*) t*el1Δ::HIS3*	This study
DMP4621/1A	W303 *TEL1-hy909::LEU2 rif1Δ::KANMX4*	This study
DMP4627/3B	W303 *TEL1-hy909::LEU2 rif2Δ::KANMX4*	This study
DMP4970/9D	W303 *xrs2-11::KANMX4*	This study
DMP4975/30B	W303 *xrs2-11::KANMX4 TEL1-hy909:: LEU2*	This study
DMP5108/19A	W303 *cdc13-1*	This study
DMP5108/20A	W303 *cdc13-1 rif2Δ::KANMX4*	This study
DMP5200/2B	W303 *TEL1-hy909::KANMX4 rad51Δ::HIS3*	This study
DMP5200/2D	W303 *rad51Δ::HIS3*	This study
DMP5201/3A	W303 *TEL1-hy909::KANMX4 rad52Δ::TRP1*	This study

DMP5201/3D	W303 *rad52Δ::TRP1*	This study
YLL1221	W303 *rif1Δ::KANMX4*	This study
YLL1334	W303 *rif2Δ::KANMX4*	This study
YLL1996	W303 *TEL1/TEL1-hy909::LEU2 EST2/est2Δ::KANMX*	This study
YLL2283	W303 *TEL1-hy909::KANMX4*	This study
YLL3001	W303 *TEL1-HA::NATMX*	This study
YLL3059	W303 *TEL1-hy909kd::KANMX4*	This study
JKM139	MATa *ho hmlΔ hmrΔ ade1 lys5 leu2-3,112 trp1::hisG ura3-52 ade3::GAL-HO*	(Lee et al., 1998)
YLL1643	JKM139 *bar1Δ::HPHMX*	This study
YLL2880	JKM139 *TEL1-hy909::LEU2 bar1Δ::HPHMX*	This study
YLL2892	JKM139 *yku70Δ::URA3 bar1Δ::HPHMX*	This study
YSN645	MATa *EST1-Myc13::HIS3, VII-L::ADE2-Dbp(amp7)-TG-250-HO site, V-R::TRP1-Dbp(amp9)-TG-80-HO*	(Negrini et al., 2007)
YLL2253	YSN645 *leu2Δ::KANMX4*	This study
YLL2255	YSN645 *TEL1-hy909::LEU2 leu2Δ::KANMX4*	This study
YLL2322	YSN645 *rif1Δ::NATMX leu2Δ::KANMX4*	This study
YLL2323	YSN645 *rif2Δ::HPHMX leu2Δ::KANMX4*	This study
YLL2324	YSN645 *TEL1-hy909::LEU2 rif1Δ::HPHMX leu2Δ::KANMX4*	This study
YLL2325	YSN645 *TEL1-hy909::LEU2 rif2Δ::HPHMX leu2Δ::KANMX4*	This study

Table 1. *Saccharomyces cerevisiae* strains used in this study. Plasmids are indicated by brackets

The strains used for monitoring telomere resection at the HO-induced telomere and HO-induced DSB were derivatives of strains UCC5913 and RMY169, respectively, kindly provided by D. Gottschling (Fred Hutchinson Cancer Research Center, USA) and T. Weinert (University of Arizona, USA). Strain RMY169 was created by replacing the ADE2-TG cassette of strain UCC5913 with the TRP1 YLL2880, respectively. To induce a persistent G1 arrest with α-factor, the *BAR1* gene, which encodes a protease that degrades the α-factor, was deleted. The cdc13-1 mutant was kindly provided by D. Lydall (University of Newcastle,

UK.). The plasmid pM585, carrying the rap1D670- 807 allele, was kindly provided by D. Shore (University of Geneva, Switzerland).

A *TEL1-hy909 xrs2-11* strain was obtained by crossing strain KSC1563 (*MAT***a**-*inc ADH4cs*::*HIS2 ade1 his2 leu2 trp1 ura3 xrs2- 11*::*KANMX4 sml1*::*LEU2*), kindly provided by K. Sugimoto (University of New Jersey, Newark, NJ), with a *TEL1-hy909* strain. Strain YLL3068, carrying a fully functional *TEL1-HA* allele at the *TEL1* chromosomal locus (the hemagglutinin [HA] tag coding sequence was located 2,394 bp down-stream of the *TEL1* start codon), was obtained by transforming strain YLL2599 with a PCR product obtained using genomic DNA of strain YLL3001 as the template together with primers PRP1297 (5'-GGC CAC CGT TAA GAA GGG TAA GCC AGA A-3') and PRP1298 (5'-GTT GCA AAG ACT CTC TGC TTC CCA CCT C-3'). Strain YLL3001 was a derivative of strain KRY22, kindly provided by T. Petes (Duke University School of Medicine, Durham, NC), in which the *NATMX* cassette was inserted upstream of the *TEL1* start codon. Strain YLL3003, carrying the HA-tagged *TEL1-hy909* allele at the *TEL1* chromosomal locus, was obtained by transforming strain YLL2836 with a PCR product obtained using genomic DNA of strain YLL3001 as the template together with primers PRP1297 and PRP1298. PCR one-step tagging was used to obtain strains carrying fully functional MYC-tagged *MRE11* and MYC-tagged *EST1* alleles. The *TEL1-hy909kd* allele, encoding a kinase-defective Tel1-hy909 variant carrying the amino acid changes G2611D, D2612A, N2616K, and D2631E, was obtained by site-directed mutagenesis. The accuracy of all gene replacements and integrations was verified by Southern blot analysis or PCR.

E. coli strains

DH5α strain (*F- φ80dlacZM15 (lacZTA-argF)U169 deoR recA1 endA1 hsdR17 (rK- mK+) phoA supE44 thi1 gyrA96 relA1 λ-*) is used as bacterial hosts for plasmid manipulation and amplification. DH5a cells competent to transformation are purchased from Invitrogen.

Growth media

Yeast media

YEP (Yeast-Extract Peptone) is the standard rich media for *S. cerevisiae* and contains 10 g/L yeast extract, 20 g/L peptone and 50 mg/L adenine. YEP must be supplemented with 2% glucose (YEPD), 2% raffinose (YEP+raf), 2% raffinose and 1% or 2% galactose (YEP+raf+gal) as carbon source. For all the experiments done with *Tel1-hy909* cells YEP was supplemented with 3% glycerol, 2% lactic acid, and 0.05% glucose or with 3% glycerol, 2% lactic acid, and 2% galactose.

YEP-based selective media are obtained including 400 μg/mL G418, 300 μg/mL hygromicin-B or 100 μg/mL nourseotricin. Solid media are obtained including 2% agar. Stock solutions are 50% glucose, 30% raffinose, 30% galactose, 80 mg/mL G418, 50 mg/mL Hygromicin-B and 50 mg/mL Nourseotricin. YEP and glucose stock solution are autoclave-sterilized and stored at RT. Sugars and antibiotics stock solutions are sterilized by micro-filtration and stored at RT and 4°C respectively.

S.C. (Synthetic Complete) is the minimal growth media for *S. cerevisiae* and contains 1.7 g/L YNB (without aminoacids), 5 g/L ammonium sulphate, 200mM inositol, 25 mg/L uracil, 25 mg/L adenine, 25 mg/L hystidine, 25 mg/L leucine, 25 mg/L tryptophan. S.C. can be supplemented with drop-out solution (20 mg/L arginine, 60 mg/L isoleucine, 40 mg/L lysine, 10 mg/L methionine, 60 mg/L phenylalanine, 50 mg/L tyrosine) based on yeast strains requirements. Different carbon sources can be used as in rich media (2% glucose, 2% raffinose or 2% raffinose and 1% galactose). One ore more aminoacid/base can be omitted to have S.C.-based selective media (e.g. S.C.-ura is S.C. lacking uracil). Solid media are obtained by including 2% agar. Stock solutions are 17 g/L YNB + 50 g/L ammonium sulphate (or 10g/L monosodic glutamic acid), 5 g/L uracil, 5 g/L adenine, 5 g/L hystidine, 5 g/L leucine, 5 g/L tryptophan, 100X drop out solution (2 g/L arginine, 6 g/L isoleucine, 4 g/L lysine, 1 g/L methionine, 6 g/L phenylalanine, 5 g/L tyrosine), 20mM inositol. All of these solutions are sterilized by micro-filtration and stored at 4°C.

VB sporulation medium contains 13.6 g/L sodium acetate, 1.9 g/L KCl, 0.35 g/L $MgSO_4$, 1.2 g/L NaCl. pH is adjusted to 7.0. To obtain solid medium include 2% agar.

5-FoA medium is obtained including 1 g/L 5-FoA, 50 mg/L uracil to S.C. medium. Solid medium contains 2% agar.

E. coli media

LD is the standard growth medium for *E. coli*. LD medium contains 10 g/L tryptone, 5 g/L yeast extract and 5 g/L NaCl. Solid medium is

obtained by including 1% agar. LD+Amp selective medium is obtained including 50 μg/mL ampicillin. Ampicillin stock solution (2.5 g/L) is sterilized by micro-filtration and stored at 4°C.

Molecular biology techniques

Agarose gel electrophoresis

Agarose gel elctrophoresis is the most easy and common way of separating and analyzing DNA molecules. This technique allows the separation of DNA fragments based on their different molecular weight. The purpose of this technique might be to visualize the DNA, to quantify it or to isolate a particular DNA fragment. The DNA is visualized by the addition in the gel of ethidium bromide.

Agarose powder is mixed with TAE (Tris-Acetate/EDTA) or TBE buffers (Tris, boric acid, EDTA ph8.0) to the desired concentration, and the solution is boiled. Most gels are made between 0.8% and 2% agarose. A 0.8% gel will show good resolution of large DNA fragments (5-10 Kb) and a 2% gel will show good resolution for small fragments (0.2-1 Kb). Ethidium bromide is added to the gel at a final concentration of 1 μg/mL to facilitate visualization of DNA after electrophoresis. After cooling the solution to about 60°C, it is poured into a casting tray containing a sample comb and allowed to solidify at RT or at 4°C. The comb is then removed and the gel is placed into an electrophoresis chamber and just covered with the buffer (TAE or TBE). Sample are loaded together with loading buffer (0.05% bromo-phenol blue and 5% glycerol). A marker

containing DNA fragments of known length and concentration is generally loaded in parallel to determine size and quantity of DNA fragments in the samples.

Restriction endonucleases

Type II endonucleases (also known as restriction endonuceases or restriction enzymes) cut DNA molecules at defined positions close to their recognitions sequences in a reaction known as enzymatic digestion. They produce discrete DNA fragments that can be separated by agarose gel electrophoresis, generating distinct gel banding patterns. For these reasons they are used for DNA analysis and gene cloning. Restriction enzymes are generally stored at -20°C in a solution containing 50% glycerol, in which they are stable but not active. Glycerol concentration in the reaction mixture must be below 5% in order to allow enzymatic reaction to occur. They generally work at 37°C with some exceptions (e.g. ApaI activity is maximal at 25°C) and they must be supplemented with a reaction buffer provided by the manufacturer, and in some cases with Bovin Serum Albumin. We use restriction endonucleases purchased from NEB.

Polymerase Chain Reaction (PCR)

PCR allows to obtain high copy number of a specific DNA fragment of interest starting from very low quantity of DNA fragment. The reaction is directed to a specific DNA fragment by using a couple of oligonucleotides flanking the DNA sequence of interest. These

oligonucleotides work as primers for the DNA polymerase. The reaction consists of a number of polymerization cycles which are based on 3 main temperature-dependent steps: denaturation of DNA (which occur over 90°C), primer annealing to DNA (typically take place at 45-55°C depending on primer characteristic), synthesis of the DNA sequence of interest by a thermophilic DNA polymerase (which usually works at 68 or 72°C). Different polymerases with different properties (processivity, fidelity, working temperature, etc) are commercially available and suitable for different purpose. Taq polymerase works at 72°C and is generally used for analytical PCR. Polymerases with higher fidelity like Pfx and VENT polymerases, which work respectively at 68 and 72°C, are generally employed when 100% polymerization accuracy is required.

The typical 50 μL PCR mixture contains 1μL of template DNA, 0.5 mM each primer, 200mM dNTPs, 5 μL of 10X Reaction Buffer, 1mM $MgCl_2$, 1-2 U DNA polymerase and water to 50 μL. The typical cycle-program for a reaction is: 1. 3' denaturation at 94-95°C; 2. 30" denaturation at 94-95°C; 3. 30" annealing at primers T_m (melting temperature); 4. 1' polymerization per Kb at 68 or 72°C (depending on polymerase); 5. repeat 30 times from step 2; 6. 5-10' polymerization at 68-72°C. The choice of primer sequences determines the working T_m, which depends on the length (L) and GC% content of the oligonucleotides and can be calculated as follows: $T_m = 59.9 + 0.41(GC\%) - 675/L$.

Plasmid DNA extraction from *E. coli*

Minipreps boiling. *E. coli* cells (2ml overnight culture) are harvested by centrifugation and resuspended in 500 μL STET buffer (8% sucrose, 5%

TRITON X-100, 50mM EDTA, 50mM Tris-HCl, pH 8). Bacterial cell wall is digested boiling the sample for 2 minutes with 1 mg/mL lysozyme. Cellular impurities are removed by centrifugation and DNA is precipitated with isopropanol and resuspended in the appropriate volume of water or TE.

QIAgen columns. See QIAprep Spin Miniprep Kit handbook.

Transformation of *E. coli*

DH5a competent cells are thawed on ice. Then, 50-100 μL cells are incubated 30 minutes in ice with 1 μL plasmid DNA. Cells are then subjected to heat shock at 37°C for 30 seconds and then incubated on ice for 2 minutes. Finally, 900 μL LD are added to the tube and cells are incubated 30 minutes at 37°C to allow expression of ampicillin resistance. Cells are then plated on LD+amp and overnight incubated at 37°C.

Transformation of *S. cerevisiae*

YEPD exponentially growing yeast cells are harvested by centrifugation and washed with 0,5 mL 1M lithium acetate (LiAc) pH 7.5. Cells are then resuspended in 1M LiAc pH 7.5 to obtain a cells/LiAc 1:1 solution. 12 μL cells/LiAc are incubated 30-45 minutes at RT with 45 μL 50% PEG (PolyEthylene-Glycol) 3350, 4 μL carrier DNA (salmon sperm DNA) and 1-4 μL DNA of interest (double each quantity when transform with PCR products). After addition of 6 μL 60% glycerol cells are incubated at RT

for 30-45 minutes, heat-shocked at 42°C for 5-10 minutes and plated on the appropriate selective medium.

Extraction of yeast genomic DNA (Teeny yeast DNA preps)

Yeast cells are harvested from overnight cultures by centrifugation, washed with 1 mL of 0.9M sorbytol 0.1M EDTA pH 7.5 and resuspended in 0.4 mL of the same solution supplemented with 14mM β-mercaptoethanol. Yeast cell wall is digested by 45 minutes incubation at 37°C with 0.4 mg/mL 100T zimoliase. Spheroplasts are harvested by 30 seconds centrifugation and resuspended in 400 μL TE. After addition of 90 μL of a solution containing EDTA pH 8.5, Tris base and SDS, spheroplasts are incubated 30 minutes at 65°C. Samples are kept on ice for 1 hour following addition of 80 μL 5M potassium acetate. Cell residues are eliminated by 15 minutes centrifugation at 4°C. DNA is precipitated with chilled 100% ethanol, resuspended in 500 μL TE and incubated 30 minutes with 25 μL 1 mg/mL RNase to eliminate RNA. DNA is then precipitated with isopropanol and resuspended in the appropriate volume (typically 50 μL) of TE.

Southern blot analysis

Yeast genomic DNA prepared with standard methods is digested with the appropriate restriction enzyme(s). The resulting DNA fragments are separated by agarose gel electrophoresis in a 0.8% agarose gel. For Southern blot analysis of telomere length we generally use 1X TBE as

buffer. When adequate migration has occurred, gel is washed 30-60 minutes with a denaturation buffer (0.2N NaOH, 0.6M NaCl), and 30-60 minutes with a neutralization buffer (1.5M NaCl, 1M Tris HCl, pH 7.4). DNA is blotted onto a nylon membrane (GeneScreen™) by overnight capillary transfer with 10X SSC buffer (20X SSC: 3M sodium chloride, 0.3M sodium citrate, pH 7.5). Membrane is then washed with 4X SSC and UV-crosslinked.

Hybridization is carried out by incubating membrane for 5 hours at 55°C with Church buffer solution (0.5M sodium phosphate buffer ph 7.2, 7% SDS, 1mM EDTA ph 8.5, 0.5% BSA, water), followed by o/n incubation at 55°C with Church buffer solution + probe. Probe is obtained by random priming method (DECAprime™ kit by Ambion) on a suitable DNA template and with ^{32}P d-ATP. Filter is then washed (45' + 15') at 55°C with a washing solution (0.2M sodium phosphate buffer pH 7.2, SDS 1%, water), air dried and then exposed to an autoradiography film.

Resection assay

Non denaturing in-gel hybridization (Dionne and Wellinger, 1996). XhoI-digested DNA samples were loaded onto 0.75% agarose gels and DNA fragments were separated by electrophoresis for 16 hr at 0.8 V/cm. The DNA was then stained with ethidium bromide for photography. The gels were immersed for 30 min in 2× SSC (0.3 M NaCl/0.03 M sodium citrate, pH 7) at 20°C and then mounted on a BIORAD gel drier. Drying was carried out for 25–30 min at 20°C. The very thin gels were then placed in sealable plastic bags and hybridized for 16 hr at 37°C to end-

labeled oligonucleotides using the hybridization buffer (Counter et al., 1992). After removal of excess hybridization buffer, gels were placed in 0.25× SSC and washed once for 30 min at 20°C, followed by two 1-hr washes at 30°C. Gels were then exposed to x-ray films for appropriate amounts of time. The oligonucleotide used as probe is a 22-mer of the sequence 5′-CCCACCACACACACCCACACCC-3′ and is referred to as the CA-oligo. The same gel was denatured and hybridized with the end-labeled C-rich oligonucleotide for loading control; alternatively the same DNA samples were separated on a 0.8% agarose gel, denatured and hybridized with the end-labeled C-rich oligonucleotide for loading and telomere length control (denatured gel).

Denaturing gel electrophoresis. Yeast genomic DNA is digested with the appropriate restriction endonuclease for at least 5 hrs at 37°C, ethanol precipitated and then resuspended in 10 μl of water. Digested genomic DNA, together with an equal amount of 1X sequencing loading dye (10mM EDTA pH 8.0, 0.025% bromo-phenol blue, formamide 95%), is denatured for 5 minutes at 95°C and then put immediately in ice. 5 μl of this solution are loaded on a 6% denaturing acrylamide gel, which is then run at 38W until the blue reaches the bottom of the gel. DNA is electro-blotted on a nylon positively charged membrane (Roche) for 1h and 30' in cold TBE0.5X at 40V. Membrane is then dried and UV cross-linked. Hybridization is carried out in a 5% SSC, 50% formamide, 5% Denhardt's solution, 1% SDS solution at 42°C o/n. Washes are done in a 0.1% SDS + 0.2% SSC solution (4x30'). Single-stranded RNA probe is

transcribed *in vitro* as described by the manufacturer (Promega) using appropriate plasmid as a template.

To monitor resection at the HO-derived telomeres, RsaI- and EcoRV-digested genomic DNA was the hybridized respectively with the single-stranded riboprobes A (plasmid pML 716.8) or B (plasmid pML 715.5), which anneal to the 5' C- strand or the 3' G-strand, respectively, to a site located 212 nt from the HO cutting site. Resection of the C-rich strand in Figure 10E and Figure 11C was monitored by hybridizing RsaI-digested genomic DNA with riboprobe A.

To monitor resection at the HO-induced DSB, EcoRV- or SspI- and XbaI-digested genomic DNA was hybridized with a single-stranded riboprobe, which anneals to the 5' strand to a site located respectively 215 or 248 nt from the HO cutting site. For quantitative analysis of resection, the ratios between the intensities of the cut 5' strand and loading control bands were calculated by using the NIH image program.

ChIP analysis

Exponentially growing cells (50ml of $8x10^6$-$1x10^7$) are treated with 1.4ml of 37% formaldehyde for 5 minutes while shaking, in order to create DNA-protein and protein-protein covalent bounds (cross-link). Then 2.5ml of 2.5M glycine are added for other 5 minutes while shaking. Treated cells are kept in ice until centrifugation at 1800rpm for 5' at 4°C. Cell pellet is then washed first with HBS buffer (50mM HEPES pH 7.5, 140mM NaCl) and then with ChIP buffer (50mM HEPES pH 7.5, 140mM NaCl, 1mM EDTA pH8, 1% IGEPAL CA-630, 0.1% Sodium deoxycholate, 1mM PMSF). Before each wash cells are pelletted by

centrifugation at 1800rpm for 5' at 4°C. After the wash with ChIP buffer and subsequent centrifugation, the supernatant is carefully and completely removed. Then add 0.4ml of ChIP buffer + complete anti-proteolitic tablets (Roche) is added. (Store at -80°C) After breaking cells for 30' at 4°C with glass beads, the latter are eliminated. This passage is followed by centrifugation at 4°C for 30'. Pellet is resuspended in 0.5ml ChIP buffer + anti-proteolitics and then sonicated, in order to share DNA in 500-1000 bp fragments (4 x 25"). At this point 5µl as "input DNA" for PCR reactions and 20µl as "input" for western blot analysis are taken. Then 400µl of the remaining solution is immunoprecipitated with specific Dynabeads-coated antibobies. After proper incubation with desired antibodies, Dynabeads can be washed RT as follow: 2X with SDS buffer (50mM Hepes pH7.5, 1mM EDTA pH8, 140mM NaCl, 0.025% SDS), 1X with High-salt buffer (50mM Hepes pH7.5, 1mM EDTA pH8, 1M NaCl), 1X with T/L buffer (20mM Tris-Cl pH7.5, 250mM LiCl, 1mM EDTA pH8, 0.05% sodium deoxycholate, 0.5% IGEPAL CA-630) and then 1X with T/E buffer (20mM Tris-Cl pH7.5, 0.1mM EDTA pH8). All washes are done by pulling down Dynabeads 1' and then nutating for 4' with the specific buffer. After the last wash Dynabeads are resuspended in 145µl TE + 1% SDS buffer, shaked on a wortex, put at 65°C for 2', shaked on wortex again and then pulled down. Now 120µl of the surnatant should be put at 65°C over-night for reverse cross-linking, while 20µl should be stored as sample for western blot analysis of the immunoprecipitated protein amount. Previously taken input DNA samples should be put at 65°C over-night together with 115µl of TE+ 1% SDS buffer. The next day DNA should be purified for PCR analysis (QIAgen columns).

Quantification of immunoprecipitated DNA was achieved by quantitative real-time PCR (qPCR) on a Bio-Rad MiniOpticon apparatus using primer pairs located at the nontelomeric *ARO1* fragment of chromosome IV (CON) and 640 bp centromere proximal (TG-HO) or 550 bp centromere distal (HO) to the HO cutting site at chromosome VII, and the amount was normalized to the input signal for each primer set; data are expressed as the fold enrichment of TG-HO or HO over the amount of CON in the immunoprecipitates.

Synchronization of yeast cells

Synchronization of yeast cells with α-factor

α-factor allows to synchronize a population of yeast cells in G1 phase of the cell cycle. This pheromone activates a signal transduction cascade that arrests yeast cells in G1-phase. Only *MAT***a** cells are responsive to a-factor. To synchronize in G1 a population of exponentially growing yeast cells in YEPD, 3 μg/mL α-factor is added to a 6 x 10^6 cells/mL culture, if the synchronization is performed on *bar1Δ* cells, 0,5 μg/mL α-factor is added to a 6 x 10^6 cells/mL colture. As the percentage of budded cells will fall below 5% cells are considered to be G1-arrested.

Synchronization of yeast cells with nocodazole

Nocodazole allow synchronizing a population of yeast cells in G2 phase. This drug causes the depolimerization of microtubules thus activating

the mitotic checkpoint that arrest cells at the G2-phase (at metaphase to anaphase transition). To synchronize in G2 a population of exponentially growing yeast cells in YEPD, 0.5 μg/mL nocodazole is added to a 6 x 10^6 cells/mL culture together with DMSO at a final concentration of 1%. As the percentage of dumbbell cells will reach 95% cells are considered to be G2-arrested. Cells are then washed and resuspended in fresh medium with or without 1.5 μg/mL nocodazole to keep cells G2-arrested or release them into the cell cycle respectively. Cells are harvested at different time points to perform several analyses.

Other techniques

FACS analysis of the DNA contents

FACS (Fluorescence-Activated Cell Sorting) analysis allow to determine the DNA content of every single cell of a given population of yeast cells. $6{\cdot}10^6$ cells are harvested by centrifugation, resuspended in 70% ethanol and incubated at RT for 1 hour. Cells are then washed with 1 mL 50mM Tris pH 7.5 and incubated overnight at 37°C in the same solution with 1 mg/mL RNase. Samples are centrifuged and cells are incubated at 37°C for 30 minutes with 5 mg/mL pepsin in 55mM HCl, washed with 1 mL FACS Buffer and stained in 0.5 mL FACS buffer with 50 μg/mL propidium iodide. 100 μL of each sample are diluted in 1 mL 50mM Tris pH 7.5 and analysed with a Becton-Dickinson FACS-Scan. The same

samples can also be analysed by fluorescence microscopy to score nuclear division.

Total protein extracts

Total protein extracts were prepared from 10^8 cells collected from exponentially growing yeast cultures. Cells are harvested by centrifugation and washed with 20% trichloracetic acid (TCA) in order to prevent proteolysis and resuspended in 50 ml 20% TCA. After addition of 200 μL of glass beads, cells are disrupted by vortexing for 8 minutes. Glass beads are washed with 400 μL 5% TCA, and the resulting extract are centrifuged at 3000 rpm for 10 minutes. The pellet is resuspended in 70 μL Laemmli buffer (0.62M Tris, 2% SDS, 10% glycine, 0.001% Bfb, 100mM DTT), neutralized with 30 μL 1M Tris base, boiled for 3 minutes, and finally clarified by centrifugation.

SDS-PAGE and western blot analysis

Protein extracts are loaded in 10% polyacrylamide gels. Proteins are separated based on their molecular weight by polyacrylamide gel electrophoresis in the presence of sodium dodecyl sulfate (SDS-PAGE). When adequate migration has occurred proteins are blotted onto nitrocellulose membrane. Membrane is saturated by 1 hour incubation with 4% milk in TBS containing 0.2% TRITON X-100 and incubated for 2 hours with primary antibodies. Membrane is washed three times with TBS for 10 minutes, incubated for 1 hour with secondary antibodies and again washed with TBS. Detection is performed with ECL (Enhanced

ChemiLuminescence – GE Healthcare) and X-ray films according to the manufacturer. Primary polyclonal rabbit anti-Rad53 antibodies are kindly provided by John Diffley (Clare Hall Laboratories, London). Primary monoclonal 12CA5 anti-HA and 9E10 anti-MYC antibodies are purchased at GE Healthcare, as well as peroxidase conjucated IgG anti-rabbit and anti-mouse secondary antibodies.

References

Abdallah, P., Luciano, P., Runge, K.W., Lisby, M., Géli, V., Gilson, E., and Teixeira, M.T. (2009). A two-step model for senescence triggered by a single critically short telomere. Nat. Cell Biol. *11*, 988–993.

Adams, K.E., Medhurst, A.L., Dart, D.A., and Lakin, N.D. (2006). Recruitment of ATR to sites of ionising radiation-induced DNA damage requires ATM and components of the MRN protein complex. Oncogene *25*, 3894–3904.

Arnerić, M., and Lingner, J. (2007). Tel1 kinase and subtelomere-bound Tbf1 mediate preferential elongation of short telomeres by telomerase in yeast. EMBO Rep. *8*, 1080–1085.

Aylon, Y., Liefshitz, B., and Kupiec, M. (2004). The CDK regulates repair of double-strand breaks by homologous recombination during the cell cycle. EMBO J. *23*, 4868–4875.

Baldo, V., Testoni, V., Lucchini, G., and Longhese, M.P. (2008). Dominant TEL1-hy mutations compensate for Mec1 lack of functions in the DNA damage response. Mol. Cell. Biol. *28*, 358–375.

Barnes, G., and Rio, D. (1997). DNA double-strand-break sensitivity, DNA replication, and cell cycle arrest phenotypes of Ku-deficient Saccharomyces cerevisiae. Proc. Natl. Acad. Sci. U.S.A. *94*, 867–872.

Baumann, P., and Cech, T.R. (2001). Pot1, the putative telomere end-binding protein in fission yeast and humans. Science *292*, 1171–1175.

Bertuch, A.A., and Lundblad, V. (2004). EXO1 contributes to telomere maintenance in both telomerase-proficient and telomerase-deficient Saccharomyces cerevisiae. Genetics *166*, 1651–1659.

Bianchi, A., Negrini, S., and Shore, D. (2004). Delivery of yeast telomerase to a DNA break depends on the recruitment functions of Cdc13 and Est1. Mol. Cell *16*, 139–146.

Bianchi, A., and Shore, D. (2007). Increased association of telomerase with short telomeres in yeast. Genes Dev. *21*, 1726–1730.

Bilaud, T., Brun, C., Ancelin, K., Koering, C.E., Laroche, T., and Gilson, E. (1997). Telomeric localization of TRF2, a novel human telobox protein. Nat. Genet. *17*, 236–239.

Bonetti, D., Clerici, M., Anbalagan, S., Martina, M., Lucchini, G., and Longhese, M.P. (2010a). Shelterin-like proteins and Yku inhibit

nucleolytic processing of Saccharomyces cerevisiae telomeres. PLoS Genet. *6*, e1000966.

Bonetti, D., Clerici, M., Manfrini, N., Lucchini, G., and Longhese, M.P. (2010b). The MRX complex plays multiple functions in resection of Yku- and Rif2-protected DNA ends. PLoS ONE *5*, e14142.

Bonetti, D., Martina, M., Clerici, M., Lucchini, G., and Longhese, M.P. (2009). Multiple pathways regulate 3' overhang generation at S. cerevisiae telomeres. Mol. Cell *35*, 70–81.

Booth, C., Griffith, E., Brady, G., and Lydall, D. (2001). Quantitative amplification of single-stranded DNA (QAOS) demonstrates that cdc13-1 mutants generate ssDNA in a telomere to centromere direction. Nucleic Acids Res. *29*, 4414–4422.

Boulton, S.J., and Jackson, S.P. (1996). Identification of a Saccharomyces cerevisiae Ku80 homologue: roles in DNA double strand break rejoining and in telomeric maintenance. Nucleic Acids Res. *24*, 4639–4648.

Broccoli, D., Smogorzewska, A., Chong, L., and de Lange, T. (1997). Human telomeres contain two distinct Myb-related proteins, TRF1 and TRF2. Nat. Genet. *17*, 231–235.

de Bruin, D., Zaman, Z., Liberatore, R.A., and Ptashne, M. (2001). Telomere looping permits gene activation by a downstream UAS in yeast. Nature *409*, 109–113.

Celli, G.B., and de Lange, T. (2005). DNA processing is not required for ATM-mediated telomere damage response after TRF2 deletion. Nat. Cell Biol. *7*, 712–718.

Chai, W., Ford, L.P., Lenertz, L., Wright, W.E., and Shay, J.W. (2002). Human Ku70/80 associates physically with telomerase through interaction with hTERT. J. Biol. Chem. *277*, 47242–47247.

Chan, A., Boulé, J.-B., and Zakian, V.A. (2008). Two pathways recruit telomerase to Saccharomyces cerevisiae telomeres. PLoS Genet. *4*, e1000236.

Chandra, A., Hughes, T.R., Nugent, C.I., and Lundblad, V. (2001). Cdc13 both positively and negatively regulates telomere replication. Genes Dev. *15*, 404–414.

Chang, M., Arneric, M., and Lingner, J. (2007). Telomerase repeat addition processivity is increased at critically short telomeres in a Tel1-dependent manner in Saccharomyces cerevisiae. Genes Dev. *21*, 2485–2494.

Chen, S., Inamdar, K.V., Pfeiffer, P., Feldmann, E., Hannah, M.F., Yu, Y., Lee, J.W., Zhou, T., Lees-Miller, S.P., and Povirk, L.F. (2001). Accurate in vitro end joining of a DNA double strand break with partially cohesive 3'-overhangs and 3'-phosphoglycolate termini: effect of Ku on repair fidelity. J. Biol. Chem. *276*, 24323–24330.

Chikashige, Y., and Hiraoka, Y. (2001). Telomere binding of the Rap1 protein is required for meiosis in fission yeast. Curr. Biol. *11*, 1618–1623.

Clerici, M., Mantiero, D., Guerini, I., Lucchini, G., and Longhese, M.P. (2008). The Yku70-Yku80 complex contributes to regulate double-strand break processing and checkpoint activation during the cell cycle. EMBO Rep. *9*, 810–818.

Clerici, M., Mantiero, D., Lucchini, G., and Longhese, M.P. (2005). The Saccharomyces cerevisiae Sae2 protein promotes resection and bridging of double strand break ends. J. Biol. Chem. *280*, 38631–38638.

Conrad, M.N., Wright, J.H., Wolf, A.J., and Zakian, V.A. (1990). RAP1 protein interacts with yeast telomeres in vivo: overproduction alters telomere structure and decreases chromosome stability. Cell *63*, 739–750.

Cooper, J.P., Nimmo, E.R., Allshire, R.C., and Cech, T.R. (1997). Regulation of telomere length and function by a Myb-domain protein in fission yeast. Nature *385*, 744–747.

Cooper, J.P., Watanabe, Y., and Nurse, P. (1998). Fission yeast Taz1 protein is required for meiotic telomere clustering and recombination. Nature *392*, 828–831.

Cortez, D., Guntuku, S., Qin, J., and Elledge, S.J. (2001). ATR and ATRIP: partners in checkpoint signaling. Science *294*, 1713–1716.

Counter, C.M., Avilion, A.A., LeFeuvre, C.E., Stewart, N.G., Greider, C.W., Harley, C.B., and Bacchetti, S. (1992). Telomere shortening associated with chromosome instability is arrested in immortal cells which express telomerase activity. EMBO J *11*, 1921–1929.

Dahlen, M., Olsson, T., Kanter-Smoler, G., Ramne, A., and Sunnerhagen, P. (1998). Regulation of telomere length by checkpoint genes in Schizosaccharomyces pombe. Mol. Biol. Cell *9*, 611–621.

Daley, J.M., Palmbos, P.L., Wu, D., and Wilson, T.E. (2005). Nonhomologous end joining in yeast. Annu. Rev. Genet. *39*, 431–451.

Diede, S.J., and Gottschling, D.E. (1999). Telomerase-mediated telomere addition in vivo requires DNA primase and DNA polymerases alpha and delta. Cell *99*, 723–733.

Diede, S.J., and Gottschling, D.E. (2001). Exonuclease activity is required for sequence addition and Cdc13p loading at a de novo telomere. Curr. Biol. *11*, 1336–1340.

Dionne, I., and Wellinger, R.J. (1996). Cell cycle-regulated generation of single-stranded G-rich DNA in the absence of telomerase. Proc. Natl. Acad. Sci. U.S.A. *93*, 13902–13907.

Edwards, R.J., Bentley, N.J., and Carr, A.M. (1999). A Rad3-Rad26 complex responds to DNA damage independently of other checkpoint proteins. Nat. Cell Biol. *1*, 393–398.

Evans, S.K., and Lundblad, V. (1999). Est1 and Cdc13 as comediators of telomerase access. Science *286*, 117–120.

Falck, J., Coates, J., and Jackson, S.P. (2005). Conserved modes of recruitment of ATM, ATR and DNA-PKcs to sites of DNA damage. Nature *434*, 605–611.

Faure, V., Coulon, S., Hardy, J., and Géli, V. (2010). Cdc13 and telomerase bind through different mechanisms at the lagging- and leading-strand telomeres. Mol. Cell *38*, 842–852.

Fisher, T.S., Taggart, A.K.P., and Zakian, V.A. (2004). Cell cycle-dependent regulation of yeast telomerase by Ku. Nat. Struct. Mol. Biol. *11*, 1198–1205.

Francia, S., Weiss, R.S., Hande, M.P., Freire, R., and d' Adda di Fagagna, F. (2006). Telomere and telomerase modulation by the mammalian Rad9/Rad1/Hus1 DNA-damage-checkpoint complex. Curr. Biol. *16*, 1551–1558.

Frank, C.J., Hyde, M., and Greider, C.W. (2006). Regulation of telomere elongation by the cyclin-dependent kinase CDK1. Mol. Cell *24*, 423–432.

Furuse, M., Nagase, Y., Tsubouchi, H., Murakami-Murofushi, K., Shibata, T., and Ohta, K. (1998). Distinct roles of two separable in vitro activities of yeast Mre11 in mitotic and meiotic recombination. EMBO J. *17*, 6412–6425.

Gallardo, F., Laterreur, N., Cusanelli, E., Ouenzar, F., Querido, E., Wellinger, R.J., and Chartrand, P. (2011). Live cell imaging of telomerase RNA dynamics reveals cell cycle-dependent clustering of telomerase at elongating telomeres. Mol. Cell *44*, 819–827.

Gao, H., Toro, T.B., Paschini, M., Braunstein-Ballew, B., Cervantes, R.B., and Lundblad, V. (2010). Telomerase recruitment in Saccharomyces cerevisiae is not dependent on Tel1-mediated phosphorylation of Cdc13. Genetics *186*, 1147–1159.

Garvik, B., Carson, M., and Hartwell, L. (1995). Single-stranded DNA arising at telomeres in cdc13 mutants may constitute a specific signal for the RAD9 checkpoint. Mol. Cell. Biol. *15*, 6128–6138.

Goudsouzian, L.K., Tuzon, C.T., and Zakian, V.A. (2006). S. cerevisiae Tel1p and Mre11p are required for normal levels of Est1p and Est2p telomere association. Mol. Cell *24*, 603–610.

Grandin, N., Damon, C., and Charbonneau, M. (2001). Ten1 functions in telomere end protection and length regulation in association with Stn1 and Cdc13. EMBO J. *20*, 1173–1183.

Grandin, N., Reed, S.I., and Charbonneau, M. (1997). Stn1, a new Saccharomyces cerevisiae protein, is implicated in telomere size regulation in association with Cdc13. Genes Dev. *11*, 512–527.

Gravel, S., Larrivée, M., Labrecque, P., and Wellinger, R.J. (1998). Yeast Ku as a regulator of chromosomal DNA end structure. Science *280*, 741–744.

Greenwell, P.W., Kronmal, S.L., Porter, S.E., Gassenhuber, J., Obermaier, B., and Petes, T.D. (1995). TEL1, a gene involved in controlling telomere length in S. cerevisiae, is homologous to the human ataxia telangiectasia gene. Cell *82*, 823–829.

Greider, C.W., and Blackburn, E.H. (1985). Identification of a specific telomere terminal transferase activity in Tetrahymena extracts. Cell *43*, 405–413.

Griffith, J.D., Comeau, L., Rosenfield, S., Stansel, R.M., Bianchi, A., Moss, H., and de Lange, T. (1999). Mammalian telomeres end in a large duplex loop. Cell *97*, 503–514.

Hardy, C.F., Sussel, L., and Shore, D. (1992). A RAP1-interacting protein involved in transcriptional silencing and telomere length regulation. Genes Dev. *6*, 801–814.

Hector, R.E., Shtofman, R.L., Ray, A., Chen, B.-R., Nyun, T., Berkner, K.L., and Runge, K.W. (2007). Tel1p preferentially associates with short telomeres to stimulate their elongation. Mol. Cell *27*, 851–858.

Hirano, Y., Fukunaga, K., and Sugimoto, K. (2009). Rif1 and rif2 inhibit localization of tel1 to DNA ends. Mol. Cell *33*, 312–322.

Hirano, Y., and Sugimoto, K. (2007). Cdc13 telomere capping decreases Mec1 association but does not affect Tel1 association with DNA ends. Mol. Biol. Cell *18*, 2026–2036.

Houghtaling, B.R., Cuttonaro, L., Chang, W., and Smith, S. (2004). A dynamic molecular link between the telomere length regulator TRF1 and the chromosome end protector TRF2. Curr. Biol. *14*, 1621–1631.

Hug, N., and Lingner, J. (2006). Telomere length homeostasis. Chromosoma *115*, 413–425.

Ira, G., Pellicioli, A., Balijja, A., Wang, X., Fiorani, S., Carotenuto, W., Liberi, G., Bressan, D., Wan, L., Hollingsworth, N.M., et al. (2004). DNA end resection, homologous recombination and DNA damage checkpoint activation require CDK1. Nature *431*, 1011–1017.

Jain, D., and Cooper, J.P. (2010). Telomeric strategies: means to an end. Annu. Rev. Genet. *44*, 243–269.

Jazayeri, A., Falck, J., Lukas, C., Bartek, J., Smith, G.C.M., Lukas, J., and Jackson, S.P. (2006). ATM- and cell cycle-dependent regulation of ATR in response to DNA double-strand breaks. Nat. Cell Biol. *8*, 37–45.

Kanoh, J., and Ishikawa, F. (2001). spRap1 and spRif1, recruited to telomeres by Taz1, are essential for telomere function in fission yeast. Curr. Biol. *11*, 1624–1630.

Kim, S.H., Kaminker, P., and Campisi, J. (1999). TIN2, a new regulator of telomere length in human cells. Nat. Genet. *23*, 405–412.

de Lange, T. (2005). Shelterin: the protein complex that shapes and safeguards human telomeres. Genes Dev. *19*, 2100–2110.

Larrivée, M., LeBel, C., and Wellinger, R.J. (2004a). The generation of proper constitutive G-tails on yeast telomeres is dependent on the MRX complex. Genes Dev. *18*, 1391–1396.

Larrivée, M., LeBel, C., and Wellinger, R.J. (2004b). The generation of proper constitutive G-tails on yeast telomeres is dependent on the MRX complex. Genes Dev. *18*, 1391–1396.

Lee, S.E., Moore, J.K., Holmes, A., Umezu, K., Kolodner, R.D., and Haber, J.E. (1998). Saccharomyces Ku70, mre11/rad50 and RPA proteins regulate adaptation to G2/M arrest after DNA damage. Cell *94*, 399–409.

Lendvay, T.S., Morris, D.K., Sah, J., Balasubramanian, B., and Lundblad, V. (1996). Senescence mutants of Saccharomyces cerevisiae with a defect in telomere replication identify three additional EST genes. Genetics *144*, 1399–1412.

Levy, D.L., and Blackburn, E.H. (2004). Counting of Rif1p and Rif2p on Saccharomyces cerevisiae telomeres regulates telomere length. Mol. Cell. Biol. *24*, 10857–10867.

Li, B., Oestreich, S., and de Lange, T. (2000). Identification of human Rap1: implications for telomere evolution. Cell *101*, 471–483.

Li, S., Makovets, S., Matsuguchi, T., Blethrow, J.D., Shokat, K.M., and Blackburn, E.H. (2009). Cdk1-dependent phosphorylation of Cdc13 coordinates telomere elongation during cell-cycle progression. Cell *136*, 50–61.

Lingner, J., Cech, T.R., Hughes, T.R., and Lundblad, V. (1997). Three Ever Shorter Telomere (EST) genes are dispensable for in vitro yeast telomerase activity. Proc. Natl. Acad. Sci. U.S.A. *94*, 11190–11195.

Liu, L., Bailey, S.M., Okuka, M., Muñoz, P., Li, C., Zhou, L., Wu, C., Czerwiec, E., Sandler, L., Seyfang, A., et al. (2007). Telomere lengthening early in development. Nat. Cell Biol. *9*, 1436–1441.

Llorente, B., and Symington, L.S. (2004). The Mre11 nuclease is not required for 5' to 3' resection at multiple HO-induced double-strand breaks. Mol. Cell. Biol. *24*, 9682–9694.

Longhese, M.P. (2008). DNA damage response at functional and dysfunctional telomeres. Genes Dev. *22*, 125–140.

Longhese, M.P., Bonetti, D., Manfrini, N., and Clerici, M. (2010). Mechanisms and regulation of DNA end resection. EMBO J. *29*, 2864–2874.

Longhese, M.P., Mantiero, D., and Clerici, M. (2006). The cellular response to chromosome breakage. Mol. Microbiol. *60*, 1099–1108.

Longhese, M.P., Paciotti, V., Neecke, H., and Lucchini, G. (2000). Checkpoint proteins influence telomeric silencing and length maintenance in budding yeast. Genetics *155*, 1577–1591.

Lydall, D. (2009). Taming the tiger by the tail: modulation of DNA damage responses by telomeres. EMBO J. *28*, 2174–2187.

Majka, J., Niedziela-Majka, A., and Burgers, P.M.J. (2006). The checkpoint clamp activates Mec1 kinase during initiation of the DNA damage checkpoint. Mol. Cell *24*, 891–901.

Makarov, V.L., Hirose, Y., and Langmore, J.P. (1997). Long G tails at both ends of human chromosomes suggest a C strand degradation mechanism for telomere shortening. Cell *88*, 657–666.

Mallory, J.C., and Petes, T.D. (2000). Protein kinase activity of Tel1p and Mec1p, two Saccharomyces cerevisiae proteins related to the human ATM protein kinase. Proc. Natl. Acad. Sci. U.S.A. *97*, 13749–13754.

Mantiero, D., Clerici, M., Lucchini, G., and Longhese, M.P. (2007). Dual role for Saccharomyces cerevisiae Tel1 in the checkpoint response to double-strand breaks. EMBO Rep. *8*, 380–387.

Marcand, S., Brevet, V., and Gilson, E. (1999). Progressive cis-inhibition of telomerase upon telomere elongation. EMBO J. *18*, 3509–3519.

Marcand, S., Brevet, V., Mann, C., and Gilson, E. (2000). Cell cycle restriction of telomere elongation. Curr. Biol. *10*, 487–490.

Marcand, S., Gilson, E., and Shore, D. (1997). A protein-counting mechanism for telomere length regulation in yeast. Science *275*, 986–990.

Marcand, S., Pardo, B., Gratias, A., Cahun, S., and Callebaut, I. (2008). Multiple pathways inhibit NHEJ at telomeres. Genes Dev. *22*, 1153–1158.

Maringele, L., and Lydall, D. (2002a). EXO1-dependent single-stranded DNA at telomeres activates subsets of DNA damage and spindle checkpoint pathways in budding yeast yku70Delta mutants. Genes Dev. *16*, 1919–1933.

Maringele, L., and Lydall, D. (2002b). EXO1-dependent single-stranded DNA at telomeres activates subsets of DNA damage and spindle checkpoint pathways in budding yeast yku70Delta mutants. Genes Dev. *16*, 1919–1933.

Matsuura, A., Naito, T., and Ishikawa, F. (1999). Genetic control of telomere integrity in Schizosaccharomyces pombe: rad3(+) and tel1(+) are parts of two regulatory networks independent of the downstream protein kinases chk1(+) and cds1(+). Genetics *152*, 1501–1512.

McGee, J.S., Phillips, J.A., Chan, A., Sabourin, M., Paeschke, K., and Zakian, V.A. (2010). Reduced Rif2 and lack of Mec1 target short telomeres for elongation rather than double-strand break repair. Nat. Struct. Mol. Biol. *17*, 1438–1445.

Metcalfe, J.A., Parkhill, J., Campbell, L., Stacey, M., Biggs, P., Byrd, P.J., and Taylor, A.M. (1996). Accelerated telomere shortening in ataxia telangiectasia. Nat. Genet. *13*, 350–353.

Michelson, R.J., Rosenstein, S., and Weinert, T. (2005). A telomeric repeat sequence adjacent to a DNA double-stranded break produces an anticheckpoint. Genes Dev. *19*, 2546–2559.

Mimitou, E.P., and Symington, L.S. (2008). Sae2, Exo1 and Sgs1 collaborate in DNA double-strand break processing. Nature *455*, 770–774.

Miyoshi, T., Kanoh, J., Saito, M., and Ishikawa, F. (2008). Fission yeast Pot1-Tpp1 protects telomeres and regulates telomere length. Science *320*, 1341–1344.

Moreau, S., Ferguson, J.R., and Symington, L.S. (1999). The nuclease activity of Mre11 is required for meiosis but not for mating type switching, end joining, or telomere maintenance. Mol. Cell. Biol. *19*, 556–566.

Moretti, P., Freeman, K., Coodly, L., and Shore, D. (1994). Evidence that a complex of SIR proteins interacts with the silencer and telomere-binding protein RAP1. Genes Dev. *8*, 2257–2269.

Myers, J.S., and Cortez, D. (2006). Rapid activation of ATR by ionizing radiation requires ATM and Mre11. J. Biol. Chem. *281*, 9346–9350.

Naito, T., Matsuura, A., and Ishikawa, F. (1998). Circular chromosome formation in a fission yeast mutant defective in two ATM homologues. Nat. Genet. *20*, 203–206.

Nakada, D., Shimomura, T., Matsumoto, K., and Sugimoto, K. (2003). The ATM-related Tel1 protein of Saccharomyces cerevisiae controls a checkpoint response following phleomycin treatment. Nucleic Acids Res. *31*, 1715–1724.

Nakamura, T.M., Moser, B.A., and Russell, P. (2002). Telomere binding of checkpoint sensor and DNA repair proteins contributes to maintenance of functional fission yeast telomeres. Genetics *161*, 1437–1452.

Negrini, S., Ribaud, V., Bianchi, A., and Shore, D. (2007). DNA breaks are masked by multiple Rap1 binding in yeast: implications for telomere capping and telomerase regulation. Genes Dev. *21*, 292–302.

Nugent, C.I., Hughes, T.R., Lue, N.F., and Lundblad, V. (1996). Cdc13p: a single-strand telomeric DNA-binding protein with a dual role in yeast telomere maintenance. Science *274*, 249–252.

Paciotti, V., Clerici, M., Lucchini, G., and Longhese, M.P. (2000). The checkpoint protein Ddc2, functionally related to S. pombe Rad26, interacts with Mec1 and is regulated by Mec1-dependent phosphorylation in budding yeast. Genes Dev. *14*, 2046–2059.

Palmbos, P.L., Wu, D., Daley, J.M., and Wilson, T.E. (2008). Recruitment of Saccharomyces cerevisiae Dnl4-Lif1 complex to a double-strand break requires interactions with Yku80 and the Xrs2 FHA domain. Genetics *180*, 1809–1819.

Pardo, B., and Marcand, S. (2005). Rap1 prevents telomere fusions by nonhomologous end joining. EMBO J. *24*, 3117–3127.

Pennock, E., Buckley, K., and Lundblad, V. (2001). Cdc13 delivers separate complexes to the telomere for end protection and replication. Cell *104*, 387–396.

Peterson, S.E., Stellwagen, A.E., Diede, S.J., Singer, M.S., Haimberger, Z.W., Johnson, C.O., Tzoneva, M., and Gottschling, D.E. (2001). The function of a stem-loop in telomerase RNA is linked to the DNA repair protein Ku. Nat. Genet. *27*, 64–67.

Polotnianka, R.M., Li, J., and Lustig, A.J. (1998). The yeast Ku heterodimer is essential for protection of the telomere against nucleolytic and recombinational activities. Curr. Biol. *8*, 831–834.

Porter, S.E., Greenwell, P.W., Ritchie, K.B., and Petes, T.D. (1996). The DNA-binding protein Hdf1p (a putative Ku homologue) is required for maintaining normal telomere length in Saccharomyces cerevisiae. Nucleic Acids Res. *24*, 582–585.

Puglisi, A., Bianchi, A., Lemmens, L., Damay, P., and Shore, D. (2008). Distinct roles for yeast Stn1 in telomere capping and telomerase inhibition. EMBO J. *27*, 2328–2339.

Ritchie, K.B., Mallory, J.C., and Petes, T.D. (1999). Interactions of TLC1 (which encodes the RNA subunit of telomerase), TEL1, and MEC1 in regulating telomere length in the yeast Saccharomyces cerevisiae. Mol. Cell. Biol. *19*, 6065–6075.

Ritchie, K.B., and Petes, T.D. (2000). The Mre11p/Rad50p/Xrs2p complex and the Tel1p function in a single pathway for telomere maintenance in yeast. Genetics *155*, 475–479.

Sabourin, M., Tuzon, C.T., and Zakian, V.A. (2007). Telomerase and Tel1p preferentially associate with short telomeres in S. cerevisiae. Mol. Cell *27*, 550–561.

Shiloh, Y. (2006). The ATM-mediated DNA-damage response: taking shape. Trends Biochem. Sci. *31*, 402–410.

Shore, D., and Bianchi, A. (2009). Telomere length regulation: coupling DNA end processing to feedback regulation of telomerase. EMBO J. *28*, 2309–2322.

Stellwagen, A.E., Haimberger, Z.W., Veatch, J.R., and Gottschling, D.E. (2003). Ku interacts with telomerase RNA to promote telomere addition at native and broken chromosome ends. Genes Dev. *17*, 2384–2395.

Strahl-Bolsinger, S., Hecht, A., Luo, K., and Grunstein, M. (1997). SIR2 and SIR4 interactions differ in core and extended telomeric heterochromatin in yeast. Genes Dev. *11*, 83–93.

Taggart, A.K.P., Teng, S.-C., and Zakian, V.A. (2002). Est1p as a cell cycle-regulated activator of telomere-bound telomerase. Science *297*, 1023–1026.

Teixeira, M.T., Arneric, M., Sperisen, P., and Lingner, J. (2004). Telomere length homeostasis is achieved via a switch between telomerase-extendible and -nonextendible states. Cell *117*, 323–335.

Tomita, K., and Cooper, J.P. (2008). Fission yeast Ccq1 is telomerase recruiter and local checkpoint controller. Genes Dev. *22*, 3461–3474.

Tomita, K., Kibe, T., Kang, H.-Y., Seo, Y.-S., Uritani, M., Ushimaru, T., and Ueno, M. (2004). Fission yeast Dna2 is required for generation of the telomeric single-strand overhang. Mol. Cell. Biol. *24*, 9557–9567.

Tseng, S.-F., Lin, J.-J., and Teng, S.-C. (2006). The telomerase-recruitment domain of the telomere binding protein Cdc13 is regulated by Mec1p/Tel1p-dependent phosphorylation. Nucleic Acids Res. *34*, 6327–6336.

Tsubouchi, H., and Ogawa, H. (1998). A novel mre11 mutation impairs processing of double-strand breaks of DNA during both mitosis and meiosis. Mol. Cell. Biol. *18*, 260–268.

Vodenicharov, M.D., Laterreur, N., and Wellinger, R.J. (2010). Telomere capping in non-dividing yeast cells requires Yku and Rap1. EMBO J. *29*, 3007–3019.

Vodenicharov, M.D., and Wellinger, R.J. (2006). DNA degradation at unprotected telomeres in yeast is regulated by the CDK1 (Cdc28/Clb) cell-cycle kinase. Mol. Cell *24*, 127–137.

Wellinger, R.J., Ethier, K., Labrecque, P., and Zakian, V.A. (1996). Evidence for a new step in telomere maintenance. Cell *85*, 423–433.

Wellinger, R.J., Wolf, A.J., and Zakian, V.A. (1993). Saccharomyces telomeres acquire single-strand TG1-3 tails late in S phase. Cell *72*, 51–60.

Wotton, D., and Shore, D. (1997). A novel Rap1p-interacting factor, Rif2p, cooperates with Rif1p to regulate telomere length in Saccharomyces cerevisiae. Genes Dev. *11*, 748–760.

Wright, J.H., and Zakian, V.A. (1995). Protein-DNA interactions in soluble telosomes from Saccharomyces cerevisiae. Nucleic Acids Res. *23*, 1454–1460.

Ye, J., Wu, Y., and Gilson, E. (2010). Dynamics of telomeric chromatin at the crossroads of aging and cancer. Essays Biochem. *48*, 147–164.

Zhang, Y., Hefferin, M.L., Chen, L., Shim, E.Y., Tseng, H.-M., Kwon, Y., Sung, P., Lee, S.E., and Tomkinson, A.E. (2007). Role of Dnl4-Lif1 in nonhomologous end-joining repair complex assembly and suppression of homologous recombination. Nat. Struct. Mol. Biol. *14*, 639–646.

Zhong, Z., Shiue, L., Kaplan, S., and de Lange, T. (1992). A mammalian factor that binds telomeric TTAGGG repeats in vitro. Mol. Cell. Biol. *12*, 4834–4843.

Zhu, Z., Chung, W.-H., Shim, E.Y., Lee, S.E., and Ira, G. (2008). Sgs1 helicase and two nucleases Dna2 and Exo1 resect DNA double-strand break ends. Cell *134*, 981–994.

Zierhut, C., and Diffley, J.F.X. (2008). Break dosage, cell cycle stage and DNA replication influence DNA double strand break response. EMBO J. *27*, 1875–1885.

Zou, L., and Elledge, S.J. (2003). Sensing DNA damage through ATRIP recognition of RPA-ssDNA complexes. Science *300*, 1542–1548.